UNIVERSITY OF CALIFORNIA,
IRVINE

Protein-Based Nanoparticles for Cancer Immunotherapy

DISSERTATION

submitted in partial satisfaction of the requirements
for the degree of

DOCTOR OF PHILOSOPHY

in Chemical and Biochemical Engineering
by

Medea Neek

Dissertation Committee:
Professor Szu-Wen Wang, Chair
Professor Nancy A. Da Silva
Professor Edward L. Nelson

2019

DEDICATION

To

my husband, my daughter, and my parents

TABLE OF CONTENTS

LIST OF ABBREVIATIONS

AA	Amino acid
Abs	Absorbance
AF	Alexa Fluor
AF488	Alexa Fluor 488
AF-E2	D381C E2 nanoparticle with AF488 conjugated internally via maleimide
APC	Antigen presenting cell
BMDC	Bone marrow-derived dendritic cell
BMDM	Bone marrow-derived macrophage
BMPH	N-β-maleimidopropionic acid hydrazide
CD	Cluster of differentiation
CpG	Nonmethylated single-stranded DNA with repeating CG motifs
CpG-E2	E2 nanoparticles with covalently encapsulated CpG 1826 (Mouse Type B)
CpG-gp-E2	E2 nanoparticles with encapsulated CpG and surface displayed gp100 25-33
CpG-PEG-E2	E2 nanoparticle with surface conjugated CpG 1826 via a 2000 Da PEG linker
CTL	$CD8^+$ cytotoxic T lymphocyte
CTLA-4	Cytotoxic T lymphocyte 4
D381C	E2 nanoparticle with an internal point mutation to cysteine at AA 381
DC	Dendritic cell
dLN	draining lymph nodes
DLS	Dynamic light scattering
E2	Catalytic subunit of the pyruvate dehydrogenase enzyme complex
E279C	E2 nanoparticle with an external point mutation to cysteine at AA 279
E2-WT	E2 nanoparticle with the native sequence from *Bacillus stearothermophilus*

ELISpot	Enzyme-linked immunospot assay
ESI-MS	Electrospray ionization mass spectrometry
FACS	Fluorescence assisted cell sorting
FBS	Fetal bovine serum
FITC	Fluorescein isothiocyanate
FoxP3	Forkhead box P3 transcription factor
FPLC	Fast protein liquid chromatography
gp100	Premelanasome protein; an overexpressed melanoma tumor antigen
$gp100_{25\text{-}33}$	KVPRNQDWL immunodominant MHC I-restricted epitope from gp100
gp-E2	E2 nanoparticle with surface displayed gp10025-33 peptides
HPLC	High performance liquid chromatography
iDC	Immature dendritic cell
IFN-γ	Interferon gamma
IM	Intramuscular
IP	Intraperitoneal
IV	Intravenous
LAL	Limulus amebocyte lysate
LPS	Lipopolysaccharide
mal-PEG	Maleimide-PEG linker
MAGE-A3	Melanoma antigen family A, 3
MHC	Major Histocompatibility complex
mPEG-E2	E2 nanoparticle with surface conjugated 2000 Da methyl-PEG
NK	Natural killer cell
NY-ESO-1	New York esophageal squamous cell carcinoma-1

OVA	Chicken ovalbumin
PBMC	Peripheral blood mononuclear cells
PD-1	Programmed cell death 1 receptor
PEG	Poly(ethylene glycol)
PHA	Phytohaemagglutinin
PLGA	Poly(lactic-co-glycolic acid)
RT	Room temperature
SC	Subcutaneous
S.D.	Standard deviation
S.E.M.	Standard error of the mean
SDS-PAGE	Sodium dodecyl sulfate polyacrylamide gel electrophoresis
SIINFEKL	MHC I-restricted epitope from the chicken ovalbumin protein (AA 257-264)
SMCC	Succinimidyl trans-4-(maleimidylmethyl)cyclohexane-1-carboxylate
TAA	Tumor-associated antigen
TCR	T cell receptor
TEM	Transmission electron microscopy
TIL	Tumor-infiltrating lymphocytes
TLR	Toll-like receptor
TME	Tumor microenvironment
VLP	Virus-like particle
WT	Wild-type

LIST OF FIGURES

LIST OF TABLES

ACKNOWLEDGMENTS

I would like to express the deepest appreciation to my committee chair, Professor Szu-Wen Wang. Without her guidance and persistent help this dissertation would not have been possible. Thank you for taking a chance on me. I truly enjoyed my research.

This work was supported by the National Institutes of Health (R21EB017995), the National Cancer Institute of the National Institutes of Health (P30CA062203), and the University of California Cancer Research Coordinating Committee.

I would like to thank my committee members, Professor Nancy A. Da Silva and Professor Edward L. Nelson for constructive feedback and helping to direct my research efforts and agreeing to evaluate my competency to enter the world as a PhD scientist.

I would like to thank all of my collaborators, including Dr. Edward Nelson and Dr. Jo Anne Tucker for their invaluable advice, direction, help on experiments, and contributions to publishing high quality research.

I would like to acknowledge everyone who allowed my use of their facilities/equipment and for providing materials, training, and advice, including Dr. Nancy Da Silva, Dr. Wendy Liu, and Dr. Sergey Ryazantsev at UCLA.

I would like to acknowledge the Mass Spectrometry Facility, Laser Spectroscopy Facility, and UCI Flow Cytometry Core Facility, Institute for Immunology.

I would like to acknowledge all of my lab mates, past and present, for useful discussions, and for maintaining the Wang Lab as a comfortable and friendly place to work every day.

I would like to acknowledge Dr. Nicholas Molino, a former Wang-lab member, for being the best mentor in the lab.

Finally, I will thank my family; My husband, Cyrus Neek, my father, Ahmad Babaie, and my mother, Mina Rostami for their continuous support.

CURRICULUM VITAE

Medea Neek

1608 Avenida Salvador, San Clemente, CA 92672
medea@neek.com

Education

- Ph.D., Chemical and Biochemical Engineering, University of California, Irvine, 2019
- M.S., Chemical and Biochemical Engineering, University of California, Irvine, 2015
- M.S., Analytical Chemistry, Sharif University of Technology, Tehran, Iran (transferred)
- B.S., Chemistry, Shahid Beheshti University, Tehran, Iran, 2010

Research Interest

- Cancer biology, treatment, and detection
- Drug delivery systems

Research Experience

- Cancer vaccine development - developing viral-mimicking nanoparticles as a platform for cancer vaccines
    - Designing biomimetic nanoparticles to improve cancer vaccine efficacy
    - Harvesting and handling immune cells such as dendritic cells and splenocytes
    - Investigating the ex-vivo efficacy of nanoparticle vaccines using various techniques such as ELISpot and CTL activity assays
    - Investigating the pre-clinical efficacy of nanoparticle vaccines in animal tumor models
- Development of immune programming polymers - synthesized TLR-agonist and studied their interaction with immune system
- Extraction of fatty acids from biological materials using analytical techniques - conducted separation & extraction of fatty acids for further investigation of their medical properties

Honors & Accomplishments

- Graduate Dean's Dissertation Fellowship, UCI, Winter 2019
- Research & Travel Grant award, The Henry Samueli School of Engineering, UCI, Spring 2017
- Ranked 12th (top 1%) in the National Master's Degree University Entrance Examination
- Full scholarship from the Department of Chemistry at Shahid Beheshti University

Leadership & Mentorship Experience

- Trained and mentored 5 undergraduate and 5 graduate level student researchers
- Volunteered & participated in UCI-affiliated FABcamp summer outreach program - science experiments were conducted and demonstrated to junior high students in order to familiarize them with basic scientific principles, 2016 & 2017
- Mentored an 8th grade student performing a science fair project who received second place in the California State Science Fair competition
- Teaching Assistant for required classes in Chemical Engineering Program
    - Chemical Engineering Design (CBEMS 149 - Spring 2014)
    - Reaction Kinetics (CBEMS 110 - Fall 2015, Fall 2016,Winter 2017, and Winter 2018)
- Tutored several high school students in Physics & Chemistry (2007-2012)

Publications

- Neek, M., Tucker, J. A., Nelson, E. L. & Wang, S. W. Combination of anti-PD-1 with protein nanoparticle vaccine induces longer survival in tumor-bearing mice (in preparation).
- Neek, M., Kim, T. Il & Wang, S. W. Protein-based nanoparticles in cancer vaccine development. *Nanomedicine Nanotechnology, Biol. Med.* **15,** 164–174 (2019).
- Neek, M., Tucker, J. A., Kim, T. Il, Molino, N. M., Nelson, E. L. & Wang, S. W. Co-delivery of human cancer-testis antigens with adjuvant in protein nanoparticles induces higher cell-mediated immune responses. *Biomaterials* **156,** 194–203 (2018).
- Molino, N. M.*****, Neek, M.*****, Tucker, J. A., Nelson, E. L. & Wang, S. W. Display of DNA on Nanoparticles for Targeting Antigen Presenting Cells. *ACS Biomater. Sci. Eng.* **3,** 496–501 (2017).
- Molino, N. M., Neek, M., Tucker, J. A., Nelson, E. L. & Wang, S. Biomaterials Viral-mimicking protein nanoparticle vaccine for eliciting anti-tumor responses. *Biomaterials* **86,** 83–91 (2016).

***** Authors contributed equally to the work and are considered co-first authors.

Provisional Patent

- Szu-Wen Wang, Nicholas Molino, Medea Neek, Edward L. Nelson, and Jo Anne Tucker. Protein nanoparticles and combination therapy for cancer immunotherapy. UCI Ref. No.: 2019-061-1, NT Ref. No.: UCI 18.27 PROV.

Conferences

- M. Neek, J. A. Tucker, E. L. Nelson, and S. W. Wang, "Protein Nanoparticle-Based Vaccines." 15th Annual UC Irvine Immunology Fair/conference, December 2017.
- M. Neek, J. A. Tucker, E. L. Nelson, and S. W. Wang, "Protein Nanoparticle-Based Vaccines for Eliciting Anti-Tumor Responses." Cancer Nanotechnology, Gordon Research Seminar, Mount Snow, VT. 18th-19th of June 2017.
- M. Neek, J. A. Tucker, E. L. Nelson, and S. W. Wang, "Protein Nanoparticle-Based Vaccines for Eliciting Anti-Tumor Responses." Cancer Nanotechnology, Gordon Research Conference, Mount Snow, VT. 19th-23rd of June 2017.
- M. Neek, J. A. Tucker, N. M. Molino, E. L. Nelson, and S. W. Wang, " Immunotherapy Using Protein Nanoparticles for Improved Response towards Human Cancer Antigens." 253rd American Chemical Society National Meeting, San Francisco, CA. April 2017.
- R.A. Que, M. Neek, N. M. Molino, E. L. Nelson, NA. Da Silva, and S.W. Wang. "Molecular Engineering of Bioinspired Materials for Therapeutic Applications." Gordon Research Conference on Bioinspired Materials, Switzerland, June 2016.
- M. Neek, N. M. Molino, J. A. Tucker, E. L. Nelson, and S. W. Wang, "Protein nanoparticle conjugates for cancer immunotherapy." 251st American Chemical Society National Meeting, San Diego, CA. March 2016.
- M. Neek, N. M. Molino, J. A. Tucker, E. L. Nelson, and S. W. Wang, "Protein nanoparticles induce tumor antigen specific CD8+ T cells and antitumor responses." 13th Annual UC Irvine Immunology Fair/conference, December 2015.
- M. Neek, N. M. Molino, J. A. Tucker, E. L. Nelson, and S. W. Wang, "Protein nanoparticles induce tumor antigen specific CD8+ T cells and antitumor responses."Chao Family Comprehensive Cancer Center Scientific Conference, Palm Springs, CA. September 2015.

Underlined represents the presenter.

ABSTRACT OF THE DISSERTATION

Protein-Based Nanoparticles for Cancer Immunotherapy

By

Medea Neek

Doctor of Philosophy in Chemical and Biochemical Engineering

University of California, Irvine, 2019

Professor Szu-Wen Wang, Chair

Although progress has been made in conventional cancer therapy, cancer is still the second leading cause of death in the United States. Recently, a new approach for cancer treatment known as immunotherapy has shown remarkable success. Within immunotherapy, cancer vaccines train the body to recognize tumor-associated antigens for targeted destruction of cancer cells. While promising, clinical success of cancer vaccines to date has been limited. Our work focuses on utilizing a viral-mimetic design to develop a new platform to improve cancer vaccine efficacy.

We have been exploring the non-viral E2 protein nanoparticle as a cancer vaccine platform. We verified that simultaneous delivery of cancer antigen epitopes (*e.g.,* gp100, NY-ESO-1, MAGE-A3) and adjuvant (CpG) within E2 nanoparticles resulted in improved anti-tumor responses. Prophylactic immunization with CpG-gp-E2 (E2 conjugated with gp100 and CpG) increased animal survival time by ~ 40% in an aggressive tumor model. Furthermore, we demonstrated that simultaneous delivery of human-restricted cancer-testis epitopes and CpG within E2 (CpG-NYESO-E2 and CpG-MAGE-E2) resulted in an increase in IFN-γ secretion and enhanced lytic activity towards human cancer cells

expressing the antigen. These results demonstrate the broad efficacy of the E2 nanoparticle platform against various target cancer antigens.

One of the promising new FDA-approved approaches in cancer immunotherapy is the obstruction of inhibitory effects of immune checkpoint molecules (*e.g.,* PD-1). However, treatments with checkpoint inhibitors are still not effective in a significant portion of patients. To address this, we examined the therapeutic effects of combination delivery of anti-PD-1 with CpG-gp-E2 nanoparticles. In the B16-F10 melanoma tumor model, ~ 50% of the mice treated with combination therapy remained tumor-free, compared with 0% and ~ 5% survival for vaccine and anti-PD-1 treatments alone, respectively. Cell uptake of the E2 nanoparticle *in vitro* was also investigated, and we demonstrated that surface display of CpG on E2 increased the nanoparticle uptake by APCs, which can potentially further increase the vaccine efficacy. Altogether, our results demonstrate the potential of the E2 protein nanoparticle as an effective cancer vaccine platform for inducing anti-tumor responses. These findings could lead to more effective cancer treatments.

CHAPTER 1

BACKGROUND: CANCER IMMUNOTHERAPY, PROTEIN NANOPARTICLE DELIVERY PLATFORMS, IMMUNE CHECKPOINT INHIBITORS

Portions of this chapter have been slightly modified and published as: Neek, M., Kim, T. I & Wang, S. W. Protein-based nanoparticles in cancer vaccine development. *Nanomedicine Nanotechnology, Biol. Med.* **15,** 164–174 (2019).

1.1. Cancer and Immune System

1.1.1. Cancer Immunoediting

Evidence has long indicated that an individual's immune system is capable of recognizing and destroying tumor cells. In the 1950's, MacFarlane Burnet and Lewis Thomas proposed the immunosurveillance hypothesis, which suggested that cancer is suppressed by the immune system.[1] However, occasional immunological escape can lead to cancer progression, a process that became known as cancer immunoediting [Figure 1.1].[2] Cancer cells alter their microenvironment to that which is more favorable for their progression. Detectable tumors, which need clinical treatments are those that have escaped the immune system. Cancer treatment by conventional strategies such as surgery, radiotherapy, and cytotoxic drugs usually result in an incomplete elimination of cancer cells. However, recent efforts in research have opened a new area in cancer treatment known as immunotherapy. Immunotherapy's main goal is to harness and boost the patient's intrinsic immune system to effectively attack cancer cells.[3–6]

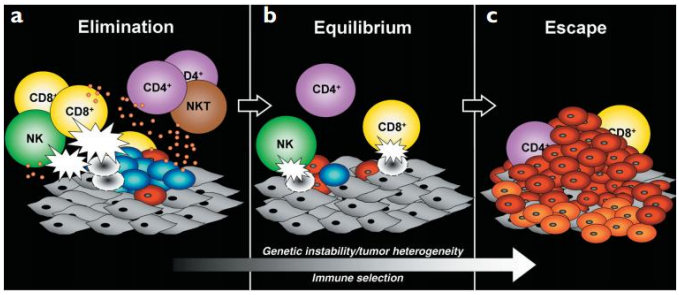

Figure 1.1. Different Phases in Cancer Immunoediting. a) Elimination phase corresponds to immunosurveillance. **b)** In the equilibrium phase, the immune system promotes the generation of tumor cell variants with increasing capacities to survive immune attack. **c)** In escape, the tumor expands in an uncontrolled manner. Figure taken from Dunn G.P. *et al*.[2] Copyright Nature Publishing Group. Reproduced with permission.

1.1.2. CD8 T Cells in Cancer Immunology

The goal of many cancer vaccines is to induce strong CD8 T cell responses which are needed to overcome the low immunogenicity of tumor cells.[7] Immature dendritic cells (DCs) residing in tissues continuously sample and process soluble extracellular antigens in their environment and respond to potential danger signals. In the presence of danger signals DCs are rapidly activated. DCs are mainly activated through the interaction of their pattern recognition receptors (e.g., Toll-like receptors) with a wide variety of conserved biological motifs known as pathogen-associated molecular patterns.[8]

Once DCs are activated, they migrate to secondary lymphoid organs to interact with T cells to achieve a more specific and longer-term anti-tumor responses. For induction of a CD8 T cell mediated response against cancer, it is required that the antigens be endocytosed by DCs and transported to MHC-I, a process known as cross-presentation.[9]

T cells activation is initiated by interactions of the T cell receptor (TCR) with an epitope-bound MHC-I molecule presented on the surface of antigen presenting cells (APCs), most importantly DCs. In addition to TCR binding, co-stimulation by receptors on the surface of activated DCs (CD80 or CD86) is also critical for activation of T cells. In the absence of co-stimulatory signals, T cell anergy could happen.[10] T cell activation is also controlled by the balance between co-stimulatory and co-inhibitory signals.[11,12] Following T cell activation, inhibitory checkpoint molecules, which exist to support self tolerance and protect individuals against autoimmunity diseases,[13,14] are expressed on surface of activated T cells. Program death 1 (PD-1) and cytotoxic T lymphocyte antigen 4 (CTLA-4) are two examples of co-inhibitory molecules that are expressed on surface of activated T

cells. Interaction of these molecules with their ligand leads to T cell suppression and deactivation, which normally aids in immune homeostasis.[15]

1.2. Cancer Vaccines

The goal of many cancer vaccines is to induce strong anti-tumor CD8 T cell responses. Cancer vaccines promote the immune system to recognize distinct antigenic epitopes expressed primarily by cancer cells and to target such cells for lysis by CD8 T cells.[16,17] These are known as tumor-associated antigens (TAAs), which vary widely among different cancer types. The identities of many TAAs have been elucidated.[18] In many clinically-examined cancer vaccines, TAAs are co-administered with adjuvant, which are immune activator molecules. Although these cancer vaccines have been shown to elicit a partial immune response, the clinical outcome is usually weak and insufficient to overcome the low immunogenicity of the tumor microenvironment.[17]

In recent years, different strategies have been developed to increase vaccine efficacy, such as vaccination with the whole tumor lysate,[19] combination of antigens with adjuvants,[20] and formulation in carriers such as nanoparticles (e.g., PLG, PLGA, gold nanoparticles),[21–23] liposomes,[24] and microparticles.[25] Protein nanoparticles have also attracted significant interest as cancer vaccine platforms for inducing antigen-specific immune responses against cancerous cells. Protein nanoparticles are self-assembled protein structures with physical properties and geometries similar to viruses but not from a viral source. These nanoparticles as vaccine platforms have the potential to improve vaccine efficacy by promoting antigen localization to dendritic cell-enriched draining lymph nodes, enhancing endocytosis of antigens by antigen presenting cells

(APCs),[26] and increasing antigen presentation to the adaptive immune cells such as T cells.[27]

1.2.1. Antigen-Based Cancer Vaccines

TAAs are typically antigenic proteins produced by tumor cells which can trigger an immune response in the host.[28] Immunotherapy using vaccines is based on the premise that TAAs can induce specific cytotoxic T cell responses to cancer cells, resulting in tumor destruction without harming normal cells.[29] However, clinically-examined cancer vaccines, consisting of whole tumor antigen (proteins) or epitopes (smaller peptides), are often insufficient to overcome the low immunogenicity of the tumor microenvironment.[28]

To address this limitation, different approaches have been examined to increase the antitumor responses for improved vaccine efficacy. One strategy is the combination of these antigen-based cancer vaccines with immune activator molecules known as adjuvants.[29,30] Common adjuvants used in clinical trials include aluminum salts, oil-in-water emulsions (MF59), and monophosphoryl lipid A (MPL) with aluminum salt.[31] Recently, ligands of Toll-like receptors in APCs such as CpG[32–34], poly-IC[35,36], and imidazoquinoline[37,38] have also attracted considerable interest as cancer vaccine adjuvants in preclinical and clinical trials.

Alternative approaches for increasing vaccine efficacy such as using multiple antigen peptide epitopes[39–41] and personalized peptide formulations have been developed and supported by clinical studies.[42,43] Vaccination with multiple-peptide epitopes from different sources can decrease the possibility of tumor escape and increase the anti-tumor responses relative to single epitope immunization.[44,45] Also, since tumor cells and TAAs are

heterogeneous among patients, a personalized selection of peptides against individually-expressed antigens could increase efficacy.[46]

Despite these improvements, however, clinical outcomes of cancer vaccines have still been limited by factors such as identification of optimal antigens, adjuvants, and importantly, delivery system. It is the goal of this dissertation research to investigate a protein nanoparticle delivery system to improve *in vivo* anti-tumor results, compared to antigen-based vaccines.

1.3. Protein Nanoparticles as Delivery Platforms

Generation of potent specific immune responses to cancer is dependent on antigen uptake by APCs, particularly DCs. Efficient uptake by DCs is subject to the important antigen properties of size, shape, and surface charge.[47,48] Additional key steps in generation of response include proper activation of DCs, trafficking of DCs to lymph nodes (LNs), sufficient communication of DCs with adaptive immune cells such as CD8 T cells, and activation of cytotoxic T cells for targeted tumor lysis [49] [Figure 1.2].

The use of nanoparticles in vaccines is supported by the premise that a higher cellular uptake and an elevated interaction of antigens with the immune cells can be achieved by using an optimally-designed delivery system.[50] Vaccine delivery materials that have been examined for cancer immunotherapy include liposomes, polymers, nanoparticles, and hydrogels.[23,51]

Nanoparticles based on proteins have symmetries and physical properties that are similar to viruses and can potentially increase the interaction of the vaccine components

with APCs. These properties, such as size, shape, and surface charge, can affect the cellular uptake and induce potentially more effective anti-tumor immune responses.

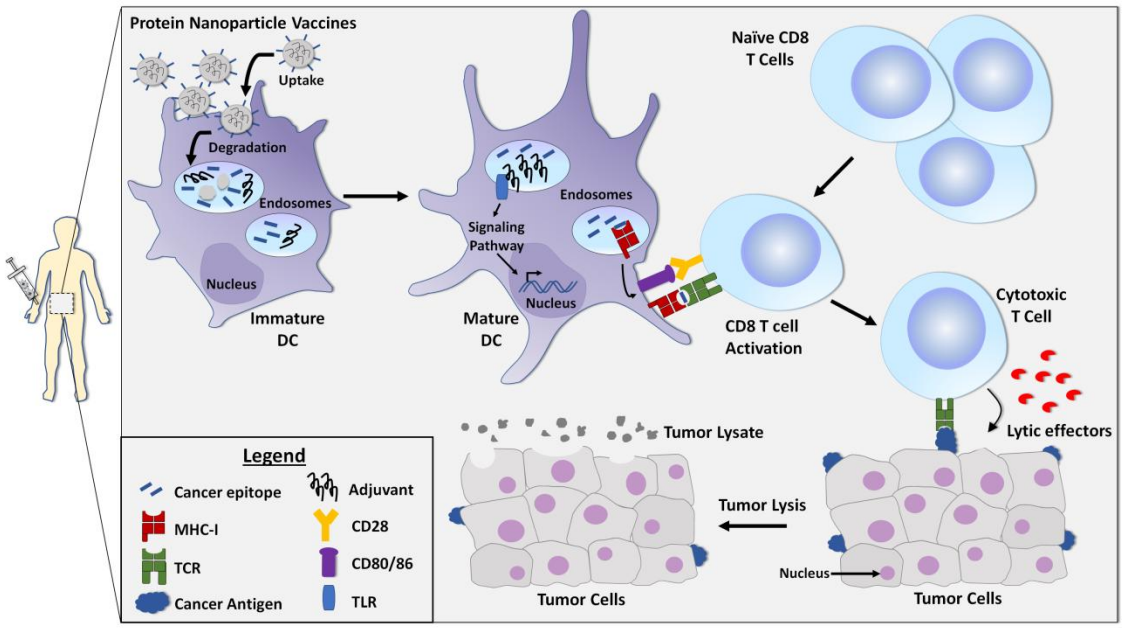

Figure 1.2. Common Mechanism of Tumor Cell Elimination. Protein nanoparticle (NP) cancer vaccines that are injected *in vivo* can accumulate in the LNs and spleen. Immature DCs residing in these tissues internalize and degrade the NPs and process the antigens and adjuvants for potential danger signals. If DCs are activated through an adjuvant-TLR interaction, they present the antigens to the T cells in the context of MHC-I molecules for specific and longer-term T cell responses (i.e., cross-presentation). Upon T cell activation and recognition of tumor-associated antigens on cancer cells, T cells secrete lytic effectors (such as perforin), leading to tumor lysis and elimination. Abbreviations in the figure include: MHC-I (major histocompatibility complex, class I), TCR (T-cell receptor), CD28 (cluster of differentiation 28, costimulatory molecule), CD80/86 (cluster of differentiation 80/86, costimulatory molecules), TLR (Toll-like receptor).

Studies have shown that there is an optimal nanoparticle size range for passive transport to the lymphatic system and APCs.[48] Particles between 20-45 nm are drained significantly by LNs, with a relatively high retention time measured up to 120 hrs post-injection.[52] Particles of this size range are internalized by almost 50% of LN-resident DCs

compared to 10% internalization by APCs of 100-nm particles.[52–54] However, particles below 10 nm are not internalized by DCs efficiently.[48] Furthermore, relatively high (~76%) lymphatic uptake was observed for 40-nm liposomes compared to larger liposomes (>150 nm), the latter of which remained almost completely at the site of injection.[55]

As discussed, conventional formulations of peptide- and protein-based cancer vaccines usually yield relatively weak immune responses, which can be attributed to insufficient uptake and interaction of antigens with APCs.[48] The size-uptake studies suggest that delivering the soluble protein or peptide antigens (which are typically much smaller than 5 nm) within nanoparticles of ~20-50 nm can lead to more efficient lymphatic drainage and a higher antigen uptake by DCs, resulting in stronger adaptive immunity to the antigens.

Particle shape can also affect the uptake of nanoparticles by immune cells.[48,56,57] Although investigations have shown that non-spherical particles such as rod-shaped particles have higher circulation times, they also demonstrated decreased cellular uptake compared to spherical NPs.[58] In fact, spherical NPs have the highest cell internalization rate compared to cubic, rod and disk-like shaped NPs.[59] Spherical polystyrene particles (diameters ~200 nm) conjugated to ovalbumin antigen (OVA) generated stronger *in vivo* Th1 and Th2 immune responses relative to rod-shaped particles.[60] In addition, enhanced LN transport and uptake by APCs was observed for the spherical virus-like particle, cowpea mosaic virus (CPMV), compared to the rod-shaped virus-like particles, potato virus X (PVX).[61]

Surface charge is another parameter that can affect the cellular uptake of NPs.[48,62] Neutral NPs demonstrated minimal cellular interaction and cellular uptake compared to

the charged NPs.[62] Positively charged nanoparticles have the greatest efficiency in cellular internalization, possibly due to their interactions with the negatively charged groups on the cell membrane.[62] However, evidence also demonstrated uptake of negatively charged nanoparticles despite their unfavorable electrostatic interaction with cell membranes. For example, cellular uptake of both negatively and positively charged micellar NPs has been observed through different endocytic pathways (*e.g.,* clathrin-mediated endocytosis, caveolae-mediated endocytosis, and macropinocytosis).[63]

With regard to tumor tissue, *in vivo* biodistribution of chitosan and micellar-based NPs suggested that NPs with relatively weak negative surface charges tend to accumulate in tumors more than NPs with positive or highly-negative zeta potential values;[63,64] this is somewhat consistent with a recent extensive survey demonstrating that NPs with neutral surface charges tend to result in higher delivery efficiencies to tumors, relative to NPs with more positive or negative charges.[65] An important, but sometimes overlooked, consideration is the adsorption of blood components on nanoparticle surfaces (called the protein corona), which can modify NP surface properties. Therefore, physicochemical properties of a NP immediately after synthesis can be different than the one that cells encounter *in vivo*.[66–68]

Highly-organized structures and symmetries of protein nanoparticles, their biodegradability, geometries, and their optimal size for delivery make them attractive vaccine platforms. Protein NPs are protein assemblies that have virus-like structures and geometries, but are not from viral sources. Examples of these particles that have been used in the field of cancer immunotherapy are heat-shock proteins (HSPs), E2, ferritin, and protein vault nanoparticles. A summary is presented in Table 1.1.

Table 1.1. Protein Nanoparticles that have been Explored as Delivery Platforms for Cancer Vaccines.

Protein NP	Antigen	Adjuvant	Target/ Cancer	*In vivo*/ *In vitro*	Clinical Study	Response Investigated	Ref
HSP	Her2/Neu	-	-	*Ex vivo*	-	T cell and antibody	[69]
HSP	MAGE-A1	-	Melanoma	*Ex vivo* and *In vivo*	-	T cell	[70]
HSP	gp100		Melanoma	*Ex vivo* and *In vivo*	-	T cell	[71]
HSP	-	-	Colorectal		Yes	T cell	[72]
HSP	-	-	Glioblastoma		Yes	T cell	[73]
HSP	-	-	Lung		Yes	NK cell	[74]
E2	SIINFEKL	CpG	-	*In vitro*	-	T cell	[27]
Ferritin	SIINFEKL	-	-	*In vitro* and *Ex vivo*	-	T cell and antibody	[75]
Ferritin	RFP	-	RFP-Melanoma	*Ex vivo* and *In vivo*	-	T cell	[76]
Vault protein	SIINFEKL	-	-	*In vitro* and *In vivo*	-	T cell and antibody	[77]
Vault protein	CCL21 ligand	-	Lung	*In vivo*	-	Immune cells	[78]

1.4. E2 Protein Nanoparticle

In our research, we have utilized the self-assembled protein nanoparticle E2. This nanoparticle is derived from the E2 subunit of the pyruvate dehydrogenase complex from *Bacillus stearothermophilus* [Figure 1.3]. The assembled NP is composed of 60 identical monomers that form a highly thermostable dodecahedral caged structure[79] with a diameter of 25 nm, which is within the favored size range for lymphatic transport and DC uptake.[52,53] This caged structure has an internal 12-nm cavity and twelve 5-nm openings leading to this hollow cavity [Figure 1.3]. The scaffold has three interfaces (internal hollow cavity, subunit-subunit interface, and the exterior surface), which can be molecularly modified for site-directed functionalization.

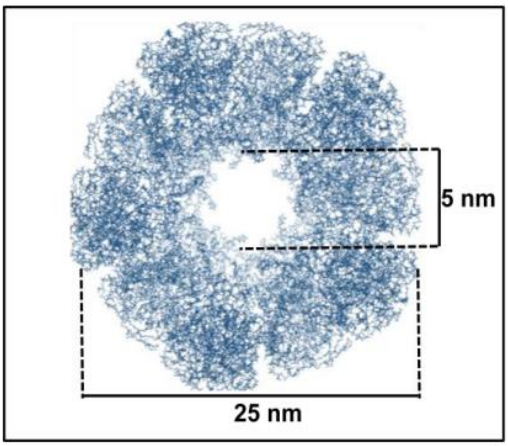

Figure 1.3. Graphic Representation of the E2 Core of Pyruvate Dehydrogenase Complex. E2 subunit is composed of 60 identical monomers, which self assemble into a highly thermo-stable dodecahedron caged structure which is 25 nm in diameter. This caged structure also has a 12-nm cavity inside and 12, 5-nm openings to the internal cavity. Structural image is from Protein Data Bank (PDB). PDB ID code:1B5S.

The E2 nanoparticle has been used in drug delivery and vaccines.[27,80–82] Our research group has demonstrated that with single amino acid (AA) mutations on E2 (e.g., D381C, E279C), we are able to chemically conjugate a variety of guest molecules to the nanoparticle.[27,81,83] Our laboratory also demonstrated that hydrophobic small drugs could be encapsulated within E2 nanoparticles designed with a hydrophobic interior surface.[81] Encapsulated therapeutic drug molecules within E2 were able to be delivered *in vitro* to cancer cells and induced cytotoxicity.[81] Others have explored the E2 nanoparticle as a vaccine vehicle for inducing a helper CD4 T cell and antibody-mediated responses against HIV antigens.[82]

Our lab has also demonstrated a significantly higher DC activation and antigen cross-presentation when an ovalbumin (OVA) antigen epitope (SIINFEKL) and DC-activating DNA (CpG) are both attached to the E2 nanoparticle.[27] Simultaneous delivery of model antigen OVA and CpG to DCs increased CD8 T cell activation *in vitro*,[27] with

concurrent delivery of antigen and CpG being essential to achieve the highest T cell activation.[27] With the use of a model antigen (OVA), our lab demonstrated the potential of the E2 nanoparticle to induce CD8 T cell mediated immune responses, which is needed to overcome the low immunogenicity of tumor cells. Higher antigen cross-presentation and CD8 T cell activation that were observed for OVA antigen provided the basis for optimizing E2 nanoparticle as a cancer vaccine platform for therapeutically relevant epitopes, which is the focus of this dissertation.

1.5. Immune Checkpoint Inhibitors in Cancer Immunotherapy

Co-inhibitory immune checkpoint molecules such as program death 1 (PD-1) and cytotoxic T lymphocyte antigen 4 (CTLA-4) are expressed on the surface of activated T cells. Interaction between these molecules and their ligands lead to T cell inactivation.[84–86] Therefore, blockade of these inhibitory molecules can release the T cell deactivation and improve the anti-tumor responses.[86–88]

Nivolumab and ipilimumab, two FDA-approved immune checkpoint inhibitor antibodies, demonstrated clinical efficacy in different advanced malignancies.[89,90] However, despite all promises, checkpoint inhibitors are still not responsive in a significant portion of patients or many cancer types. Only ~ 20% of patients benefit from a long-term survival of about 3 years post treatment.[91,92] Therefore, it is hypothesized that combination approaches with immune checkpoint inhibitors are needed to improve efficacy. Treatment with immune checkpoint inhibitors only release the general T cell suppression, without boosting the specific T cell responses towards tumors. On the other hand, cancer vaccines aim to prime the immune system to recognize specific TAA which results in an expansion of

specific CD8 T cell responses.[30,93] Therefore, combination of cancer vaccines [to increase T cell responses] with checkpoint inhibitors [to release the T cell deactivation] could improve the efficacy of immune checkpoint inhibitors.[94,95] In this dissertation, we investigated the possibility of using the E2-antigen vaccine in combination with immune checkpoint inhibitor antibody to improve the checkpoint inhibitor efficacy.

1.6. Project Goals and Specific Aims of Each Chapter

Our overall goal was to use the non-viral E2 protein nanoparticle as a platform to deliver TAA for induction of anti-tumor cell-mediated immune responses. Further, we wanted to examine if we can increase the efficacy of an FDA-approved treatment by combining this treatment with our developed nanoparticle vaccine formulation. The particular Specific Aims of each chapters are listed below.

Chapter 2: To examine the functionality of E2 nanoparticles for eliciting anti-tumor responses in a mouse model. We hypothesized that combination of CpG, a DC activator molecule, and gp100, a melanocytes-TAA epitope, within the E2 nanoparticle (CpG-gp-E2) could increase the anti-tumor responses. Our data demonstrated that in a very aggressive B16-F10 melanoma murine tumor model, immunization with CpG-gp-E2 delayed the onset of tumor growth.

Chapter 3: To examine the functionality of E2 nanoparticles for eliciting anti-tumor responses to human cancer antigens in a humanized mouse model. We hypothesized that combination of CpG and human cancer-testis antigen epitopes from NY-ESO-1 and MAGE-

A3 antigens within the E2 nanoparticle could increase cell-mediated immune responses in a humanized mouse model. Our data confirmed an increase in specific IFN-γ secretion and human tumor cell lysis after nanoparticle immunization. Furthermore, combined delivery of NY-ESO-1 and MAGE-A3 antigens in E2 nanoparticles yielded an additive effect that increased lytic activity towards cells bearing NY-ESO-1^{+} and MAGE-A3^{+}.

Chapter 4: To examine the functionality of E2 nanoparticles in combination with immune checkpoint inhibitor treatment. We hypothesized that combination of antigen-E2 nanoparticle vaccine with immune checkpoint inhibitor treatments could increase the animal survival. Our data demonstrated that combination of CpG-gp-E2 nanoparticle with anti-PD-1 treatment significantly increased the survival of tumor-bearing mice in a B16-F10 melanoma cancer model.

Chapter 5: To examine E2 nanoparticle uptake and biodistribution. Since DCs play a significant role in CD8 T cell activation, we wanted to alter E2 surface properties to enhance specificity and cell uptake by DCs. We hypothesized that surface display of CpG, a ligand of DC receptor, on E2 nanoparticles would increase cell uptake by DCs. Then we showed a higher cell uptake by DCs for E2 nanoparticles that were functionalized with CpG, compared to non-functionalized E2. However, this increase in uptake was not specific only to DCs.

Chapter 6: A brief summary followed by future directions on developing E2 platform.

1.7. References

1. Burnet M: Cancer; a biological approach. I. The processes of control. *Br Med J.* ***1,*** 779-786 (1957).
2. Dunn, G. P., Bruce, A. T., Ikeda, H., Old, L. J. & Schreiber, R. D. Cancer immunoediting: from immunosurveillance to tumor escape. *Nat. Immunol.* **3,** 991–998 (2002).
3. Berzofsky, J. A., Terabe, M., Oh, S. K., Belyakov, I. M., Ahlers, J. D., Janik, J. E. & Morris, J. C. Progress on new vaccine strategies for the immunotherapy and prevention of cancer. *J. Clin. Invest.* **113,** 1515–1525 (2004).
4. Yang, Y. Cancer immunotherapy : harnessing the immune system to battle cancer. *J Clin Invest.* **125,** 3335–3337 (2015).
5. Rosenberg, S. a, Yang, J. C. & Restifo, N. P. Cancer immunotherapy: moving beyond current vaccines. *Nat. Med.* **10,** 909–915 (2004).
6. Palucka, K., Ueno, H. & Banchereau, J. Recent Developments in Cancer Vaccines. *J. Immunol.* **186,** 1325–1331 (2011).
7. Speiser, D. E. & Romero, P. Molecularly defined vaccines for cancer immunotherapy, and protective T cell immunity. *Semin. Immunol.* **22,** 144–154 (2010).
8. Takeuchi, O. & Akira, S. Pattern Recognition Receptors and Inflammation. *Cell* **140,** 805–820 (2010).
9. Belz, G. T., Carbone, F. R. & Heath, W. R. Cross-presentation of antigens by dendritic cells. *Crit. Rev. Immunol.* **22,** 439–448 (2002).
10. Schwartz, R.H. T cell anergy. *Annu. Rev. Immunol*. **21,** 305–34 (2003).
11. Chambers, C. a & Allison, J. P. Co-stimulation in T cell responses. *Curr. Opin. Immunol.* **9,** 396–404 (1997).
12. Chen, L. Co-inhibitory molecules of the B7-CD28 family in the control of T-cell immunity. *Nat. Rev. Immunol.* **4,** 336–347 (2004).
13. Fife, B. T. & Bluestone, J. A. Control of peripheral T-cell tolerance and autoimmunity via the CTLA-4 and PD-1 pathways. *Immunol. Rev.* **224,** 166–182 (2008).
14. Francisco, L. M., Sage, P. T. & Sharpe, A. H. The PD-1 pathway in tolerance and autoimmunity. *Immunol. Rev.* **236,** 219–242 (2010).
15. Butte, M. J., Keir, M. E., Phamduy, T. B., Sharpe, A. H. & Freeman, G. J. Programmed Death-1 Ligand 1 Interacts Specifically with the B7-1 Costimulatory Molecule to Inhibit T Cell Responses. *Immunity* **27,** 111–122 (2007).
16. Even-desrumeaux, K., Baty, D. & Chames, P. State of the Art in Tumor Antigen and Biomarker Discovery. *Cancer* **3,** 2554–2596 (2011).
17. Rosenberg, S. A., Yang, J. C. & Restifo, N. P. Cancer immunotherapy : moving beyond current vaccines. *Nat. Med.* **10,** 909–915 (2004).
18. Vesely, M. D. & Schreiber, R. D. Cancer immunoediting: Antigens, mechanisms, and implications to cancer immunotherapy. *Ann. N. Y. Acad. Sci.* **1284,** 1–5 (2013).
19. Reyes, D., Salazar, L., Espinoza, E., Pereda, C., Castellón, E., Valdevenito, R., Huidobro, C., Inés Becker, M., Lladser, A., López, M N. & Salazar-Onfray, F. Tumour cell lysate-loaded dendritic cell vaccine induces biochemical and memory immune response in castration-resistant prostate cancer patients. *Br. J. Cancer* **109,** 1488–1497 (2013).
20. Reed, S. G., Orr, M. T. & Fox, C. B. Key roles of adjuvants in modern vaccines. *Nat. Med.* **19,** 1597–1608 (2013).

21. Zhao, L., Seth, A., Wibowo, N., Zhao, C., Mitter, N., Yu, C. & Middelberg, A. P. J. Nanoparticle vaccines. *Vaccine* **32,** 327–337 (2014).
22. Park, Y. M., Lee, S. J., Kim, Y. S., Lee, M. H., Cha, G. S., Jung, I. D., Kang, T. H. & Han, H. D. Nanoparticle-based vaccine delivery for cancer immunotherapy. *Immune Netw* **13,** 177–183 (2013).
23. Krishnamachari, Y., Geary, S. M., Lemke, C. D. & Salem, A. K. Nanoparticle delivery systems in cancer vaccines. *Pharm. Res.* **28,** 215–236 (2011).
24. Schwendener, R. A. Liposomes as vaccine delivery systems: a review of the recent advances. *Ther. Adv. Vaccine* **2,** 159–182 (2014).
25. Jiang, W., Gupta, R. K., Deshpande, M. C. & Schwendeman, S. P. Biodegradable poly(lactic-co-glycolic acid) microparticles for injectable delivery of vaccine antigens. *Adv. Drug Deliv. Rev.* **57,** 391–410 (2005).
26. Manolova, V., Flace, A., Bauer, M., Schwarz, K., Saudan, P. & Bachmann, M. F. Nanoparticles target distinct dendritic cell populations according to their size. *Eur. J. Immunol.* **38,** 1404–1413 (2008).
27. Molino, N. M., Anderson, A. K. L., Nelson, E. L. & Wang, S. W. Biomimetic protein nanoparticles facilitate enhanced dendritic cell activation and cross-presentation. *ACS Nano* **7,** 9743–9752 (2013).
28. Ie, E. V, Novellino, L., Castelli, C. & Parmiani, G. A listing of human tumor antigens recognized by T cells. *Cancer Immunol. Immunother.* **54,** 187–207 (2005).
29. Parmiani, G., Castelli, C., Dalerba, Piero., Mortarini, R., Rivoltini, L., Marincola, F. M., Anichini, A. Cancer Immunotherapy With Peptide-Based Vaccines : What Have We Achieved ? Where Are We Going ? *J. Natl. Cancer Inst.* **94,** 805–818 (1991).
30. Melero, I., Gaudernack, G., Gerritsen, W., Huber, C., Parmiani, G., Scholl, S., Thatcher, N., Wagstaff, J., Zielinski, C., Faulkner, I. & Mellstedt, HMelero, I., Gaudernack, G., Gerritsen, W., Huber, C., Parmiani, G., Scholl, S., Thatcher, N., Wagstaff, J, H. Therapeutic vaccines for cancer: an overview of clinical trials. *Nat Rev Clin Oncol* **11,** 509–524 (2014).
31. Temizoz, B., Kuroda, E. & Ishii, K. J. Vaccine adjuvants as potential cancer immunotherapeutics. *Int. Immunol.* **28,** 329–338 (2016).
32. Higgins, D., Marshall, J. D., Traquina, P., Nest, G. V. & Livingston, B. D. Immunostimulatory DNA as a vaccine adjuvant. *Expert Rev Vaccines* **6,** 747–759 (2007).
33. Shirota, H., Tross, D. & Klinman, D. M. CpG Oligonucleotides as Cancer Vaccine Adjuvants. *Vaccines* **3,** 390–407 (2015).
34. Scheiermann, J. & Klinman, D. M. Clinical evaluation of CpG oligonucleotides as adjuvants for vaccines targeting infectious diseases and cancer. *Vaccine* **32,** 6377–6389 (2014).
35. Ammi, R., Waele, J., Willemen, Y., Brussel, I. V., Schrijvers, . M., Lion, E. & Smits, E. L. J. Pharmacology & Therapeutics Poly (I:C) as cancer vaccine adjuvant : Knocking on the door of medical breakthroughs. *Pharmacol. Ther.* **146,** 120–131 (2015).
36. Wischke, C., Zimmermann, J., Wessinger, B., Schendler, A., Borchert, H. H., Peters, J. H., Nesselhut, T., Lorenzen, D. R. Poly(I:C) coated PLGA microparticles induce dendritic cell maturation. *Int. J. Pharm.* **365,** 61–68 (2009).
37. Johnston, D. & Zaidi, B. TLR7 imidazoquinoline ligand 3M-019 is a potent adjuvant for pure protein prototype vaccines. *Cancer Immunol. Immunother.* **56,** 1133–1141

(2007).
38. Smith, A. J., Li, Y., Bazin, H. G., Stjean, J. R., Larocque, D., Evans, J. T. & Baldridge, J. R. Evaluation of novel synthetic TLR7/8 agonists as vaccine adjuvants. *Vaccine* **34,** 4304–4312 (2016).
39. Yoshitake, Y., Fukuma, D., Yuno, A., Hirayama, M., Nakayama, H., Tanaka, T., Nagata, M., Takamune, Y., Kawahara, K., Nakagawa, Y., Yoshida, R., Hirosue, A., Ogi, H., Hiraki, A., Jono, H., Hamada, A., Yoshida, K. & Nishimura, Y. Phase II Clinical Trial of Multiple Peptide Vaccination for Advanced Head and Neck Cancer Patients Revealed Induction of Immune Responses and Improved OS. *Clin. Cancer Res.* **21,** 312–21 (2014).
40. Yoshitake, Y., Fukuma, D., Yuno, A., Hirayama, M., Nakayama, H., Tanaka, T., Nagata, M., Takamune, Y., Kawahara, K., Nakagawa, Y., Yoshida, R., Hirosue, A., Ogi, H., Hiraki, A., Jono, H., Hamada, A., Yoshida, K. & Nishimura, Y. A phase I study of combination vaccine treatment of five therapeutic epitope-peptides for metastatic colorectal cancer ; safety , immunological response , and clinical outcome. *J. Transl. Med.* **2014,** 1–11 (2014).
41. Aruga, A., Takeshita, N., Kotera, Y., Okuyama, R., Matsushita, N. & Ohta, T. Phase I clinical trial of multiple-peptide vaccination for patients with advanced biliary tract cancer. *J. Transl. Med.* **12,** 1–11 (2014).
42. Sasada, T., Yamada, A., Noguchi, M. & Itoh, K. Personalized Peptide Vaccine for Treatment of Advanced Cancer. *Curr Med Chem* **21,** 2332–2345 (2014).
43. Sakamoto, S., Yamada, T., Terazaki, Y., Yoshiyama, K., Sugawara, S., Takamori, S., Matsueda, S., Shichijo, S., Yamada, A., Noguchi, M., Itoh, K., Hattori, N., Kohno, N. & Sasada, T. Feasibility Study of Personalized Peptide Vaccination for Advanced Small Cell Lung Cancer. *Clin. Lung Cancer* **18,** 1–10 (2017).
44. Vaccine, P. D. C., Banchereau, J., Palucka, a K., Dhodapkar, M., Burkeholder, S., Taquet, N., Rolland, A., Taquet, S., Coquery, S., Wittkowski, K. M., Bhardwaj, N., Pineiro, L., Steinman, R. & Fay, J. Immune and Clinical Responses in Patients with Metastatic Melanoma to $CD34^{+}$. *Cancer Res.* **61,** 6451–6458 (2001).
45. Fay, J. W., Palucka, A. K., Johnston, D. A. & Burkeholder, S. Long-term outcomes in patients with metastatic melanoma vaccinated with melanoma peptide-pulsed $CD34^{+}$ progenitor-derived dendritic cells. *Cancer Immunol. Immunother.* **55,** 1209–1218 (2006).
46. Kimura, T., Egawa, S. & Uemura, H. Personalized peptide vaccines and their relation to other therapies in urological cancer. *Nat. Rev. Urol.* **14,** 501–510 (2017).
47. Fehres, C. M., Unger, W. W. J., Garcia-Vallejo, J. J. & van Kooyk, Y. Understanding the biology of antigen cross-presentation for the design of vaccines against cancer. *Front. Immunol.* **5,** 1–10 (2014).
48. Bachmann, M. F. & Jennings, G. T. Vaccine delivery: a matter of size, geometry, kinetics and molecular patterns. *Nat. Rev. Immunol.* **10,** 787–96 (2010).
49. Bousso, P. & Robey, E. Dynamics of CD8 + T cell priming by dendritic cells in intact lymph nodes. *Nat. Immunol.* **4,** 579–585 (2003).
50. Bertrand, N., Wu, J., Xu, X., Kamaly, N. & Farokhzad, O. C. Cancer nanotechnology: The impact of passive and active targeting in the era of modern cancer biology. *Adv. Drug Deliv. Rev.* **66,** 2–25 (2014).
51. Lichty, B. D., Breitbach, C. J., Stojdl, D. F. & Bell, J. C. Going viral with cancer immunotherapy. *Nat. Rev. Cancer* **14,** 559–567 (2014).

52. Reddy, S. T., Rehor, A., Schmoekel, H. G., Hubbell, J. A. & Swartz, M. A. In vivo targeting of dendritic cells in lymph nodes with poly (propylene sulfide) nanoparticles. *J. Control. Release* **112,** 26–34 (2006).
53. Reddy, S. T., van der Vlies, A. J., Simeoni, E., O'Neil, C. P., Swartz, M. A. & Hubbell, J. A. Exploiting lymphatic transport and complement activation in nanoparticle vaccines. *Nat. Biotechnol.* **14,** 103 (2007).
54. Swartz, M. A. The physiology of the lymphatic system. *Adv. Drug Deliv. Rev.* **50,** 3–20 (2001).
55. Oussoren, C., Zuidema, J., Crommelin, D. J. A. & Storm, G. Lymphatic uptake and biodistribution of liposomes after subcutaneous injection. II. Influence of liposomal size, lipid composition and lipid dose. *Biochim. Biophys. Acta - Biomembr.* **1328,** 261–272 (1997).
56. Niikura, K., Matsunaga, T., Suzuki, T., Kobayashi, S. & Yamaguchi, H. Gold Nanoparticles as a Vaccine Platform : Influence of Size and Shape on Immunological Responses in Vitro and in Vivo. *ACS Nano* **7,** 3926–3938 (2013).
57. Champion, J. A. & Mitragotri, S. Role of target geometry in phagocytosis. *Proc. Natl. Acad. Sci.* **103,** 4930–4934 (2006).
58. Conniot, J., Silva, J. M., Fernandes, J. G., Silva, L. C., Gaspar, R., Brocchini, S., Florindo, H. F. & Barata, T. S. Cancer immunotherapy: nanodelivery approaches for immune cell targeting and tracking. *Front. Chem.* **2,** 1–27 (2014).
59. Li, Y., Kröger, M. & Liu, W. K. Shape effect in cellular uptake of PEGylated nanoparticles: comparison between sphere, rod, cube and disk. *Nanoscale* **7,** 16631–16646 (2015).
60. Kumar, S., Anselmo, A. C., Banerjee, A., Zakrewsky, M. & Mitragotri, S. Shape and size-dependent immune response to antigen-carrying nanoparticles. *J. Control. Release* **220,** 141–148 (2015).
61. Shukla, S., Myers, J. T., Woods, S. E., Gong, X., Czapar, A. E., Commandeur, U., Huang, A., Levine, A. D. & Steinmetz, N. F. Plant viral nanoparticles-based HER2 vaccine : Immune response in fl uenced by differential transport, localization and cellular interactions of particulate carriers. *Biomaterials* **121,** 15–27 (2017).
62. Verma, A. & Stellacci, F. Effect of surface properties on nanoparticle-cell interactions. *Small* **6,** 12–21 (2010).
63. Xiao, K., Li, Y., Luo, J., Lee, J. S., Xiao, W., Gonik, A. M., Agarwal, R. G. & Lam, K. S. The effect of surface charge on in vivo biodistribution of PEG-oligocholic acid based micellar nanoparticles. *Biomaterials* **32,** 3435–3446 (2011).
64. He, C., Hu, Y., Yin, L., Tang, C. & Yin, C. Effects of particle size and surface charge on cellular uptake and biodistribution of polymeric nanoparticles. *Biomaterials* **31,** 3657–3666 (2010).
65. Wilhelm, S., Tavares, A. J., Dai, Q., Ohta, S., Audet, J., Dvorak, H. F., Chan, W. C. W. & Chatterley, A. Analysis of Nanoparticle Delivery to Tumours. *Nat. Rev. Mater.* **1,** 1–12 (2016).
66. Walkey, C. D., Olsen, J. B., Song, F., Liu, R., Guo, H., Olsen, D. W. H., Cohen, Yoram Emili, A. & Chan, W. C. W. Protein corona fingerprinting predicts the cellular interaction of gold and silver nanoparticles. *ACS Nano* **8,** 2439–2455 (2014).
67. Ritz, S., Schöttler, S., Kotman, N., Baier, G., Musyanovych, A., Kuharev, J., Landfester, K., Schild, H., Jahn, O., Tenzer, S. & Mailänder, V. Protein Corona of Nanoparticles:

Distinct Proteins Regulate the Cellular Uptake. *Biomacromolecules* **16,** 1311–1321 (2015).
68. Walkey, C. D., Olsen, J. B., Guo, H., Emili, A. & Chan, W. C. W. Nanoparticle size and surface chemistry determine serum protein adsorption and macrophage uptake. *J. Am. Chem. Soc.* **134,** 2139–2147 (2012).
69. Manjili MH, Henderson R, Wang X, Chen X, Li Y, Repasky E, Kazim L, Subjeck JR. Development of a recombinant HSP110-HER-2 / neu vaccine using the chaperoning properties of HSP110. *Cancer Res.* **62,** 1737–1742 (2002).
70. Ge W, Li Y, Zhang ZLS, Hu YSP, Yang XW, Si HS, Sui XZY. The antitumor immune responses induced by nanoemulsion-encapsulated MAGE1-HSP70/SEA complex protein vaccine following peroral administration route. *Cancer Immunol. Immunother.* **58,** 201–208 (2009).
71. Wang X, Chen X, Manjili MH, Repasky E, Henderson R, Subjeck JR. Targeted Immunotherapy Using Reconstituted Chaperone Complexes of Heat Shock Protein 110 and Melanoma-associated Antigen gp100 1. *Cancer Res.* **63,** 2553–2560 (2003).
72. Mazzaferro V, Coppa J, Carrabba MG, Rivoltini L, Schiavo M, Regalia E, et al. Vaccination with Autologous Tumor-derived Heat-Shock Protein Gp96 after Liver Resection for Metastatic Colorectal Cancer. *Clin Cancer Res.* **9,** 3235–3245 (2003).
73. Crane, C. A., Han, S. J., Ahn, B., Oehlke, J., Kivett, V., Fedoroff, A., Butowski, N., Chang, S. M., Clarke, J., Berger, M. S., McDermott, M. W., Prados, M. D. & Parsa, A. T. Individual patient-specific immunity against high-grade glioma after vaccination with autologous tumor derived peptides bound to the 96 KD chaperone protein. *Clin. Cancer Res.* **19,** 205–214 (2013).
74. Specht HM, Ahrens N, Blankenstein C, Duell T, Fietkau R, Gaipl US, et al. Heat shock protein 70 (Hsp70) peptide activated Natural Killer (NK) cells for the treatment of patients with non-small cell lung cancer (NSCLC) after radiochemotherapy (RCTx) – from preclinical studies to a clinical phase II trial. *Front. Immunol.* **6,** 1–9 (2015).
75. Han, J., Kang, Y. J., Shin, C., Ra, J., Shin, H., Hong, S. Y., Do, Y. & Kang, S. Ferritin protein cage nanoparticles as versatile antigen delivery nanoplatforms for dendritic cell (DC)-based vaccine development. *Nanomedicine Nanotechnology, Biol. Med.* **10,** 561–569 (2014).
76. Lee, B., Ko, H. K., Ryu, J. H., Ahn, K. Y., Lee, Y., Oh, S. J., Na, J. H., Kim, T. W., Byun, Y., Kwon, I. C., Kim, K. & Lee, J. Engineered Human Ferritin Nanoparticles for Direct Delivery of Tumor Antigens to Lymph Node and Cancer Immunotherapy. *Nat. Publ. Gr.* 1–12 (2016). doi:10.1038/srep35182
77. Kar, U. K., Jiang, J., Champion, C. I., Salehi, S., Srivastava, M., Sharma, S., Rabizadeh, S., Niazi, K., Kickhoefer, V., Rome, L. H. & Kelly, K. A. Vault Nanocapsules as Adjuvants Favor Cell-Mediated over Antibody-Mediated Immune Responses following Immunization of Mice. *PLoS One* **7,** 1–13 (2012).
78. Baratelli F, Huang M, Valerie A, Kar UK, Srivastava MK, Rome LH, et al. Novel CCL21-Vault Nanocapsule Intratumoral Delivery Inhibits Lung Cancer Growth. *PLoS One***. 6,** 4–11 (2011).
79. Dalmau, M., Lim, S., Chen, H. C., Ruiz, C. & Wang, S. W. Thermostability and molecular encapsulation within an engineered caged protein scaffold. *Biotechnol. Bioeng.* **101,** 654–664 (2008).
80. Ren, D., Kratz, F. & Wang, S. W. Engineered drug-protein nanoparticle complexes for

folate receptor targeting. *Biochem. Eng. J.* **89,** 33–41 (2014).
81. Ren, D., Kratz, F. & Wang, S. W. Protein nanocapsules containing doxorubicin as a pH-responsive delivery system. *Small* **7,** 1051–1060 (2011).
82. Jaworski, J. P., Krebs, S. J., Trovato, M., Kovarik, D. N., Brower, Z., Sutton, W. F., Waagmeester, G., Sartorius, R., D'Apice, L., Caivano, A., Doria-Rose, N. A., Malherbe, D., Montefiori, D. C., Barnett, S., de Berardinis, P. & Haigwood, N. L. Co-immunization with multimeric scaffolds and DNA rapidly induces potent autologous HIV-1 neutralizing antibodies and CD8 + T cells. *PLoS One* **7,** 1-15 (2012).
83. Molino, N. M., Bilotkach, K., Fraser, D. Ren, D. & Wang, S.-W. Complement activation and cell uptake responses toward polymer-functionalized protein nanocapsules. *Biomacromolecules* **13,** 974–81 (2012).
84. Sansom, D. M. CD28, CTLA-4 and their ligands: Who does what and to whom? *Immunology* **101,** 169–177 (2000).
85. Linsley, P. S., Greene, J. L., Brady, W., Bajorath, J., Ledbetter, J. A. & Peach, R. Human B7-1 (CD80) and B7-2 (CD86) bind with similar avidities but distinct kinetics to CD28 and CTLA-4 receptors. *Immunity* **1,** 793–801 (1994).
86. Blank, C., Gajewski, T. F. & Mackensen, A. Interaction of PD-L1 on tumor cells with PD-1 on tumor-specific T cells as a mechanism of immune evasion: Implications for tumor immunotherapy. *Cancer Immunol. Immunother.* **54,** 307–314 (2005).
87. Iwai, Y., Ishida, M., Tanaka, Y., Okazaki, T., Honjo, T. & Minato, N. Involvement of PD-L1 on tumor cells in the escape from host immune system and tumor immunotherapy by PD-L1 blockade. *Proc. Natl. Acad. Sci.* **99,** 12293–12297 (2002).
88. Buchbinder, E. I. & Desai, A. CTLA-4 and PD-1 pathways similarities, differences, and implications of their inhibition. *Am. J. Clin. Oncol. Cancer Clin. Trials* **39,** 98–106 (2016).
89. Lipson, E. J. & Drake, C. G. Ipilimumab: An anti-CTLA-4 antibody for metastatic melanoma. *Clin. Cancer Res.* **17,** 6958–6962 (2011).
90. Larkin, J., Chiarion-Sileni, V., Gonzalez, R., Grob, J. J., Cowey, C. L., Lao, C. D., Schadendorf, D., Dummer, R., Smylie, M., Rutkowski, P., Ferrucci, P. F., Hill, A., Wagstaff, J., Carlino, M. S., Haanen, J. B., Maio, M., Marquez-Rodas, I., McArthur, G. A., Ascierto, P. A., Long, G. V., Callahan, M. K., Postow, M. A., Grossmann, K., Sznol, M., Dreno, B., Bastholt, L., Yang, A., Rollin, L. M., Horak, C., Hodi, F. S. & Wolchok, J. D. Combined Nivolumab and Ipilimumab or Monotherapy in Untreated Melanoma. *N. Engl. J. Med.* **373,** 23–34 (2015).
91. Postow, M. A., Callahan, M. K. & Wolchok, J. D. Immune checkpoint blockade in cancer therapy. *J. Clin. Oncol.* **33,** 1974–1982 (2015).
92. Maio, M., Grob, J. J., Aamdal, S., Bondarenko, I., Robert, C., Thomas, L., Garbe, C., Chiarion-Sileni, V., Testori, A., Chen, T. T., Tschaika, M. & Wolchok, J. D. Five-year survival rates for treatment-naive patients with advanced melanoma who received ipilimumab plus dacarbazine in a phase III trial. *J. Clin. Oncol.* **33,** 1191–1196 (2015).
93. Van Der Burg, S. H., Arens, R., Ossendorp, F., Van Hall, T. & Melief, C. J. M. Vaccines for established cancer: Overcoming the challenges posed by immune evasion. *Nat. Rev. Cancer* **16,** 219–233 (2016).
94. Chowdhury, P. S., Chamoto, K. & Honjo, T. Combination therapy strategies for improving PD-1 blockade efficacy: a new era in cancer immunotherapy. *J. Intern. Med.* **283,** 110–120 (2018).

95. Ali, O. A., Lewin, S. A., Dranoff, G. & Mooney, D. J. Vaccines Combined with Immune Checkpoint Antibodies Promote Cytotoxic T-cell Activity and Tumor Eradication. *Cancer Immunol. Res.* **4,** 95–100 (2016).

CHAPTER 2

E2 PROTEIN NANOPARTICLE VACCINE ENHANCES ANTI-TUMOR RESPONSES

Portions of this chapter have been modified and published as: Molino, N. M., Neek, M., Tucker, J. A., Nelson, E. L. & Wang, S. Viral-mimicking protein nanoparticle vaccine for eliciting anti-tumor responses. *Biomaterials* **86,** 83–91 (2016).

2.1. Abstract

The immune system is a powerful resource for the eradication of cancer, but to overcome the low immunogenicity of tumor cells, a sufficiently strong $CD8^+$ T cell-mediated adaptive immune response is required. Nanoparticulate biomaterials represent a potentially effective delivery system for cancer vaccines, as they can be designed to mimic viruses, which are potent inducers of cellular immunity. We have been exploring the non-viral pyruvate dehydrogenase E2 protein nanoparticle as a biomimetic platform for cancer vaccine delivery. Our data shows that simultaneous delivery of a gp100 epitope and CpG using the E2 nanoparticle (CpG-gp-E2) enhance the anti-tumor responses. In the very aggressive B16 melanoma murine tumor model, prophylactic immunization with CpG-gp-E2 delayed the onset of tumor growth by approximately 5.5 days and increased animal survival time by approximately 40%, compared to PBS treated animals. These results show that by combining optimal particle size and simultaneous co-delivery of molecular vaccine components, anti-tumor immune responses can be significantly increased.

2.2. Introduction

Recent years have brought an improved understanding of the interaction between cancer and the immune system, increasing clinical interest in cancer immunotherapy.[1] Strategies for therapeutic vaccination against tumor-associated antigens (TAAs) have included administration of whole protein antigen,[2] immunodominant peptide epitopes,[3] and cell lysate.[4] In particular, immunization with peptide vaccines represent an attractive strategy, however, suboptimal responses are typically observed in clinical trials, prompting the need for enhanced approaches.[5] Low efficacy to TAAs using peptide (and protein)

vaccines may be related to physical size, peptide and protein are typically below the size range reported to be optimal for efficient vaccine delivery to antigen presenting cells (APCs).[6] Delivery of TAAs within synthetic nanostructured biomaterials (e.g., liposomes, metals, and polymers) have been explored as cancer vaccine delivery vehicles, to improve efficacy.[7–9] In this chapter we investigated whether the E2 protein nanoparticle could be used as a cancer antigen delivery platform to increase the peptide epitope vaccine efficacy.

Viruses are effective inducers of cytotoxic T lymphocyte (CTL) immunity.[10] They are generally comprised of one or a few protein monomers that self-assemble into symmetrical hollow structures packaged with genetic material.[11] Dendritic cells (DCs), the most potent APC for CTL responses, have evolved sensing mechanisms (*e.g.*, Toll-like receptors; TLRs) to recognize common features of pathogens for activation and orchestration of immune responses responses.[12] In particular, the size and repetitive structural features of immune-inducing viral components have been attributed to effective immunogenic response.[6] Therefore, mimicking the pathogenic features of viruses with biomaterials represents a potentially effective approach of delivering TAA epitopes.[11]

Since the first clinically approved virus-like particle (VLP)-based vaccine (Gardasil), many other protein-based assemblies have been clinically developed, primarily for infectious disease.[11,13] To induce CTL responses, nanoparticulate scaffolds based on proteins and viruses have been explored. For example, VLP-based vaccines toward influenza were previously shown to induce protective $CD8^+$ T cell responses following a single immunization.[14] In cancer therapy, tumor-derived heat shock proteins, hypothesized to bind TAAs, have been explored clinically for cancer vaccination, supporting interest in natural protein-derived nanoassemblies that carry antigens.[15,16]

Our research group has previously demonstrated that by externally displaying an ovalbumin model peptide epitope and internally packaging TLR9-activating CpG DNA for simultaneous delivery to DCs, significantly enhanced DC activation and cross-presentation ~~was observed~~.[17] In this chapter, we investigated whether simultaneous delivery of a melanoma-associated gp100 antigen with CpG increases anti-tumor responses toward a $gp100^+$ cancer cell line, and *in vivo* tumor model. *In vitro* work (section 2.4.2) was performed by Dr. Nickolas Molino, but it is included here to give context to the *in vivo* results. Our target epitope, gp100 melanocyte differentiation protein, is a TAA that is a tumor regression antigen and a clinically-pursued target antigen in humans.[18] The antigen is highly conserved between human and mouse, enabling testing of human vaccines in a murine model.[19]

2.3. Methods

2.3.1. Materials

All buffer reagents were purchased from Fisher Scientific, unless otherwise noted. The oligodeoxynucleotide TLR9 ligand CpG 1826 (5'-tccatgacgttcctgacgtt-3') (CpG) was synthesized with a phosphorothioated backbone and 5' benzaldehyde modification by TriLink Biotechnologies. The KVPRNQDWL peptide ($gp100_{25\text{-}33}$, herein abbreviated as "gp100") was from Genscript, and the custom gp100 peptide (for conjugation to E2) was synthesized with an N-terminal cysteine by Thinkpeptides (Proimmune).

2.3.2. Mice and Cell Lines

All animal studies were carried out in accordance with protocols approved by the Institute for Animal Care and Use Committee (IACUC) at the University of California, Irvine. Female C57BL/6 mice were purchased from Jackson Laboratories and used at 6-8 weeks of age. The B16-F10 murine melanoma cell line was purchased from ATCC and cultured in DMEM media supplemented with 10% FBS according to vendor instructions.

2.3.3. E2 Purification and Characterization

The D381C E2 protein nanoparticle (E2) was prepared and characterized as previously described.[17] D381C is an E2 mutant with a non-native cysteine introduced to the internal cavity of the nanoparticle at amino acid location 381 for site-specific conjugation. Briefly, proteins were expressed in *E. coli* and soluble cell lysates were applied to a HiPrep Q Sepharose anion exchange column (GE Healthcare) followed by a Superose 6 size exclusion column (GE Healthcare) for purification. The hydrodynamic diameter of the purified proteins was analyzed by dynamic light scattering (DLS; Zetasizer Nano ZS, Malvern). Electrospray ionization mass spectrometry and SDS-PAGE confirmed molecular weight and purity. Final protein preparations were stored in 50 mM potassium phosphate at pH 7.4 with 100 mM NaCl (phosphate buffer) at 4 °C for short-term and -80 °C for long-term storage. Residual LPS was removed using Triton X-114 and endotoxin levels were checked as previously described.[17] Briefly, Triton X-114 [Sigma] was added to the E2 nanoparticle at 1% [v/v] ratio, incubated at 4°C for 5 min, vortexed, and incubated at 37°C for 5 min. The mixture was then centrifuged at 18,000 × g and 37°C for 30 seconds. E2-containing aqueous portion was transferred to a new microcentrifuge tube. This process

was repeated ≥ 8 times. Triton was removed with detergent removal spin columns [Pierce]. LPS levels were below 5 EU/mg of E2 protein nanoparticle [LAL ToxinSensor gel clot assay, Genscript].

2.3.4. CpG and gp100 Conjugation

Aldehyde-terminated CpG were covalently packaged internally and cysteine-terminated peptide epitopes displayed externally on the E2 nanoparticle. The CpG 1826 DNA oligodeoxynucleotide (sequence: 5'-tccatgacgttcctgacgtt-3' ; phosphorothioted bases) was synthesized with a 5' aldehyde group. CpG is recognized by Toll-like receptor 9 (TLR9) leading to DC activation. N-beta-maleimidopropionic acid hydrazide (BMPH) linker was used to conjugate the aldehyde-CpG to the internal cysteines of the E2-D381C nanoparticle (CpG-E2), through the maleimide and hydrazide functional groups [Figure 2.1.A]. The MHC I-restricted gp100 epitope was synthesized with cysteine on the N-terminus, and this epitope was conjugated to the external lysines of the E2-D381C (gp-E2) through sulfo-SMCC linker [Figure 2.1.B].

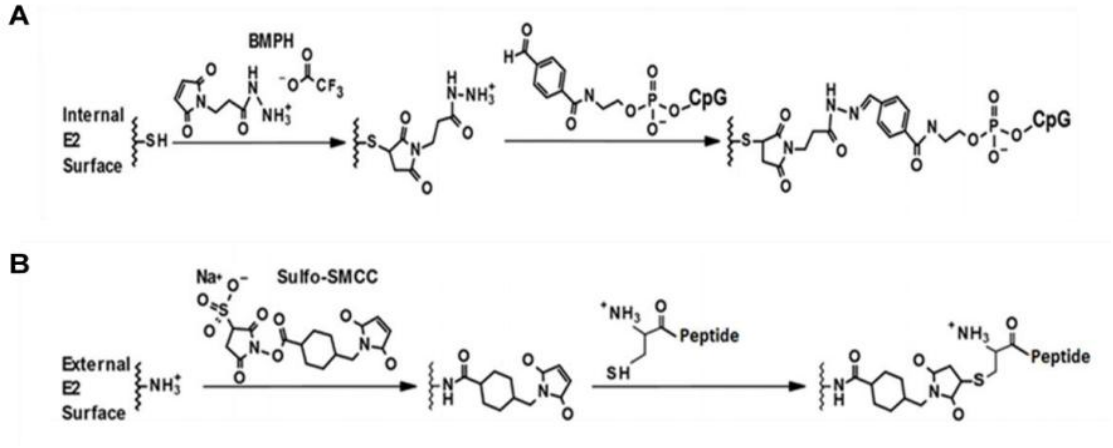

Figure 2.1. Schematic of Antigen and Adjuvant Conjugation to the E2 Nanoparticle. A) Conjugation of 5'-aldehyde-terminated CpG to E2's internal cysteines. **B)** Conjugation of peptide to E2's external lysines. Reprinted from Molino et al., *ACS Nano* **7,** 9743–9752, copyright (2013); with permission from American Chemical Society.[17]

2.3.5. IFN-γ ELISpot & CTL Lysis Assays

Mice (C57BL/6) were subcutaneously immunized with 100 ml formulations containing 5 μg each of gp100 peptide and CpG in PBS (either free or E2-bound; equivalent to 50 μg of E2-based nanoparticle formulations) bilaterally at the base of the tail. After 7 days, single cell suspensions were prepared from the spleen and draining lymph nodes (inguinal, axillary, brachial, and iliac). RBCs were depleted from splenocytes with ACK lysing buffer. For IFN-γ ELISpot, cells were resuspended in complete RPMI and added at 4 × 10^5 and 8 × 105 cells/well to ELISpot plates (PVDF membrane 96-well plates, Millipore), pre-coated overnight with anti-mouse IFN-γ antibody from the Mouse IFN-γ ELISpot ReadySet-Go kit (eBioscience). Cells were incubated for 24 h at 37^{oC} with either 10 μg/mL (~10 μM) gp100 peptide or irrelevant peptide (ovalbumin peptide, SIINFEKL). Negative control consisted of media only and positive control wells contained 1.5% PHA-M. Spots were developed according to the kit manufacturer's protocol and were detected and

analyzed by the Cellular Technology Ltd. ELISpot reader and Immunospot Analysis Pack software, respectively. To examine the specific lysis of cells bearing the gp100 TAA, splenocytes were cultured in complete RPMI at 5 × 10^6 cells/mL with 10 μg/mL free gp100 for 24 h, washed twice with PBS to remove unbound peptide, and cultured in fresh complete RPMI for an additional 48 h. B16-F10 melanoma cells ($gp100^+$) were plated at 5 × 10^3 cell/well in a round-bottom 96 well tissue culture-treated plate along with the gp100-stimulated splenocytes at a 50:1 effector-to-target ratio. Cytotoxicity was measured by lactate dehydrogenase release with the CytoTox 96 non-radioactive cytotoxicity assay (Promega) following the manufacturer's instructions. Data is reported as % lysis, calculated as:

$$\%\ Lysis = \frac{(coculture\ LDH\ release) - (background\ LDH\ release)}{(maximum\ B16\ LDH\ release) - (background\ B16\ LDH\ release)} \times 100$$

2.3.6. Immunization & Tumor Challenge

C57BL/6 mice (6-10 week) were immunized subcutaneously, bilaterally at the base of the tail with 50 μg CpG-gp-E2 in 100 ml PBS or with an equivalent volume of PBS on days -28 and -14. On day 0, 10^5 B16-F10 melanoma cells were subcutaneously inoculated in the right flank, and tumor size was measured daily with a caliper. Tumor volume was calculated as (0.5 × shortest diameter^2 × longest diameter) and mice were sacrificed when tumor volumes reached 500 mm^3

2.3.7. Statistical Analysis

Data are presented as mean ± standard deviation for particle characterization of at least 3 independent experiments, using Microsoft Excel. For in ex vivo studies, statistical

analyses were carried out using Microsoft Excel and GraphPad Prism. Data is reported as mean ± standard error of the mean (S.E.M.) of at least three independent experiments. Statistical significance was determined by performing a one-way analysis of variance (ANOVA) followed by a Dunnett's test, comparing formulations to the viral-mimicking CpG-gp-E2 protein. Statistical analysis of survival curve was determined by Log-rank [Mantel-Cox] of 2 independent experiments; n = 5 for each independent experiment [n_{total} =10], using GraphPad Prism. P-values less than 0.05 were considered significant.

2.4. Results and Discussion

2.4.1. Conjugation of CpG and gp100 Peptide to E2 Yields Intact Nanoparticles

CpG and gp100 peptides were successfully conjugated to the E2 nanoparticle, and results are consistent with those previously published for conjugation using an ovalbumin peptide epitope [Figure 2.2.A].[17] The gp-E2 nanoparticle displayed a broad band on SDS-PAGE in the molecular weight range of 30-35 kDa, consistent with multiple gp100 peptides (with linker) that add 1592 Da to the E2 monomer (which is 28105 Da). These comparable results between different peptides demonstrate the ability to apply the same conjugation strategy. CpG attached to the internal E2 cysteine at site 381 yielded two distinct bands, one at 28 kDa (28105 Da for unconjugated E2 monomer and 28288 for E2 monomer with linker) and one at 35 kDa (34879 Da for E2 with CpG), which were confirmed with mass spectrometry. Our previous study quantified this covalent encapsulation to be 22 ± 3 CpG per E2 nanoparticle (CpG-E2).[17] CpG molecules are released from E2 under acidic endolysosomal conditions, and the CpG-E2 particle facilitated enhanced DC uptake and activation, compared to free CpG.[17]

Simultaneous attachment of both CpG (internally) and gp100 peptide (externally) to the E2 monomers was also confirmed. Two distinct broad bands in the molecular weight ranges of 30-35 kDa (gp-E2) and 35-40 kDa (CpG-gp-E2) were observed [last lane of Figure 2.2.A]. DLS measurements of the gp-E2 and CpG-gp-E2 nanoparticles measured a hydrodynamic diameter of 31.6 ± 1.3 nm and 30.2 ± 0.7 nm, respectively, consistent with short peptides attached on the surface of an intact E2 core [Figure 2.2.B]. Furthermore, particle sizes show a lack of large aggregates and are within the reported optimal range for viral-based vaccines.[6] These nanoparticle diameters are also consistent with sizes observed for our conjugation with other peptides and guest molecules,[17,20–22] further demonstrating the versatility of the E2 platform for attachment of various molecules (*e.g.,* epitopes). TEM analysis further confirmed intact non-aggregated CpG-gp-E2 nanoparticles [Figure 2.2.C] that are within the reported optimal range for viral-based vaccines.[6]

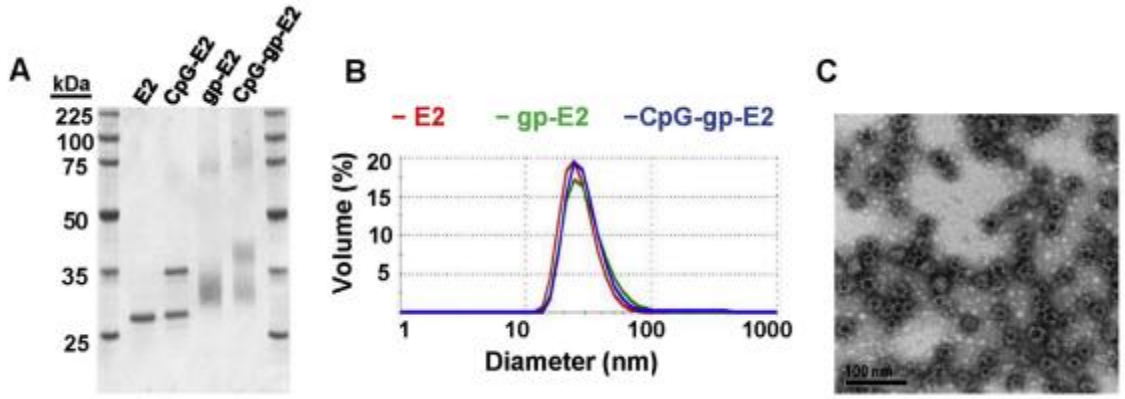

Figure 2.2. Physicochemical Characterization of Functionalized Nanoparticles. A) Functionalization of the E2 nanoparticle (E2; 28105 Da monomer) with the CKVPRNQDWL peptide (gp-E2) shows a broad band in the 30e35 kDa range, supporting heterogeneous conjugation of the gp100 peptide to the external E2 lysines. Simultaneous conjugation of gp100 peptide and CpG (lane CpG-gp-E2) shows two distinct broad signals in the 30e35 kDa and 35e40 kDa range. **B)** Representative DLS data reveal nanoparticle sizes within the optimal reported vaccine size range. **C)**Transmission electron micrograph of CpG-gp-E2 stained with 2% uranyl acetate confirms monodisperse, intact nanoparticles. Scale bar is 100 nm.

2.4.2. A single Immunization with CpG-gp-E2 Increases Specific IFN-γ Secretion and In Vitro Lytic Activity

Immunization with CpG-gp-E2 nanoparticles resulted in increased frequencies of gp100-specific IFN-γ secretion, as compared to other formulations of the peptide vaccine components [Figure 2.3]. We observed large increases in the number of gp100 peptide-specific spots in the IFN-γ ELISpot analysis of dLN cells [Figure 2.3.A] and splenocytes [Figure 2.3.B] from mice that received a single immunization with the CpG-gp-E2 viral-mimicking antigen formulation compared to all other formulations (either free or E2-bound peptide), with the exception of gp100 + CpG-E2 in the dLNs. In fact, frequencies of specific IFN-γ due to CpG-gpE2 were 30-fold and 120-fold higher in spleen and dLNs, respectively, relative to numbers from free gp100 with free CpG. Additionally, the lack of

spots observed for cells pulsed with the SIINFEKL ovalbumin epitope confirmed that the immune response was specific to gp100, rather than non-specific activation. We observed spot frequencies among total cells that were comparable to previously reported nanoparticle formulations delivering the gp100 epitope.[23] However, when compared to this previous report, we observed the expansion of gp100-specific IFN-γ following only a single injection, rather than multiple immunizations. Our IFN-g ELISpot frequencies are also similar to previous reports using nanoparticle formulations for melanoma-specific TAAs (other than gp100) and which also demonstrated strong anti-tumor activity.[24,25] Interestingly, the gp100 + CpG-E2 nanoparticle formulation exhibited similar spot frequencies to CpG-gp-E2 within the dLN, implying that packaging CpG within the E2 nanoparticle enhanced local APC activation and antigen presentation and $CD8^+$ T cell definitively test this possibility are not warranted at this stage of development of the E2 platform.

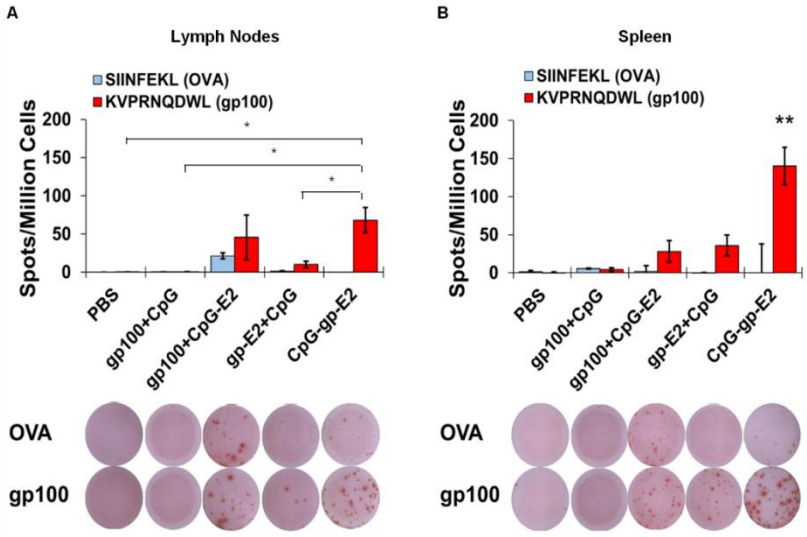

Figure 2.3. IFN-γ Responses after CpG-gp-E2 Immunization. Immunization with the CpG-gp-E2 nanoparticle increased the gp100-specific CTL response. Cells were isolated from the **A)** draining lymph nodes and **B)** spleens of mice immunized with different formulations (5 μg gp100 peptide and 5 μg CpG; unbound or bound to E2) and were cultured ex vivo in the presence of KVPRNQDWL peptide (gp100) or irrelevant SIINFEKL peptide (OVA) and analyzed for IFN-γ-secreting cells by ELISpot. The lower panels show representative wells from the immunization groups for negative control irrelevant peptide (OVA) and tumor antigen peptide (gp100). Data is presented as average ± S.E.M. spots per million cells from at least 3 independent experiments. Statistical significance was determined by ANOVA followed by Dunnett's test, comparing all means to CpG-gp-E2 (*$p < 0.05$; **$p < 0.01$).

Also, CpG-containing E2 nanoparticles co-delivering surface-bound gp100 epitopes induce increased TAA-specific lysis of syngeneic tumor cells [Figure 2.4]. Splenocytes from CpG-gp-E2-immunized animals had greater lytic activity toward the $gp100^{+}$ metastatic melanoma B16-F10 cell line, relative to other formulations. This CpG-gp-E2 formulation gave statistically significant increased lysis of the B16-F10 melanoma cells at a 50:1 effector-to-target ratio over the gp100 + CpG-E2 control formulation. Pairwise comparisons of the gp100 + CpG-E2 control formulation with all the remaining formulations did not exhibit any statistical differences. Lysis of the gp100-expressing B16

cell line is an important observation, as this particular melanoma is known to exhibit low immunogenicity.[26] Similarly, while immunogenicity may be low for the gp100 TAA, it is an effective immunotherapeutic target antigen in humans, and therefore an attractive vaccine target.

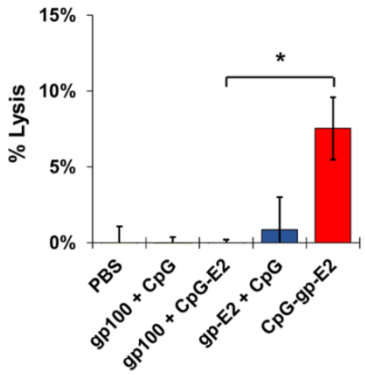

Figure 2.4. Lysis Activity of CpG-gp-E2. Splenocytes from mice receiving a single immunization of the CpG-gp-E2 (50 μg) nanoparticle formulation exhibited enhanced lytic ability toward B16-F10 melanoma cells (measured by release of lactate dehydrogenase). Data is presented as average ± S.E.M. % lysis of at least 3 independent experiments. Statistical significance was determined by ANOVA followed by Dunnett's test, comparing all means to CpGgp-E2 (*$p < 0.05$).

2.4.3. CpG-gp-E2 Immunization Delays Tumor Growth

Based on the in vitro and ex vivo data described above, we examined the therapeutic effects of the CpG-gp-E2 nanoparticle immunization in mice challenged with B16-F10 melanoma tumor cells. Our data shows that double immunization with the CpG-gp-E2 nanoparticle formulation significantly delayed tumor growth onset (15.0 ± 3.0 days), compared to PBS-treated mice (9.4 ± 0.9 days; $p < 0.05$). Tumor growth kinetic profiles further demonstrate slower tumor progression in mice immunized with CpG-gp-E2 [Figure 2.5.A], which exhibited a median survival time of 18 days [Figure 2.5.B], significantly greater than the PBS-treated median survival time of 13 days ($p < 0.002$). Our observed

B16-F10 tumor growth kinetics following prophylactic immunization with CpG-gp-E2 are similar to those reported for PLGA and heat shock protein nanoparticle immunotherapy studies delivering gp100 antigen/epitopes.[24,27] However, one major difference in our vaccination regimen, compared to these previous studies, is our schedule of a prime immunization followed by a single booster, in contrast to the two boosters administered in these previous reports.[24,27] In fact, a prime plus single booster of the heat shock protein did not demonstrate the same protective capacity compared to our single booster regimen of CpG-gp-E2, further demonstrating the advantage of our approach to deliver antigen and immune activator simultaneously in a viral-mimicking format.[27] Our anti-tumor observations support the concept that the increased antigen specific IFN-γ [Figure 2.1] and induction of antigen specific in vitro lytic activity [Figure 2.2] following CpG-gp-E2 immunization translates to a significant in vivo anti-tumor activity toward a self-antigen expressed by an aggressive, poorly immunogenic, syngeneic tumor.[26,28] gp100 is a self-antigen; therefore our results indicate that we have broken central tolerance to this antigen. These important results render the E2 nanoparticle an attractive viral-mimicking platform for further development and optimization to deliver tumor antigens and adjuvant.

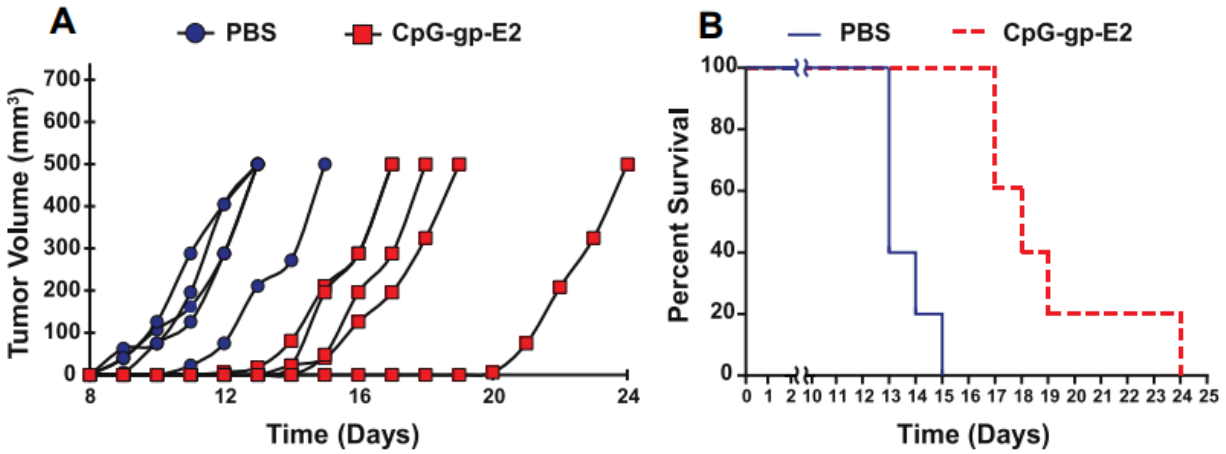

Figure 2.5. Anti-tumor Responses from CpG-gp-E2. Immunization with the CpG-gp-E2 nanoparticle delayed B16-F10 tumor growth and increased animal survival time. Data is representative of a duplicate set of independent experiments. Mice (n = 5 per group) were immunized subcutaneously with CpG-gp-E2 (50 μg per injection; equivalent to 5 μg each of gp100 peptide and CpG ODN) or PBS at Days 28 and 14, followed by tumor challenge at Day 0. A) Immunization with CpG-gp-E2 exhibited a delayed tumor growth, compared to PBS-treated control. Each line represents the tumor growth of a single animal. B) Immunization with CpG-gp-E2 significantly prolonged animal survival, compared to PBS-treated controls ($p < 0.002$, log-rank test).

2.5. Conclusion

We have simultaneously packaged CpG within the interior of the E2 nanoparticle and displayed multiple copies of an MHC I-restricted epitope from the melanocyte differentiation antigen gp100. Immunization of mice with CpG-gp-E2 nanoparticles followed by challenge with the B16- F10 melanoma tumor line resulted in a significant delay in tumor growth and prolonged life, compared to PBS-treated controls, confirming the anti-tumor capabilities generated with the viral-mimicking E2 formulation. We have achieved the ability to overcome tolerance to a self TAA, without the need for using live or attenuated pathogens. Altogether, this work supports the hypothesis that simultaneous

delivery of antigen and immune activator in a virus-mimicking format can enhance cell-mediated anti-tumor antigen responses and, importantly, demonstrates the therapeutic potential of the virus-mimicking E2 nanoparticle as a biomaterial-based vaccine platform for delivering tumor associated antigens.

2.6. Acknowledgments

DLS was carried out at the UCI Laser Spectroscopy Facility. We are grateful to Dr. Sergey Ryazantsev at the California NanoSystems Institute at UCLA for assistance with obtaining TEM images. We also thank Dr. Michael Phelan at UCI's Chao Family Comprehensive Cancer Center's Biostatistics Shared Resource Facility for consultation and advice with statistical analyses. The work in this chapter was supported by the National Institutes of Health (R21EB017995), the National Cancer Institute of the National Institutes of Health (P30CA062203), and the University of California Cancer Research Coordinating Committee (UCCRCC-101868).

2.7. References

1. Schreiber, R. D., Old, L. J. & Smyth, M. J. Cancer Immunoediting: Integrating Immunity's Roles in Cancer Suppression and Promotion. *Science* **331,** 1565–1570 (2011).
2. Hariharan K, Braslawsky G, Black A, Raychaudhuri S, Hanna N. The Induction of Cytotoxic T-Cells and Tumor-Regression by Soluble-Antigen Formulation. *Cancer Research* **55,** 3486-9 (1995).
3. Rosenberg, S. a, Yang, J. C. & Restifo, N. P. Cancer immunotherapy: moving beyond current vaccines. *Nat. Med.* **10,** 909–915 (2004).
4. Fadul CE, Fisher JL, Hampton TH, Lallana EC, Li Z, Gui J, et al. Immune response in patients with newly diagnosed glioblastoma multiforme treated with intranodal autologous tumor lysate-dendritic cell vaccination after radiation chemotherapy. *J immunother.* **34,** 382-9 (2011).
5. Yamada A, Sasada T, Noguchi M, Itoh K. Next-generation peptide vaccines for advanced cancer. *Cancer science* **104,** 15-21 (2013).
6. Bachmann, M. F. & Jennings, G. T. Vaccine delivery: a matter of size, geometry, kinetics and molecular patterns. *Nat. Rev. Immunol.* **10,** 787–96 (2010).
7. Tan A, De La Pena H, Seifalian AM. The application of exosomes as a nanoscale cancer vaccine. *International journal of nanomedicine* **5,** 889-900 (2010).
8. Lichty, B. D., Breitbach, C. J., Stojdl, D. F. & Bell, J. C. Going viral with cancer immunotherapy. *Nat. Rev. Cancer* **14,** 559–567 (2014).
9. Krishnamachari, Y., Geary, S. M., Lemke, C. D. & Salem, A. K. Nanoparticle delivery systems in cancer vaccines. *Pharm. Res.* **28,** 215–236 (2011).
10. Kolumam GA, Thomas S, Thompson LJ, Sprent J, Murali-Krishna K. Type I interferons act directly on CD8 T cells to allow clonal expansion and memory formation in response to viral infection. *The Journal of experimental medicine* **202,** 637-50 (2005).
11. Plummer EM, Manchester M. Viral nanoparticles and virus-like particles: platforms for contemporary vaccine design. *Reviews-Nanomedicine and Nanobiotechnology* **3,** 174-96 (2011).
12. Steinhagen, F., Kinjo, T., Bode, C. & Klinman, D. M. TLR-based immune adjuvants. *Vaccine* **29,** 3341–3355 (2011).
13. Kushnir, N., Streatfield, S. J. & Yusibov, V. Virus-like particles as a highly efficient vaccine platform : Diversity of targets and production systems and advances in clinical development. *Vaccine* **31,** 58–83 (2012).
14. Patterson, D. P., Rynda-Apple, A., Harmsen, A. L., Harmsen, A. G. & Douglas, T. Biomimetic antigenic nanoparticles elicit controlled protective immune response to influenza. *ACS Nano* **7,** 3036–3044 (2013).
15. Ciocca DR, Cayado-Gutierrez N, Maccioni M, Cuello-Carrion FD. Heat Shock Proteins (HSPs) Based Anti-Cancer Vaccines. *Curr Mol Med*. **12,** 1183-97 (2012).
16. Calderwood SK, Stevenson MA, Murshid A. Heat shock proteins, autoimmunity, and cancer treatment. *Autoimmune diseases* **48,** 60-69 (2012)
17. Molino, N. M., Anderson, A. K. L., Nelson, E. L. & Wang, S. W. Biomimetic protein nanoparticles facilitate enhanced dendritic cell activation and cross-presentation. *ACS Nano* **7,** 9743–9752 (2013).

18. Kirkin AF, Dzhandzhugazyan K, Zeuthen J. The immunogenic properties of melanoma-associated antigens recognized by cytotoxic T lymphocytes. *Exp Clin immunogenet.* **15,** 19-32 (1998).
19. Overwijk, W. W., Theoret, M. R., Finkelstein, S. E., Surman, D. R., de Jong, L. a, Vyth-Dreese, F. a, Dellemijn, T. a, Antony, P. a, Spiess, P. J., Palmer, D. C., Heimann, D. M., Klebanoff, C. a, Yu, Z., Hwang, L. N., Feigenbaum, L., Kruisbeek, A. M., Rosenberg, S. a & Restifo, N. P. Tumor regression and autoimmunity after reversal of a functionally tolerant state of self-reactive CD8+ T cells. *J. Exp. Med.* **198,** 569–580 (2003).
20. Dalmau, M., Lim, S., Chen, H. C., Ruiz, C. & Wang, S. W. Thermostability and molecular encapsulation within an engineered caged protein scaffold. *Biotechnol. Bioeng.* **101,** 654–664 (2008).
21. Ren, D., Kratz, F. & Wang, S. W. Protein nanocapsules containing doxorubicin as a pH-responsive delivery system. *Small* **7,** 1051–1060 (2011).
22. Ren, D., Kratz, F. & Wang, S. W. Engineered drug-protein nanoparticle complexes for folate receptor targeting. *Biochem. Eng. J.* **89,** 33–41 (2014).
23. Wang XY, Chen X, Manjili MH, Repasky E, Henderson R, Subjeck JR. Targeted immunotherapy using reconstituted chaperone complexes of heat shock protein 110 and melanoma-associated antigen gp100. Cancer Res. **63,** 2553-60 (2003).
24. Zhang, Z., Tongchusak, S., Mizukami, Y., Kang, Y. J., Ioji, T., Touma, M., Reinhold, B., Keskin, D. B., Reinherz, E. L. & Sasada, T. Induction of anti-tumor cytotoxic T cell responses through PLGA-nanoparticle mediated antigen delivery. *Biomaterials* **32,** 3666–3678 (2011).
25. Xu, Z., Ramishetti, S., Tseng, Y. C., Guo, S., Wang, Y. & Huang, L. Multifunctional nanoparticles co-delivering Trp2 peptide and CpG adjuvant induce potent cytotoxic T-lymphocyte response against melanoma and its lung metastasis. *J. Control. Release* **172,** 259–265 (2013).
26. Finkelstein SE, Heimann DM, Klebanoff CA, Antony PA, Gattinoni L, Hinrichs CS, et al. Bedside to bench and back again: how animal models are guiding the development of new immunotherapies for cancer. *Journal of leukocyte biology*. **76,** 333-7 (2004).
27. Wang, X. Y., Chen, X., Manjili, M. H., Repasky, E., Henderson, R. & Subjeck, J. R. Targeted immunotherapy using reconstituted chaperone complexes of heat shock protein 110 and melanoma-associated antigen gp100. *Cancer Res.* **63,** 2553–2560 (2003).
28. Zoller M. IFN-treatment of B16-F1 versus B16-F10: relative impact on non-adaptive and T-cell-mediated immune defense in metastatic spread. *Clin. Expel metastasis*. **6,** 411-29 (1988).

CHAPTER 3

CO-DELIVERY OF HUMAN CANCER-TESTIS ANTIGENS WITH ADJUVANT IN E2 NANOPARTICLE INDUCES HIGHER CELL-MEDIATED IMMUNE RESPONSES

Portions of this chapter have been slightly modified and published as: Neek, M., Tucker, J. A., Kim, T. Il, Molino, N. M., Nelson, E. L. & Wang, S. W. Co-delivery of human cancer-testis antigens with adjuvant in protein nanoparticles induces higher cell-mediated immune responses. *Biomaterials* **156,** 194–203 (2018).

3.1. Abstract

Nanoparticles have attracted considerable interest as cancer vaccine delivery vehicles for inducing sufficient $CD8^+$ T cell-mediated immune responses to overcome the low immunogenicity of the tumor microenvironment. Our studies described here are the first to examine the effects of clinically-tested human cancer-testis (CT) peptide epitopes within a synthetic nanoparticle. Specifically, we focused on two significant clinical CT targets, the HLA-A2 restricted epitopes of NY-ESO-1 and MAGE-A3, using a viral-mimetic packaging strategy. Our data shows that simultaneous delivery of a NY-ESO-1 epitope (SLLMWITQV) and CpG using the E2 subunit assembly of pyruvate dehydrogenase (E2 nanoparticle), resulted in a 25-fold increase in specific IFN-γ secretion in HLA-A2 transgenic mice. This translated to a 15-fold increase in lytic activity toward target cancer cells expressing the antigen. Immunization with a MAGE-A3 epitope (FLWGPRALV) delivered with CpG in E2 nanoparticles yielded an increase in specific IFN-γ secretion and cell lysis by 6-fold and 9-fold, respectively. Furthermore, combined delivery of NY-ESO-1 and MAGE-A3 antigens in E2 nanoparticles yielded an additive effect that increased lytic activity towards cells bearing NY-ESO-1^+ and MAGE-$A3^+$. Our investigations demonstrate that formulation of CT antigens within a nanoparticle can significantly enhance antigen-specific cell-mediated responses, and the combination of the two antigens in a vaccine can preserve the increased individual responses that are observed for each antigen alone.

3.2. Introduction

Boosting a patient's immune system by immunotherapy represents a promising approach in cancer treatment,[1] and cancer vaccines in particular enable the recognition of tumor-associated antigens for targeted destruction.[2] Although these cancer vaccines have

been shown to elicit CD8 T cell immune responses, the typical response levels generated are usually clinically insufficient to overcome the low immunogenicity and immunosuppressive microenvironment of tumors.[3,4] For example, in a review of clinical studies, an overall objective response rate (50% tumor size reduction) of only 2.6% was observed with peptide vaccines derived from gp100, MART-1, TRP-2, cancer testis NY-ESO-1, MAGE-A12, or HER2 antigens (alone or in combination with adjuvant); these results suggest the need for development of more effective strategies and therapies.[1]

In Chapter 2, we demonstrated higher cell-mediated immune responses to gp100 antigen, while delivered with E2. While the gp100 antigen is an overexpressed differentiation antigen, we evaluated the CT class of antigen in this chapter. Vaccination with overexpressed antigens (*e.g.,* gp100) is usually in association with high risk of autoimmunity and inflammatory reactions. However, expression of cancer-testis is restricted in testes, an immune-privileged site; therefore the risk of autoimmune reactions in normal tissues is decreased.

Given the wide range of tumors that express CT antigens, their relatively high expression level in cancer, their restricted expression, and their potential for vaccine improvement, the CT class of antigens is an important and significant clinical target. In this study, we examined the feasibility of using the E2 nanoparticle to induce cell-mediated immune responses against NY-ESO-1 and MAGE-A3 in a mouse model that is transgenic for the human major histocompatibility complex, HLA-A2. While our prior work examined gp100, an antigen that has mouse and human analogues, this current study focuses on antigens that are specifically expressed in humans.

The application of nanotechnology has shown an exceptional promise towards improvement of cancer diagnosis and treatment in recent years.[5–7] Antigen uptake by dendritic cells (DCs) depends on the antigen properties such as geometry,[8] surface charge,[9] and importantly, size.[10,11] Some nanoparticles have the advantage of being in the optimal size for DCs uptake and passive transport to the lymphatic system, with prior research demonstrating that particles between approximately 20-45 nm are taken up more effectively by the DCs residing in the lymph-nodes.[8,12,13] Therefore, delivery of vaccine components with these nanoparticles may facilitate and increase DC interaction, resulting in a more effective immune responses.[14-15]

One nanoparticle with favorable DC uptake properties is the E2 nanoparticle.[15–17] E2 is a 25-nm non-viral protein nanoparticle derived from the pyruvate dehydrogenase complex of *Bacillus stearothermophilus*.[18] It is composed of 60 identical monomer subunits that self assemble into a highly thermostable dodecahedral caged structure with a hollow 12-nm cavity,[19] and it can be engineered at the internal, external, and inter-subunit interfaces to change the properties and functionality of the nanoparticle.[20–23] Our research group has also previously demonstrated that the viral-mimetic, simultaneous delivery of adjuvant (internally packaged) and MHC-I restricted antigens (bound on the surface) via E2 nanoparticles resulted in an increase in DCs activation and antigen cross-presentation.[16] This was associated with a significant increase in antigen-specific IFN-γ secretion, tumor cell lysis, delayed B16-F10 tumor growth, and increased survival time in C57BL/6 mice.[15]

The target epitopes in this current study are HLA-A2 restricted peptide sequences from New York esophageal squamous cell carcinoma-1 (NY-ESO-1) and melanoma antigen family A, 3 (MAGE-A3).[24] While other tumor-associated antigens (TAAs) are often

expressed at low levels in healthy tissue, expression of CTs is restricted only to cancer cells and the immune-privileged cells in the testis. Furthermore, CT antigens exist in a high proportion of different human tumors such as melanoma, bladder, lung, prostate, and breast cancers.[25,26] In particular, NY-ESO-1 is expressed in 82% of neuroblastomas and 46% melanomas[27] while MAGE-A3 is also expressed in 76% of melanoma cancers.[28] A phase II clinical trial of NY-ESO-1/ISCOMATRIX vaccine which was recently completed in June 2017 (NCT00518206, ClinicalTrials.gov) resulted in 4% partial response (based on a standard of 30% reduction in tumor size), 48% stable disease, and 48% progressive disease; this result highlights the generation of response to NY-ESO-1, but also the need and potential for development of alternative strategies that will yield more effective therapies.

In this study, we examined the feasibility of using the E2 nanoparticle to induce cell-mediated immune responses against NY-ESO-1 and MAGE-A3 in a mouse model that is transgenic for the human major histocompatibility complex, HLA-A2. We also investigated the extent of cell-mediated and cytolytic responses by simultaneous delivery of NY-ESO-1- and MAGE-A3-containing nanoparticles. Tumor escape after single-epitope vaccination is common since cancers often lose expression of the targeted antigen to evade the immune system.[29] Immunization with combined antigens can possibly decrease the risk of tumor escape resulting from antigen loss.[30,31] Furthermore, increasing the number of different antigen targets in a vaccine can induce a broader range of T cell responses simultaneously, which could be effective in a higher number of patients. Because there is a lack of immune-competent murine tumor models expressing these CT antigens to examine *in vivo* anti-tumor efficacy in the most physiologically relevant way possible, we examined lytic ability

ex vivo using human cancer cell lines expressing both NY-ESO-1 and MAGE-A3. To our knowledge, our study is the first to test the efficacy of cell-mediated responses to clinically-relevant CT peptide epitopes formulated as a nanoparticle, and it examines these human epitopes in nanoparticles both individually and in combination.

3.3. Methods

3.3.1. Materials

Reagents were purchased from Fisher Scientific unless otherwise noted. Complete RPMI used in this study for splenocytes was compromised of RPMI 1640 (Mediatech) with 10% heat-inactivated FBS (Hyclone), 1mM sodium pyruvate (Hyclone), 100 μg/ml of streptomycin (Hyclone), 0.1 mM nonessential amino acids (Lonza), 2 mM L-glutamine (Lonza), and 100 units/ml penicillin. Cancer cell lines used in this study were cultured in DMEM media (Sigma) supplemented with 10% heat-inactivated FBS (Hyclone).

3.3.2. Peptides and CpG

CpG 1826, a bacterial DNA ligand for TLR9, was purchased from Invivogen, and 5' benzaldehyde-modified CpG 1826 with a phosphorothioated backbone was synthesized by Trilink. The NY-ESO-1 and MAGE-A3 peptide epitopes were synthesized by Genscript or Genemed Synthesis (Table 3.1). Peptides were synthesized both with and without an N-terminal cysteine; the functionalized thiol on the cysteine-modified peptides was used for conjugation to E2, whereas peptides with no cysteine were used as controls. In this study, the abbreviation (e.g., NYESO, MAGE) refers to the peptide, while the names NY-ESO-1 and MAGE-A3 refer to the whole protein.

Table 3.1. List of Peptide Epitopes Sequences and their Respective Abreviations in this Study. Conventional single-letter abbreviations for amino acids (aa) are used in the peptide epitope sequence.

Abbreviation	Antigen source	Sequence	Serotype	Reference
NYESO	NY-ESO-1	C-SLLMWITQV (aa 157-165)	HLA-A2	32, 33
NYESO(p2)	NY-ESO-1	C-ILTIRLTAA (aa 132-140)	HLA-A2	34
MAGE	MAGE-A3	C-FLWGPRALV (aa 271-279)	HLA-A2	35, 36
MAGE(p2)	MAGE-A3	C-KVAELVHFL (aa 112-120)	HLA-A2	36

3.*3.3. E2 Purification and Characterization*

In this study, we used the D381C mutant of the E2 nanoparticle, which has an aspartic acid-to-cysteine mutation at position 381 in the internal hollow cavity of the nanoparticle. The cysteine of D381C can be used for site-directed conjugation, and this nanoparticle is abbreviated as "E2" in this study. Expression, purification, and characterization of E2 (D381C mutant) were performed as previously described.[19] In summary, *E. coli* strain BL21 (DE3) containing E2 gene was cultured in Luria-Bertani medium containing 100 μg/ml ampicillin. Expression was induced by adding 1mM of IPTG when the culture reached the optical density of 0.7-0.9 measured at 600 nm. Cells were harvested and stored at -80^{o}C. Cells were lysed using French pressure cell (Thermo Scientific), and insoluble fraction was removed by centrifugation. Soluble part was heated at 70^{o}C for 20 min. Denatured native *E.coli* protein aggregates were removed by centrifugation. The recovered supernatant was loaded to a HiPrep Q Sepharose anion exchange column followed by a Superose 6 size exclusion column.[19] Purity and the

molecular weight of purified E2 were confirmed with SDS-PAGE and electrospray ionization mass spectrometry. Dynamic light scattering and transmission electron microscopy were used to check the size, assembly, and monodispersity of the particles. As previously described, lipopolysaccharide was removed using Triton X-114 (Sigma) extraction, and endotoxin levels were evaluated using an LAL ToxinSensor kit (Genscript).[16]

3.3.4. CpG and peptides Conjugation

CpG 1826 modified with a 5'-benzaldehyde was attached to the TCEP-reduced cysteines in the internal cavity of E2 nanoparticles using a N-β-maleimidopropionic acid hydrazide (BMPH) linker. The average number of CpG molecules conjugated to the internal cavity of E2 nanoparticle was estimated with intensity analysis in ImageJ software, using standardized concentrations.[16] Peptides with N-terminal cysteines were conjugated to the native lysines on the surface of the E2 nanoparticle by mixing the nanoparticle with a sulfo-SMCC linker in the presence of a 10-fold excess of TCEP-reduced peptides (relative to E2 monomer), and incubating overnight at 4°C. HPLC was used for peptide quantification as previously described,[15] and details are in Supplementary Materials.

3.3.5. Zeta Potential Measurements

To measure zeta potential, the diffusion barrier method with monomodal analysis were used because they are compatible with the amounts and physiological ionic strengths of our samples. Malvern capillary cells were filled with buffer (50 mM potassium phosphate at pH 7.4 with 100 mM NaCl), and 150 µl of nanoparticles (at 1.3 mg/ml) were gently

injected to the bottom of the buffer-filled capillary cells. Zeta potential was measured with a Malvern Zetasizer (Nano ZS).

3.3.6. Mice

Transgenic mice expressing the human HLA-A2 gene were obtained from Jackson Laboratory. All animal studies were carried out in accordance with protocols approved by the Institute for Animal Care and Use Committee (IACUC) at the University of California, Irvine. Briefly, 6-8 week old female HLA-A2 transgenic C57BL/6 mice were immunized subcutaneously at the base of the tail at Day 0. A priming immunization was followed by a booster after 14 days. Injections were 120 μl and contained specific amounts of peptide, E2, and CpG, based on the formulations tested. Seven days after the last immunization, mice were sacrificed and spleens were isolated.

3.3.7. IFN-γ ELISpot

For IFN-γ ELISpot, we used the Ready-Set-Go kit (eBioscience). Single-cell suspensions in RPMI were prepared from the spleens isolated from immunized mice, and added at 5 x 10^5 and 10^6 cells/well to PVDF ELISpot plates that were pre-coated with an anti-mouse IFN-γ antibody. Cells were incubated with either 10 μg/ml of the relevant peptide or an irrelevant peptide (SIINFEKL) for 24 hrs at 37°C. Unstimulated cells in RPMI were plated and served as a negative control. Positive control wells contained 2% PHA-M (Gibco). IFN-γ spots were developed following the manufacturer's protocol. Plates were scanned and quantified using an ELISpot reader (Cellular Technology) and immunospot analysis software (Immunospot Analysis Pack).

3.3.8. Cell Lines

A375, a human malignant melanoma cell line, and MCF-7, a human breast cancer cell line, were purchased from ATCC. A375 was cultured in DMEM supplemented with 10% FBS, and MCF-7 was cultured in DMEM supplemented with 10% FBS and 0.01 mg/ml human recombinant insulin. Cells were incubated at 37°C, under 5% CO2, and were passaged 2-3 times a week.

3.3.9. Cell Lysis Assay

Single cell suspensions prepared from splenocytes isolated from immunized mice were cultured in RPMI at 5 x 10^6 cell/ml and incubated overnight at 37°C. On day 1, 10 µg/ml of target peptide was added to the cells, incubated for 24 hrs at 37°C, and washed twice with PBS to remove the unbound peptide. On day 3, culture was supplemented with 0.4 ng/ml of IL-2. Peptide stimulated splenocytes were collected on day 5 to perform the cytotoxicity assay. LDH release was measured with a calorimetric assay, CytoTox 96 (Promega), to examine the specific lysis of target cancer cell lines expressing NY-ESO-1 and MAGE-A3 antigens. A375 expresses both NY-ESO-1[37] and MAGE-A3,[38] while MCF7 has low expression of these antigens.[39,40] Splenocytes were counted with a hemocytometer, co-cultured with the target cancer cell lines at effector-to-target ratios of 100:1, 50:1, and 25:1, and evaluated for LDH release following the manufacturer's protocol. Data is reported as "% Lysis", calculated as

$$\%Lysis = \frac{Experimental\ LDH\ Release}{Maximum\ LDH\ Release} \times 100$$

where "experimental LDH release" is the LDH release from cancer cells co-cultured with splenocytes minus the sum of LDH release from the cancer cells and the splenocytes

cultured separately. "Maximum LDH release" is from lysed cancer cells using the kit's lysis buffer minus background LDH release from cancer cells.

3.3.10. Statistical Analysis

Statistical analysis was carried out using GraphPad Prism. Data are presented as mean ± standard error of the mean (S.E.M.) of at least three independent experiments (n ≥ 3). Statistical analysis was determined by a two-way ANOVA over all groups followed by a Tukey's multiple comparison test, unless otherwise noted. P-values less than 0.05 were considered significant.

3.4. Results and Discussion

3.4.1. Conjugation of CpG and Cancer-Testis Peptides to E2 Nanoparticle Yielded Intact Nanoparticles

Both CpG and peptides were successfully conjugated to the E2 nanoparticle, and the results are consistent with those previously described for conjugation of other epitopes to the E2 nanoparticle.[15,16] The CpG-conjugated nanoparticle (CpG-E2) displayed two distinct bands on SDS-PAGE [Figure 3.1.A]; the lower band at ~28 kDa is the unconjugated E2 monomer and coincides with 28118 ± 13 Da measured by mass spectrometry, and the band at ~ 35 kDa is indicative of the conjugation of one CpG molecule attached to one 28-kDa E2 monomer. By analyzing band intensities, we estimate a conjugation ratio of 21 ± 4 CpG molecules encapsulated per (60-mer) protein particle, similar to prior studies.[16]

Simultaneous conjugation of CpG to the internal cavity and peptides to external surface of E2 resulted in two distinct broad bands [Figure 3.1.A]. The broad band between

30-35 kDa shows the heterogeneous conjugation of peptides (from Table 3.1) to the surface of E2 monomers (peptide-E2), and the band between 35-40 kDa confirms the simultaneous conjugation of peptide and CpG to the E2 monomers (CpG-peptide-E2). We quantified the number of peptides conjugated to the E2 nanoparticle with HPLC,[15] and found that on average, 140 ± 16 NYESO or 155 ± 21 MAGE peptides were attached on each protein nanoparticle. Conjugation of CpG and peptides to the E2 nanoparticle resulted in a 1:1 mass ratio. This 1:1 mass ratio of CpG and peptide has been used in other studies to induce CD8 T cell responses.[41,42]

Dynamic light scattering revealed a hydrodynamic diameter of 28.4 ± 0.7, 30 ± 1.3, and 30 ± 0.9 nm for E2, CpG-NYESO-E2, and CpG-MAGE-E2 respectively [Figure 3.1.B]. DLS data confirmed that particles remained unaggregated and within the optimal reported size for lymphatic drainage (20-45 nm),[5,12,13] even after conjugation. This data verifies that attachment of short peptides (9 amino acid length) on the surface of the nanoparticle does not result in a dramatic change in size. TEM analysis further confirmed intact, non-aggregated CpG-NYESO-E2 [Figure 3.1.C] and CpG-MAGE-E2 [Figure 3.1.D] nanoparticles. The zeta potential of E2, CpG-NYESO-E2, and CpG-MAGE-E2 nanoparticles were -11.7 ± 1 mV, -12.8 ± 1 mV, and -11.1 ± 1.8 mV, respectively. This data confirmed that conjugation of NYESO or MAGE peptides on the surface and CpG inside of the nanoparticles did not change the overall surface charge compared to the E2 nanoparticle itself.

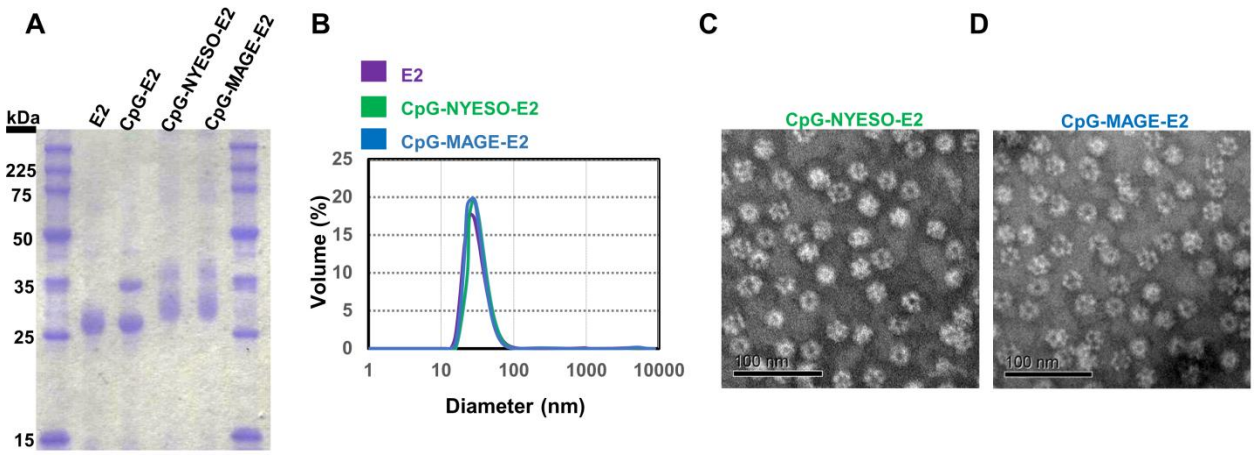

Figure 3.1. Characterization of Functionalized Nanoparticles. A) SDS-PAGE shows successful conjugation of CpG and peptides (NYESO, MAGE) to E2 nanoparticles. **B)** DLS reveals nanoparticle sizes of about 30 nm, before and after conjugation. **C)** TEM of CpG-NYESO-E2 nanoparticles**. D)** TEM of CpG-MAGE-E2 nanoparticles. Scale bars are 100 nm.

3.4.2. Immunization with CpG-NYESO-E2 Nanoparticles Yielded Increased Antigen-Specific IFN-γ Secretion

Different vaccine formulations of NY-ESO-1 antigen peptide, CpG, and E2 were investigated, and ELISpot results are presented in Figure 3.2. Immunization with the CpG-NYESO-E2 nanoparticle significantly increased the NY-ESO-1 epitope-specific IFN-γ secretion by 25-fold, compared to immunization with unbound CpG and NYESO, at an equivalent amount of antigen and adjuvant [Figure 3.2.B,C]. In contrast, we observed negligible IFN-γ response by the cells pulsed with an irrelevant SIINFEKL peptide [Figure 3.2.C], confirming that the immune response generated from immunization was specific to the NYESO epitope. Splenocytes isolated from mice immunized with bare E2 nanoparticle also lacked significant amounts of NYESO-specific IFN-γ secretion [Figure 3.2.C], confirming that higher IFN-γ secretion resulting from CpG-NYESO-E2 immunization was not a result of non-specific immune responses to the E2 delivery platform itself.

We previously observed higher DC activation towards CpG-E2 nanoparticles and also an elevated antigen cross-presentation when a model ovalbumin peptide and CpG were delivered within an E2 nanoparticle, relative to unbound antigen and adjuvant.[16] This suggests that our observed increase in IFN-γ secretion in this experiment results from higher DCs activation and more efficient cross-presentation of the NYESO epitope. This mechanism of improving T cell immunity by increasing DC uptake and activation is supported by Dhodapkar et al., who observed higher antigen-specific CD8 T cell responses with a vaccine that targeted NY-ESO-1 antigen to the DEC205 receptor of DCs.[43] The high IFN-γ secretion specific to NYESO epitope (aa 157-165) in our study is consistent with ELISpot/IFN-γ data previously reported on a NY-ESO-1 protein with ISCOMATRIX vaccine[44] and a lentiviral vector encoding the NY-ESO-1 gene. [45] However, in contrast to those cases, our vaccine formulation contains only a single NY-ESO-1 epitope rather than the whole protein or gene, respectively, used in the previous studies.

We also observed higher peptide-specific IFN-γ secretion for the group receiving immunizations of 50 μg CpG-NYESO-E2 compared to 25 μg CpG-NYESO-E2 [Figure 3.2.C; groups e, f]. This demonstrates dose dependency of the generated cell-mediated immune response to the NYESO epitope. However, immunization with 100 μg of CpG-NYESO-E2 did not increase the IFN-γ secretion compared to 50 μg, and in fact showed a significant decreased across the cohort of mice [see Appendix B]. This could be due to increased levels of suppressive T cells,[46] T cell exhaustion,[47] or high antigen doses leading to increase tolerance.[48]

In addition to the NY-ESO-1 peptide epitope examined in Figure 3.2 (NYESO), we examined another epitope [NYESO(p2)] (see Table 3.1) that had been previously reported

to yield a relatively low lysis of NYESO(p2)-pulsed T2 cells when incubated with T lymphocytes isolated from a patient.[34] In contrast to that study, however, our data showed that immunization with nanoparticle formulations of the NYESO(p2) epitope [CpG-NYESO(p2)-E2] did not result in any significant increase in the IFN-γ secretion [see Appendix B]. To our knowledge, there have been no additional reports regarding the immunogenicity of this peptide. One explanation for this apparent discrepancy is that the *in vitro* data using T2 cells[34] may not recapitulate what happens *in vivo*.

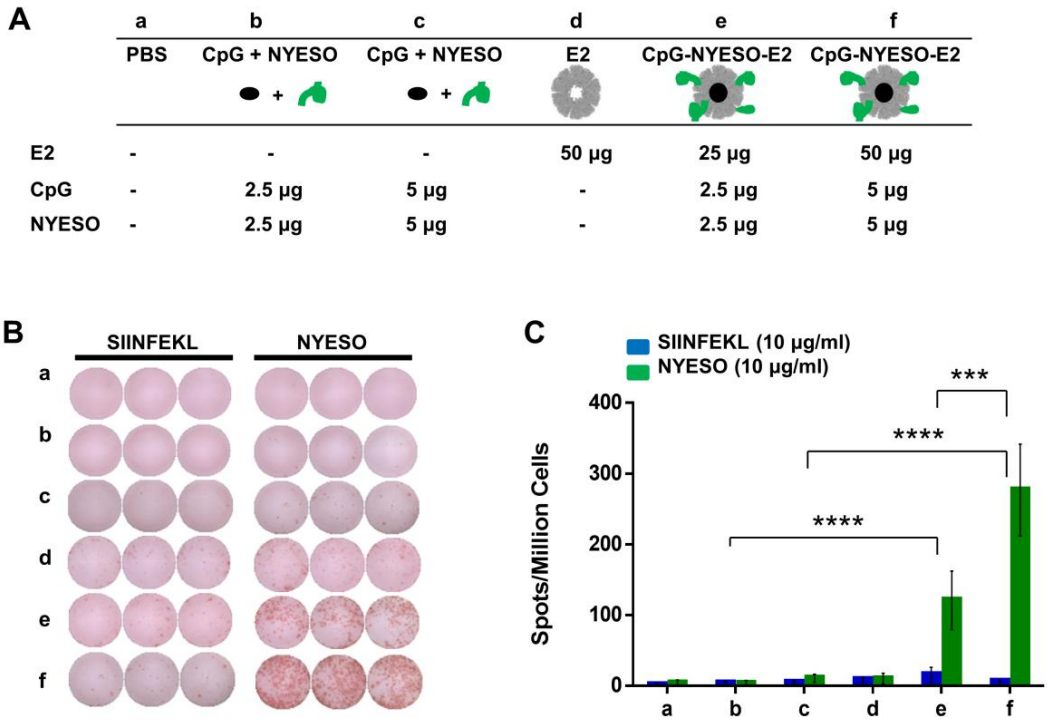

Figure 3.2. ELISpot Analysis of Splenocytes from Immunization with NY-ESO-1 Formulations. A) Vaccine components per dose of different formulation groups (a-f). **B)** Representative ELISpot data from splenocytes of immunized group, pulsed with irrelevant peptide (SIINFEKL) or relevant epitope peptide (NYESO). **C)** Summary of averaged ELISpot data, which evaluated antigen-specific IFN-γ secretion. HLA-A2 mice were immunized with different formulations (a-f), and splenocytes were pulsed *ex vivo* in the presence of relevant peptide (NYESO) or irrelevant peptide (SIINFEKL) and analyzed for specific IFN-γ secretion. Higher NY-ESO-1 epitope-specific IFN-γ secretion was observed for the group that received CpG-NYESO-E2. Data is presented as average ± S.E.M. of at least 3 independent experiments ($n \geq 3$). Statistical significance was determined by two-way ANOVA followed by a Tukey's test (***$p < 0.001$; ****$p < 0.0001$).

3.4.3. Higher Lysis Activity toward NY-ESO-1⁺ Cancer Cells Was Observed for the Group Immunized with CpG-NYESO-E2 Nanoparticles

Lytic capacity of splenocytes isolated from immunized mice was tested on a human melanoma cell line expressing NY-ESO-1 (A375)[49-50] and on a human breast cancer cell line negative for NY-ESO-1 expression (MCF-7)[39], both positive for HLA-A2.[39,49] The increase in

antigen-specific IFN-γ levels that resulted from CpG-NYESO-E2 immunization [Figure 3.2] translated to a 15-fold increase in the lysis activity towards A375, compared to unbound peptide and CpG [Figure 3.3.A]. In contrast, no significant lysis was observed for the control cell line, MCF-7 [Figure 3.3.A]. This data supports the specificity of the immune response for the NY-ESO-1 antigen.

Our data also confirms that lysis activity towards the target cancer cell line is dose-dependent; higher activity toward A375 can be achieved by increasing the effector-to-target ratio [Figure 3.3.B], where the effector cells are the splenocytes isolated from the immunized mice and the target cells are the cancer cells. Our lysis data is comparable to those previously reported on the NY-ESO-1/ISCOMATRIX vaccine by which the entire NY-ESO-1 protein was delivered.[44] Remarkably, we observed almost the same extent of lysis by delivering a single NY-ESO-1 epitope rather than the whole antigen with multiple epitopes, albeit toward a different target cell line.

Splenocytes isolated from mice immunized with bare E2 nanoparticles or antigen/CpG alone did not increase specific lysis [Figure 3.3.A]; this confirms that the significant increase in lysis resulting from the CpG-NYESO-E2 immunization is due to the complete nanoparticle-adjuvant-antigen delivery system, and not the effect of E2 or antigen alone. The E2 data is consistent with prior work by Perham and De Berardinis, which previously demonstrated a negligible lysis activity towards the mouse lymphoma RMA-S cell line by splenocytes isolated from mice immunized with bare E2 nanoparticle.[51] Taken together, our data show that conjugation of the NY-ESO-1 epitope and CpG adjuvant to the nanoparticle is an effective delivery strategy for increasing INF-γ response, and it results in a functional lysis activity that is specific towards the NY-ESO-1 epitope.

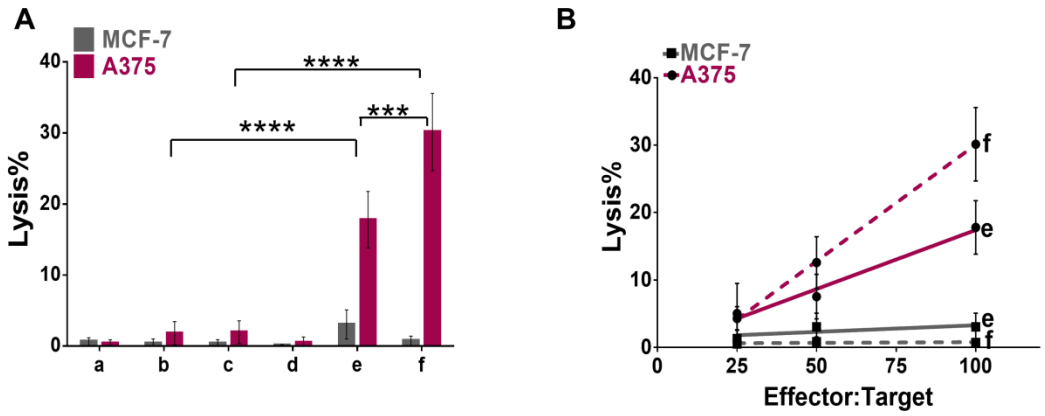

Figure 3.3. Results of Cell Lysis Assays Using Splenocytes from Immunization with NY-ESO-1 Formulations. A) Summary of average lysis data at 100:1 effector:target ratio. HLA-A2 mice were immunized with different formulations (a-f; see Fig. 2A for schematic), and splenocytes were pulsed *ex vivo* in the presence of NYESO peptide. Splenocytes isolated from mice immunized with CpG-NYESO-E2 nanoparticles enhanced lysis activity toward A375, relative to free peptide and CpG. **B)** Cell lysis results at different effector:target ratios. HLA-A2 mice were immunized with different formulations (a-f; see Fig. 2A for schematic), and splenocytes were pulsed *ex vivo* in the presence of NYESO peptide. Lytic ability toward A375 cell line resulted from CpG-NYESO-E2 nanoparticles immunization is dose dependent. Data is presented as average ± S.E.M. of at least 3 independent experiments. Statistical significance was determined by two-way ANOVA followed by a Tukey's test (***p < 0.001; ****p <0.0001).

3.4.4. Immunization with CpG-MAGE-E2 Nanoparticles Yielded Increased Antigen-Specific IFN-γ Secretion

Peptide epitopes for MAGE-A3 were conjugated to the E2 nanoparticle bearing the CpG adjuvant. The ELISpot results of immunizations with the different MAGE formulations are presented in Figure 3.4. Vaccination with the CpG-MAGE-E2 nanoparticles increased the number of IFN-γ spots, relative to free CpG and MAGE [Figure 3.4.B]. We also observed a dose-dependent response, where significantly higher IFN-γ secretion was obtained for mice immunized with the 50 μg dose compared to the 25 μg dose. Similar to CpG-NYESO-E2, CpG-MAGE-E2 increased the specific IFN-γ secretion compared to the free peptide/CpG

control group, but to a lower extent (6-fold for MAGE vs. 25-fold for NYESO for the comparable 50 μg dose). High IFN-γ secretion to this MAGE epitope was also observed in a previous study, where HLA-A2 mice were immunized with DNA vaccine encoding 5 epitopes, followed by a booster of peptide epitopes in solution plus a hepatitis B virus core containing a T helper peptide.[35] In contrast to the previous study, however, we obtained high IFN-γ secretion to the MAGE epitope without a need for T helper peptides or a separate DNA vaccine.

The second MAGE-A3 epitope in this study, MAGE(p2), did not affect the splenocyte IFN-γ secretion when conjugated to E2-CpG compared to unbound peptide and CpG [see Appendix B]. The apparent discrepancy between our study compared to a previous investigation[52] could be due to the different experimental conditions. In the prior study, much higher doses of peptide MAGE(p2) was used (200 μg total) compared to ours (10 μg total), together with an additional 120 μg of hepatitis B virus core containing a T helper epitope.[52]

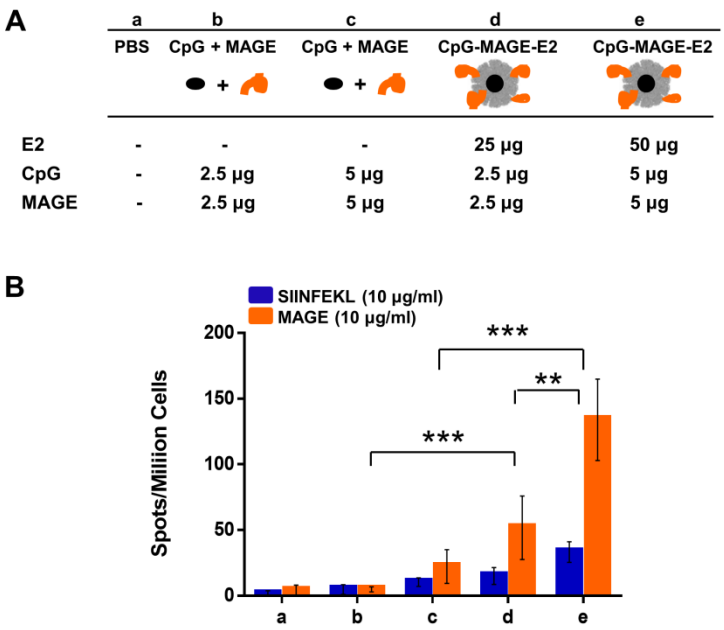

Figure 3.4. ELISpot Analysis of Splenocytes from Immunization with MAGE-A3 Formulations. **A)** Vaccine components per dose of different formulation groups (a-e). **B)** Summary of averaged ELISpot data, which evaluated antigen-specific IFN-γ secretion. HLA-A2 mice were immunized with different formulations (a-e), and splenocytes were pulsed *ex vivo* in the presence of relevant peptide (MAGE) or irrelevant peptide (SIINFEKL) and analyzed for specific IFN-γ secretion. Higher MAGE-A3 epitope-specific IFN-γ secretion was observed for the group that received CpG-MAGE-E2. Data is presented as average ± S.E.M. of 3 independent experiments (n ≥ 3). Statistical significance was determined by two-way ANOVA followed by a Tukey's test (**p < 0.01; ***p < 0.001).

3.4.5. Higher Lysis Activity toward MAGE-A3⁺ Cancer Cells Was Observed for the Group Immunized with CpG-MAGE-E2 Nanoparticles.

MAGE-specific lytic activity of splenocytes isolated from immunized mice was tested using A375 and MCF-7, which are positive[38,53] and negative[40] for MAGE-A3, respectively, and results are presented in Figure 3.5. Splenocytes isolated from mice immunized with CpG-MAGE-E2 nanoparticles significantly enhanced the lytic activity toward A375 by 9-fold at a 100:1 effector-to-target ratio [Figure 3.5.A], compared to free peptide and CpG. As expected, lytic activity observed for the mice immunized with CpG-MAGE-E2 is specific to

the cell line expressing MAGE, where no significant lysis was observed for the control cell line MCF-7. As with the results for the NY-ESO-1 antigen on our nanoparticle, our data confirms dose dependency of lysis activity toward target cell line [Figure 3.5.B]. Our data is also consistent with results previously reporting that the MAGE-specific CD8 T cells generated from immunization of MAGE epitope within bacteriophage are capable of recognizing and lysis of the MAGE-A3^{+} cell line.[54] This data, together with the data generated for NYESO epitope, confirms that the E2 nanoparticle can be used as an effective platform to simultaneously deliver clinically-tested CT antigens and CpG, resulting in an increase in the cellular-mediated immune responses generated to the target epitope.

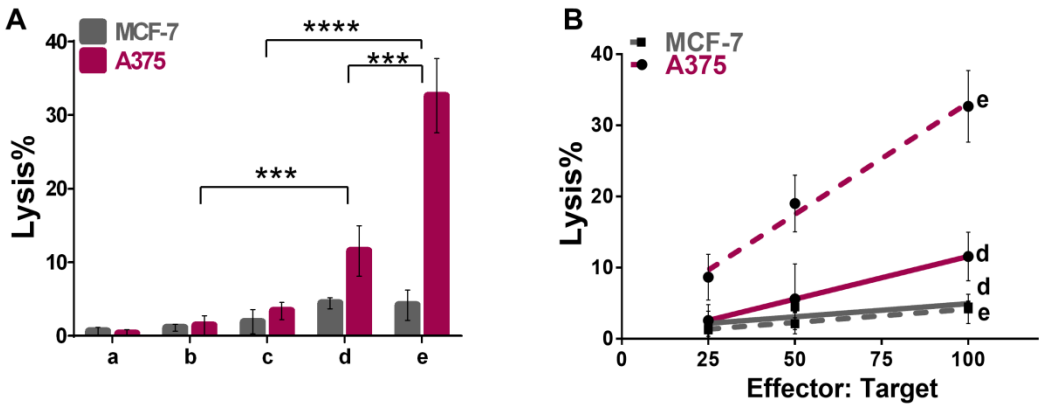

Figure 3.5. Results of Cell Lysis Assays Using Splenocytes from Immunization with MAGE-A3 Formulations**. A)** Summary of average lysis data at 100:1 effector:target ratio. HLA-A2 mice were immunized with different formulations (a-e; see Fig. 4A for schematic), and splenocytes were pulsed *ex vivo* in the presence of MAGE. Splenocytes isolated from mice immunized with CpG-MAGE-E2 nanoparticles enhanced lysis activity toward A375, relative to free peptide and CpG. **B)** Cell lysis results at different effector:target ratios. HLA-A2 mice were immunized with different formulations (a-e; see Fig. 4A for schematic), and splenocytes were pulsed *ex vivo* in the presence of MAGE peptide. Lytic ability toward A375 cell line resulted from CpG-MAGE-E2 nanoparticles immunization is dose dependent. Data is presented as average ± S.E.M. of at least 3 independent experiments. Statistical significance was determined by two-way ANOVA followed by a Tukey's test (***$p < 0.001$, ****$p < 0.0001$).

3.4.6. Co-Immunization with Nanoparticles Bearing both NYESO and MAGE Epitopes Yielded an Additive IFN-γ Effect and Increased the Lysis Activity

Prior studies have demonstrated that targeting a tumor through multiple antigen sources can decrease the possibility of tumor escape. For example, Banchereau et al. demonstrated clinical benefit for patients who received vaccines composed of four different melanoma antigens if at least two out of four antigen peptides were immunogenic in patients, rather than one peptide alone.[55-56] Similar observations have been made for

renal cell cancer.[57] Therefore, we investigated the effects of simultaneous immunization with CpG-NYESO-E2 and CpG-MAGE-E2 nanoparticles.

We observed that immunization with the CpG-NYESO-E2 and CpG-MAGE-E2 nanoparticles together (25 μg each, 50 μg total per dose) significantly increased the NYESO and MAGE epitope-specific IFN-γ secretion, compared to immunization with simultaneous vaccination of unbound CpG, NYESO, and MAGE peptides [Figure 3.6.B]. As expected, we observed negligible IFN-γ for the cells pulsed with an irrelevant SIINFEKL peptide [Figure 3.6.B], confirming the specificity of immune response generated from immunization.

We also obtained the same levels of IFN-γ secretion to the individual NYESO and MAGE epitopes when CpG-NYESO-E2 and CpG-MAGE-E2 nanoparticles were co-administered, relative to each nanoparticle formulation separately [Figure 3.6.B]; this shows that the specific IFN-γ responses to individual epitopes were preserved after co-immunization. The result is an additive effect to IFN-γ secretion, with the total IFN-γ frequencies of group f (sum of NYESO- and MAGE-specific IFN-γ) being approximately equal to the sum of individual NYESO-specific IFN-γ (group b) and MAGE-specific IFN-γ (group d). Furthermore, this additive effect to IFN-γ secretion from the simultaneous immunization is entirely antigen-specific and is not due to the adjuvant effect of CpG-E2 nanoparticle, since the addition of CpG-E2 alone did not further promote the specific IFN-γ secretion (compare formulations a to b, and c to d; Figure 3.6.B).

Consistent with the ELISpot data, splenocytes isolated from mice simultaneously immunized with CpG-NYESO-E2 and CpG-MAGE-E2 nanoparticles (25 μg each, 50 μg total per dose) significantly enhanced the lytic activity toward A375 [Figure 3.6.C], in a dose dependent manner [Figure 3.6.D], relative to unbound CpG, NYESO, and MAGE epitopes. As

expected, the lytic activity was specific to A375, with no lysis observed for the control cell line MCF-7 [Figure 3.6.C]. Furthermore, an elevated and additive lysis activity was observed for the mice that were co-immunized with CpG-NYESO-E2 and CpG-MAGE-E2 formulations compared to each formulation separately [Figure 3.6.C].

However, co-immunization with higher doses of CpG-NYESO-E2 and CpG-MAGE-E2 nanoparticles (50 μg each, 100 μg total per dose) did not amplify the specific-IFN-γ secretion [see Appendix B] or lysis activity [see Appendix B], relative to each formulation separately; in fact, both IFN-γ and lysis effects were lower than the effects of each individual antigen-nanoparticle alone. This observation could be due to T cell exhaustion[47] or peptide competition on the MHC of the antigen presenting cells (e.g., DCs) or on the T cell receptors.[58,59] This data, together with our data for the 100 μg CpG-NYESO-E2 results [see Appendix B], shows that for our current immunization schedule, the optimal dose for maximal immunogenic response is 50 μg total nanoparticle (either 50 μg for one antigen, or 25 μg for two antigens).

Overall, our results show that co-delivery of a multi-epitope nanoparticle vaccine can elicit higher cell-mediated immune responses than single-epitope formulations. Although dosing multiple (unconjugated) peptides in solution has shown to increase immune responses in the clinic,[39-41] and others have investigated other classes of antigen combinations,[60,61] our study is the first investigation, to our knowledge, that has examined the efficacy of administering multiple cancer-testis epitopes peptides within the context of nanoparticles. Our data show that (1) co-immunization of our E2 nanoparticle vaccines can preserve the individual cell-mediated effects against cancer-testis antigens and (2) that these IFN-γ and lytic effects are additive.

On the other hand, some groups have shown vaccination with cytotoxic T-cell epitopes can be more successful in combination with helper epitopes.[62] However, other evidence has shown that the CD8 T cell response in melanoma patients can actually be reduced after co-immunization with T helper epitopes.[62,63] Using T helper epitopes in our vaccines could be another important approach towards increasing efficacy, which will be examined in a future study.

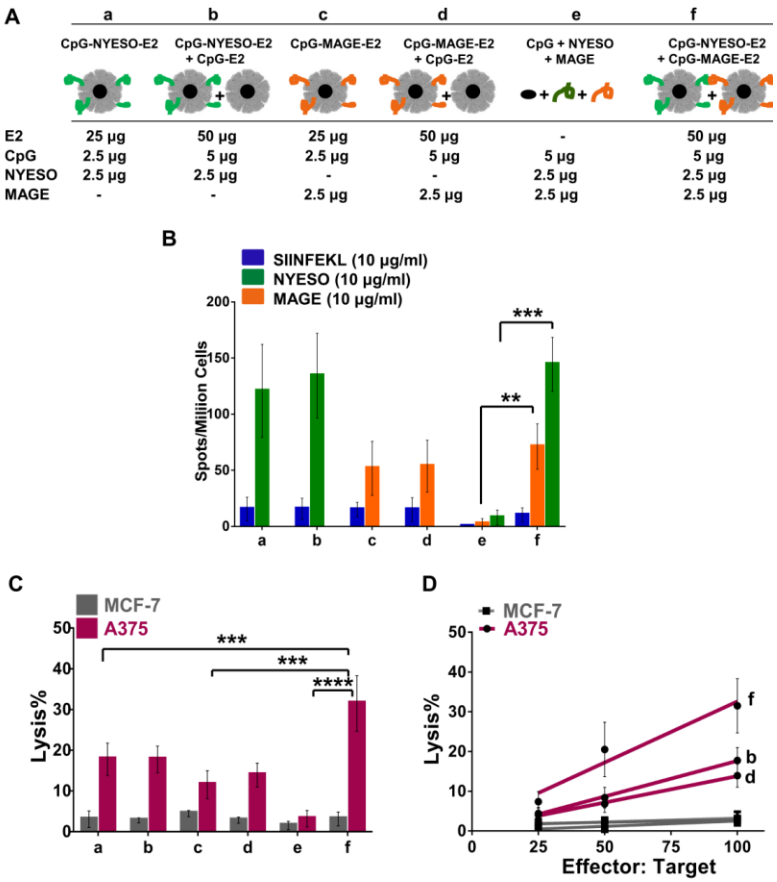

Figure 3.6. Cell-Mediated Immune Responses Using Splenocytes from Co-Immunization with NY-ESO-1 and MAGE-A3 Formulations. A) Vaccine components per dose of different formulation groups (a-f). **B)** Summary of averaged ELISpot data, which evaluated antigen-specific IFN-γ secretion. HLA-A2 mice were immunized with different formulations (a-f). Splenocytes of immunized mice were pulsed *ex vivo* in the presence of relevant peptide (NYESO or MAGE) or irrelevant peptide (SIINFEKL) and analyzed for specific IFN-γ secretion. Data is presented as average ± S.E.M. of at least 3 independent experiments. Statistical significance was determined by two-way ANOVA followed by a Bonferroni's test (**p < 0.01; ***p < 0.001). **C)** Summary of average lysis activity at 100:1 effector: target ratio. Mice received immunizations with different formulations (a-f), and splenocytes were incubated with target cells (A375 or MCF-7). Co-immunization with CpG-NYESO-E2 and CpG-MAGE-E2 nanoparticles significantly enhanced the lytic activity toward HLA-A2$^+$ and MAGE-A3$^+$ cell line (A375), relative to immunization with one antigen. **D)** Cell lysis results at different effector:target ratios. Data show dose-dependent cell lysis for both individual and combined antigens when bound to E2 and CpG, relative to unconjugated peptides and CpG. Data is presented as average ± S.E.M. of at least 3 independent experiments. Statistical significance was determined by two-way ANOVA followed by a Tukey's test (**p < 0.01; ***p < 0.001).

3.5. Conclusion

In this study, we have investigated the effects of incorporating clinically-relevant human CT antigens into a nanoparticle platform that had been previously shown to increase cancer vaccine efficacy. We examined whether higher cell-mediated immune responses can be achieved by simultaneously packaging of CT antigens and CpG adjuvant to the E2 nanoparticle. In a HLA-A2 transgenic mouse model, we found that immunization with nanoparticle formulations containing CpG and CT antigens resulted in a significantly higher specific IFN-γ frequencies compared to unbound antigen and CpG. Further, we observed an elevated lysis activity towards a target cancer cell line (A375). Additionally, simultaneous delivery of CpG-NYESO-E2 and CpG-MAGE-E2 nanoparticles preserved the effects of the individual antigen-nanoparticles, and resulted in an additive IFN-γ secretion and lysis activity relative to each separate nanoparticle formulation. Altogether, this work shows the advantages of using the E2 nanoparticle as an effective vaccine platform to deliver cancer-testis antigens for higher cell-mediated activation.

3.6. Acknowledgment

We thank Dr. Jin Wook Choi, Pamela B. Besada-Lombana, and Dr. Nancy Da Silva for access to and assistance with HPLC. DLS measurements and mass spectrometry analysis were carried out at the UCI Laser Spectroscopy Facility and the UCI Mass Spectrometry Facility, respectively. We are grateful to Dr. Sergey Ryazantsev at the California NanoSystems Institute at UCLA for assistance with obtaining TEM images. We also thank Dr. Christine E. McLaren at UCI's Chao Family Comprehensive Cancer Center's Biostatistics Shared Resource Facility for consultation and advice with statistical analyses. This work

was supported by the National Institute of Health (R21EB017995) and the National Cancer Institute of the National Institutes of Health (P30CA062203).

3.7. References

1. Rosenberg, S. A., Yang, J. C. & Restifo, N. P. Cancer immunotherapy: moving beyond current vaccines. *Nat. Med.* **10,** 909–915 (2004).
2. Even-Desrumeaux, K., Baty, D. & Chames, P. State of the art in tumor antigen and biomarker discovery. *Cancers.* **3,** 2554–2596 (2011).
3. Parmiani, G., Castelli,C., Dalerba, P., Mortarini, R., Rivoltini, L., Marincola, F. M. & Anichini, A. Cancer immunotherapy with peptide-based vaccines : what have we achieved ? where are we going ? *Journal of the National Cancer Institute.* **94,** 805–818 (1991).
4. Melero, I., Gaudernack, G., Gerritsen, W., Huber, C., Parmiani,G., Scholl, S., Thatcher, N., Wagstaff, J., Zielinski, C., Faulkner,I. & Mellstedt,H. Therapeutic vaccines for cancer : an overview of clinical trials. *Nat. Publ. Gr.* **11,** 509–524 (2014).
5. Ferrari, M. Cancer nanotechnology: opportunities and challenges. *Nat. Rev. Cancer* **5,** 161– 171 (2005).
6. Gao, F., Sun, M., Ma, W., Wu, X., Liu, L., Kuang, ., Xu, C. A Singlet Oxygen Generating Agent by Chirality-dependent Plasmonic Shell-Satellite Nanoassembly. *Adv. Mater.* **29,** 1–8 (2017).
7. Ma, W., Fu, P., Sun, M., Xu, L., Kuang, H., Xu, C. Dual Quantification of MicroRNAs and Telomerase in Living Cells. *J. Am. Chem. Soc.* **139,** 11752–11759 (2017).
8. Bachmann, M. F. & Jennings, G. T. Vaccine delivery: a matter of size, geometry, kinetics and molecular patterns. *Nat. Rev. Immunol.* **10,** 787–96 (2010).
9. Soema, P. C., Willems, G., Jiskoot, W., Amorij, J. & Kersten, G. F. European Journal of Pharmaceutics and Biopharmaceutics Predicting the influence of liposomal lipid composition on liposome size, zeta potential and liposome-induced dendritic cell maturation using a design of experiments approach. *Eur. J. Pharm. Biopharm.* **94,** 427–435 (2015).
10. Niikura, K., Matsunaga, T., Suzuki, T., Kobayashi, S. & Yamaguchi, H. Gold Nanoparticles as a vaccine platform : influence of size and shape on immunological responses in vitro and in vivo. *ACS Nano*. **7,** 3926-3938 (2013).
11. Manolova, V. Flace, A., Bauer, M., Schwarz, K., Saudan, P. & Bachmann, M. F. Nanoparticles target distinct dendritic cell populations according to their size. *Eur. J. Immunol.* **38,** 1404–1413 (2008).
12. Reddy, S. T., Rehor, A., Schmoekel, H. G., Hubbell, J. A. & Swartz, M. A. In vivo targeting of dendritic cells in lymph nodes with poly (propylene sulfide) nanoparticles. *J. of Controlled Release.* **112,** 26-34 (2006).
13. Reddy, S. T., van der Vlies, A. J., Simeoni, E., Angeli, V., Randolph, G. J., O'Neil, C. P., Lee, L. K., Swartz. M. A. & Hubbell, J. A. Exploiting lymphatic transport and complement
activation in nanoparticle vaccines. *Nature Biotechnology.* **25,** 1159-1164 (2007).
14. Wilson, J. T. Keller, S., Manganiello, M.J., Cheng,C., Lee,C.C., Opara,C., Convertine, A. & Stayton, P.S. pH-responsive nanoparticle vaccines for dual-delivery of antigens and immunostimulatory oligonucleotides. *ACS Nano.* **7,** 3912–3925 (2013).
15. Molino, N. M., Neek, M., Tucker, J., Nelson, E. L. & Wang, S. Biomaterials Viral-mimicking protein nanoparticle vaccine for eliciting anti-tumor responses. *Biomaterials.* **86,** 83–91 (2016).

16. Molino, N. M., Anderson, A. K. L., Nelson, E. L. & Wang, S. W. Biomimetic protein nanoparticles facilitate enhanced dendritic cell activation and cross-presentation. *ACS Nano.* **7,** 9743–9752 (2013).
17. Molino, N. M., Neek, M., Tucker, J. A., Nelson, E. L. & Wang, S. W. Display of DNA on Nanoparticles for Targeting Antigen Presenting Cells. *ACS Biomater. Sci. Eng.* **3,** 496–501 (2017).
18. Domingo, G. J., Chauhan, H. J., Lessard, I. A. D., Fuller, C. & Perham, R. N. Self-assembly and catalytic activity of the pyruvate dehydrogenase multienzyme complex from Bacillus stearothermophilus. *Eur. J. Biochem.* **266,** 1136–1146 (1999).
19. Dalmau, M., Lim, S., Chen, H. C., Ruiz, C. & Wang, S. W. Thermostability and molecular encapsulation within an engineered caged protein scaffold. *Biotechnol. Bioeng.* **101,** 654–664 (2008).
20. Dalmau, M., Lim, S. & Wang, S. Design of a pH-Dependent Molecular Switch in a Caged Protein Platform. *Nano Lett.* **9.** 160-166 (2009).
21. Ren, D., Dalmau, M., Randall, A., Shindel, M. M, Baldi, P. & Wang, S. W. Biomimetic design of protein nanomaterials for hydrophobic molecular transport. *Adv. Funct. Mater.* **22,** 3170–3180 (2012).
22. Ren, D., Kratz, F. & Wang, S. W. Engineered drug-protein nanoparticle complexes for folate receptor targeting. *Biochem. Eng. J.* **89,** 33–41 (2014).
23. Ren, D., Kratz, F. & Wang, S. W. Protein nanocapsules containing doxorubicin as a pH-responsive delivery system. *Small.* **7,** 1051–1060 (2011).
24. Krishnadas, D. K., Bai, F. & Lucas, K. Cancer testis antigen and immunotherapy. *ImmunoTargets Ther.* **2,** 1-19 (2013).
25. Fratta, E., Coral, S., Covre, A., Parisi, G., Colizzi, F., Danielli, R., Nicolay,H., Sigalotti,L. & Maio,M. The biology of cancer testis antigens : Putative function, regulation and therapeutic potential. *Mol. Oncol.* **5,** 164–182 (2011).
26. Caballero, O. L. & Chen, Y. Cancer/testis (CT) antigens: potential targets for immunotherapy. *JCA*. **100,** 2014-2021 (2009).
27. Nicholaou, T., Ebert, L., Davi, I.D., Robson, N., Klein, O., Maraskovsky, E., Chen ,W. & Cebon, J. Directions in the immune targeting of cancer: Lessons learned from the cancer-testis Ag NY-ESO-1. *Immunol and Cell Biology.* **84,** 303–317 (2006).
28. Kobayashi, H., Song, Y., Hoon, D. S. B., Appella, E. & Celis, E. Tumor-reactive T helper lymphocytes recognize a promiscuous MAGE-A3 epitope presented by various major histocompatibility complex class II alleles. *Cancer Res.* **61,** 4773–4778 (2001).
29. Olson, B. M. & McNeel, D. G. Antigen loss and tumor-mediated immunosuppression facilitate tumor recurrence. *Expert Rev. Vaccines* **11,** 1315–7 (2012).
30. Marincola, F. M., Jaffee, E. M., Hicklin, D. J. & Ferrone, S. Escape of Human Solid Tumors from T–Cell Recognition: Molecular Mechanisms and Functional Significance. *Adv. Immunol.* **74,** 181–273 (1999).
31. Petrulio, C. A. & Kaufman, H. L. Development of the PANVAC-VF vaccine for pancreatic cancer. *Expert Rev Vaccines* **5,** 9–19 (2006).
32. Chen, J. L. Dunbar, P. R., Gilead,i U., Jäger, E., Gnjatic, S., Nagata, Y., Stockert, E., Panicali, D. L., Chen, Y. T., Knuth, A., Old, L. J. & Cerundolo, V. Identification of NY-ESO-1 Peptide Analogues Capable of Improved Stimulation of Tumor-Reactive CTL. *J. Immunol.* **165,** 948–955 (2000).

33. Khong, H. T., Yang, J. C., Topalian, S. L., Sherry, R. M., Mavroukakis, S. A., Whit, D. E. & Rosenberg, S. A. Immunization of HLA-A*0201 and/or HLA-DPbeta1*04 patients with metastatic melanoma using epitopes from the NY-ESO-1 antigen. *J. Immunother.* **27,** 472–7 (2004).
34. Jäger, E., Chen, Y. T., Drijfhout, J. W., Karbach, J., Ringhoffer, M., Jäger, D., Arand, M., Wada, H., Noguchi, Y., Stockert, E., Old, L.J. & Knuth, A. Simultaneous humoral and cellular immune response against cancer-testis antigen NY-ESO-1: definition of human histocompatibility leukocyte antigen (HLA)-A2-binding peptide epitopes. *J. Exp. Med.* **187,** 265–270 (1998).
35. Song, S., Wang, F., He, X., He, Y., Li, D. & Sun, H. Evaluation of antitumor immunity efficacy of epitope-based vaccine with B16 cell line coexpressing HLA-A2/H-2kb and CTL multiepitope in HLA transgenic mice. *Vaccine.* **25,** 4853–4860 (2007).
36. Voskens, C. J., Sewell, D., Hertzano, R., DeSanto, J., Rollins, S., Lee, M., Taylor, R., Wolf, J Suntharalingam, M., Gastman, B., Papadimitriou J. C., Lu, C., Tan M., Morales, R., Cullen, K., Celis, E., Mann, D & Strome, S. E. Induction of mage-A3 and HPV-16 immunity by Trojan vaccines in patients with head and neck carcinoma. *Head Neck.* **34,** 1734–1746 (2012).
37. Gunda, V., Frederick, D. T., Bernasconi, M. J., Wargo, J. A. & Parangi, S. A potential role for immunotherapy in thyroid cancer by enhancing NY-ESO-1 cancer antigen expression.*Thyroid.* **24,** 1241–1250 (2014).
38. Rapoport , A. P., Aqui, N. A, Stadtmauer, E. A., *et al.* Combination immunotherapy after asct for multiple myeloma using MAGE-A3/Poly-ICLC immunizations followed by adoptive transfer of vaccine-primed and costimulated autologous T cells. *Clin. Cancer Res.* **20,** 1355–1365 (2014).
39. Klar, A. S., Gopinadh, J., Kleber, S. & Wadle, A. Treatment with 5-Aza-2'-Deoxycytidine Induces Expression of NY-ESO-1 and Facilitates Cytotoxic T Lymphocyte-Mediated Tumor Cell Killing. *PLoS One.* **1,** 1–15 (2015).
40. Kayser, S., Watermann, I., Rentzsch, C., Weinschenk, T., Wallwiener, D. & Gückel, B. Tumor-associated antigen profiling in breast and ovarian cancer : mRNA, protein or T cell recognition?*Journal of Cancer Research and Clinical Oncology*. **129,** 397–409 (2003).
41. Kochenderfer, J. N., Chien, C. D., Simpson, J. L. & Gress, R. E. Maximizing CD8+ T cell responses elicited by peptide vaccines containing CpG oligodeoxynucleotides. *Clin. Immunol.* **124,** 119–130 (2007).
42. Davila, E., Kennedy, R. & Celis, E. Generation of Antitumor Immunity by Cytotoxic T Lymphocyte Epitope Peptide. *Cancer Res*. **63,** 3281–3288 (2003).
43. Dhodapkar, M. V., Sznol, M., Zhao, B., Wang, D., Carvajal,R.D., Keohan, M. L., Chuang, E., Sanborn, R.E., Lutzky, J., Powderly, J., Kluger, H., Tejwani, S., Green, J., Ramakrishna, V., Crocker, A., Vitale, L., Yellin, M., Davis,T. & Keler, T. Induction of antigen-specific immunity with a vaccine targeting NY-ESO-1 to the dendritic cell receptor DEC-205. *Sci Transl Med.* **6,** 1-11 (2014).
44. Maraskovsky E., Sjölander,S., Drane,D.P., Schnurr,M., Thuy,T. T. Le, Mateo,L., Luft,T., Masterman, K.N., Tai, T-Y., Chen,Q., Green, S., Sjölander, A., Pearse, M.J., Lemonnier, F.A., Chen, W., Cebon. J. & Suhrbier.A. NY-ESO-1 protein formulated in ISCOMATRIX adjuvant is a potent anticancer vaccine inducing both humoral and $CD8^+$ T-cell-mediated immunity and protection against NY-ESO-1+ tumors. *Clin Cancer Res.* **10,**

2879–2890 (2004).
45. Palmowski, M. J. Lopes,L., Ikeda,Y., Salio, M., Cerundolo,V. & Collins, M.K. Intravenous Injection of a Lentiviral Vector Encoding NY-ESO-1 Induces an Effective CTL Response. *J. Immunol.* **172,** 1582-1587 (2004).
46. Fontenot, J. D., Gavin, M. A. & Rudensky, A. Y. Foxp3 programs the development and function of CD4 + CD25 + regulatory T cells. *Nature Immunology*. **4,** 330-336 (2003).
47. Yi, J. S., Cox, M. A. & Zajac, A. J. T-cell exhaustion: characteristics, causes and conversion. *Immunology.* **2,** 474–481 (2010).
48. Miller, S. D., Turley, D. M. & Podojil, J. R. Antigen-specific tolerance strategies for the prevention and treatment of autoimmune disease. *Nat. Rev. Immunol.* **7,** 665–677 (2007).
49. Pollack, S.M., Jones, R.L., Farrar, E.A., Lai, I.P., Lee, S.M., Cao, J., Pillarisetty, V.G., Hoch, B.L., Gullett, A., Bleakley, M., Conrad, E.U., Eary, J.F., Shibuya, K.C., Warren, E.H., Carstens, J.N., Heimfeld, S., Riddell, S.R. & Yee, C. Tetramer guided cell sorter assisted production of clinical grade autologous NY-ESO-1 specific $CD8^+$ T cells. *Journal for Immunotherpay of Cancer.* **2,** 1–10 (2014).
50. Wargo, J. A., Robbins, P. F., Li, Y., Zhao, Y., El-Gamil, M., Caragacianu, D., Zheng, Z., Hong, J.A., Downey, S., Schrump, D.S., Rosenberg, S. A. & Morgan, R. A. Recognition of NY-ESO-1^+ tumor cells by engineered lymphocytes is enhanced by improved vector design and epigenetic modulation of tumor antigen expression. *Cancer Immunol Immunother.* **58,** 383–394 (2009).
51. Domingo, G. J., Caivano, A., Sartorius, R., Barba, P., Bäckströma, M., Piatier-Tonneau, D., Guardiola, J., Berardinis, P. & Perham. R.N. Induction of specific T-helper and cytolytic responses to epitopes displayed on a virus-like protein scaffold derived from the pyruvate dehydrogenase multienzyme complex. *Vaccine.* **21,** 1502–1509 (2003).
52. Chinnasamy, N., Wargo, J., Yu, Z., Rao, M., Frankel, T., Riley, J., Hong, J., Parkhurst, M., Feldman, S., Schrump, D., Restifo, N., Robbins, P., Rosenberg, S. & Morgan, R. A TCR targeting the HLA-A*0201-restricted epitope of MAGE-A3 recognizes multiple epitopes of the MAGE-A antigen superfamily in several types of cancer. *J. Immunol.* **186,** 685–96 (2011).
53. Cameron, B. J., Gerry, A. B., Dukes, J., Harper, J. V., Kannan,V., Bianchi, F. C., Grand,F., Brewer, J. E., Gupta, M., Plesa, F., Bossi, G., Vuidepot,A., Powlesland, A. S., Legg, A., Adams, K. J., Bennett,A. D., Pumphrey, N. J., Williams, D. D., Binder-Scholl, G., Kulikovskaya, I., Levine, B. L., Riley, J. L., Varela-Rohena, A., Stadtmauer, E. A., Rapoport, A. P., Linette, G. P., June, C. H., Hassan, N. J., Kalos, M. & Jakobsen, B. K. Identification of a titin-derived HLA-A1-presented peptide as a cross-reactive target for engineered MAGE-A3– directed T cells. *Science Translational Medicine.* **5,** 1-11 (2013).

54. Sartorius, R., Pisu, P., D'Apice, L., Pizzella, L., Romano, C., Cortese, G., Giorgini, A., Santoni, A., Velotti, F. & De Berardinis. P. The use of filamentous bacteriophage *fd* to deliver MAGE-A10 or MAGE-A3 HLA-A2-restricted peptides and to induce strong antitumor CTL responses. *J. Immunol.* **180,** 3719-3728 (2008).
55. Banchereau, J., Palucka,A. K., Dhodapkar, M., Burkeholder, S., Taquet, N., Rolland, A., Taquet, S., Coquery, S., Wittkowski, K. M., Bhardwaj, N., Pineiro, L., Steinman, R. & Fay, J. Immune and clinical responses in patients with metastatic melanoma to C D34+ progenitor-derived dendritic cell vaccine. *Cancer Res.* **61,** 6451–6458 (2001).
56. Fay, J. W., Palucka,. A. K., Johnston, D. A. & Burkeholder, S. Long-term outcomes in patients with metastatic melanoma vaccinated with melanoma peptide-pulsed CD34+ progenitor-derived dendritic cells. *Cancer Immunol.* **10,** 1209–1218 (2006).
57. Walter, S*.,* Weinschenk, T., Stenzl, A., Zdrojowy, R., Pluzanska, A., Szczylik, C. Staehler,M., Brugger, W., Dietrich, P., Mendrzy, R., Hilf, N., Schoor, O., Fritsche, J., Mahr, A., Maurer, D., Vass, V., Trautwein, C., Lewandrowski, P., Flohr, C., Pohla, H., Stanczak, J. J., Bronte, V., Mandruzzato, S., Biedermann, T., Pawelec, G., Derhovanessian, E., Yamagishi, H.,Miki, T., Hongo, F., Takaha, N., Hirakawa, K., Tanaka, H., Stevanovic, S., Frisch, J., Mayer-Mokler, A., Kirner, A., Rammensee, H. G., Reinhardt, C. & Singh-Jasuja, H. Multipeptide immune response to cancer vaccine IMA901 after single-dose cyclophosphamide associates with longer patient survival. *Nature Medicine.* **18,** 1254-1261 (2012).
58. Adodni, L. & Nagy, Z. A. Peptide competition for antigen presentation. *Immunology Today*. **11,** 21-24 (1990).
59. Rosenberg, S. A., Sherry, R.M., Morton, K.E., Yang, J.C., Topalian, S.L., Royal, R.E., Kammula, U.S., Restifo, N.P., Hughes, M.S., Schwarz. S,L., Ngo, L. T., Mavroukakis, S.A. & White. D.E. Altered CD8(+) T-cell responses when immunizing with multiepitope peptide vaccines. *J Immunother*. **29,** 224–231 (2006).
60. McCormick, A. A., Corbo, T. A., Wykoff-Clary, S., Palmer, K. E. & Pogue, G. P. Chemical conjugate TMV-Peptide bivalent fusion vaccines improve cellular immunity and tumor protection. *Bioconjug. Chem.* **17,** 1330–1338 (2006).
61. Tan, S., Sasada, T., Bershteyn, A., Yang, K., Ioji, T. & Zhang, Z. Combinational delivery of lipid-enveloped polymeric nanoparticles carrying different peptides for anti-tumor immunotherapy. *Nanomedicine.* **9,** 635–647 (2014).
62. Slingluff, C. L. The Present and Future of Peptide Vaccines for Cancer: Single or Multiple, Long or Short, Alone or in Combination? *Cancer J.* **17,** 343–350 (2012).
63. Noguchi, M., Moriya, F., Koga, N. & Matsueda, S. A randomized phase II clinical trial of personalized peptide vaccination with metronomic low - dose cyclophosphamide in patients with metastatic castration-resistant prostate cancer. *Cancer Immunol. Immunother.* **65,** 151–160 (2016).

CHAPTER 4

COMBINATION OF PROTEIN NANOPARTICLE VACCINE WITH IMMUNE CHECKPOINT INHIBITOR, ANTI-PD-1, INCREASES TUMOR-BEARING ANIMAL SURVIVAL

4.1. Abstract

Obstruction of inhibitory effects of immune checkpoint molecules is a promising approach in cancer treatment. However, treatments with checkpoint inhibitors are still not effective in a significant portion of patients. Cancer treatments are often most effective when performed in combination with one another. Vaccination is a promising approach to increase immune checkpoint inhibitors efficacy, due to their individual mechanism of action. We have been exploring the non-viral E2 protein nanoparticle as a platform for cancer vaccine delivery. Simultaneous delivery of melanoma gp100 antigen and CpG adjuvant within E2 nanoparticle (CpG-gp-E2) resulted in an improved survival of tumor-bearing animals, enhanced IFN-γ secretion, and increased T cell population, compared to the PBS control group. Furthermore, in an aggressive B16-F10 tumor model, ~50% of the mice treated with combination of anti-PD-1 with CpG-gp-E2 nanoparticle remained tumor-free, compared with 0% and ~5% survival for CpG-gp-E2 and anti-PD-1 treatment groups alone, respectively. These results show that combination of protein-based cancer vaccines with anti-PD-1 can significantly increase the immune checkpoint inhibitor efficacy.

4.2. Introduction

One of the promising approaches in cancer immunotherapy is the obstruction of inhibitory effects of immune checkpoint molecules[1,2] which exist to support self tolerance and protect individuals against autoimmunity diseases.[3,4] Despite all promises, however, treatments with checkpoint inhibitors are still not responsive in a significant portion of patients; only ~20% of patients have long-term survival, with the longest reported survival of ~10 years.[5,6] Also, many aggressive cancer types do not respond to these immune checkpoint therapies.[7,8] Treatment with immune checkpoint inhibitors only release the

general T cell suppression (release the brake on existing T cells), without boosting the specific T cell responses towards tumors. Therefore, poor outcomes of checkpoint inhibitors may signify the absence of a strong specific anti-tumor T cell response in the tumor microenvironment (TME). Thus, the efficacy could possibly be improved in the presence of higher anti-tumor T cell responses. In Chapters 2 and 3, we demonstrated the ability of antigen-E2 delivery system in inducing strong specific anti-tumor responses. Therefore, combination of immune checkpoint inhibitors with antigen-E2 delivery system could increase the checkpoint inhibitor efficacy. In this chapter, we investigated whether a prolonged animal survival can be achieved if immune checkpoint inhibitor treatment is administered in combination with our nanoparticle vaccine.

Antigen-specific T cell responses, which are needed to overcome the low immunogenicity of cancer cells, are controlled by the balance between co-stimulatory and co-inhibitory signals.[9,10] Generation of CD8 T cell response is a complex multi-step process. The first step is recognition of the tumor antigen in the context of human leukocyte antigen (HLA) molecules by T cell receptors (TCR).[11] After antigen recognition by TCR, T cells are only activated if CD28, a stimulatory molecule expressed on T cells, binds to the ligands CD80 and CD86 on APCs.[9,10] Following T cell activation, inhibitory checkpoint molecules such as program death 1 (PD-1) and cytotoxic T lymphocyte antigen 4 (CTLA-4) are expressed on the surface of activated T cells. Interaction between these molecules and their ligands lead to T cell inactivation.[12–14] Therefore, blockade of PD-1, CTLA-4 and/or their ligands can release the T cell deactivation and improve the anti-tumor responses.[14–16]

Nivolumab and ipilimumab, two FDA-approved immune checkpoint inhibitor antibodies, demonstrated clinical efficacy in different advanced malignancies.[17,18] However,

despite all promises, only ~ 20% of patients benefit from a long-term survival of about 3 years post treatment.[5,6] Therefore, it is hypothesized that combination approaches with immune checkpoint inhibitors are needed to improve the efficacy. Treatment with immune checkpoint inhibitors only release the general T cell suppression, without boosting the specific T cell responses towards tumors. On the other hand, cancer vaccines aim to prime the immune system to recognize specific tumor antigens which results in an expansion of specific CD8 T cell responses.[19,20] Therefore, combination of cancer vaccines (to increase T cell responses) with checkpoint inhibitors (to release the T cell deactivation) could improve the efficacy of immune checkpoint inhibitors.[21,22]

Although conventional cancer vaccines (peptide and protein-based vaccines) usually fail to efficiently trigger immune responses against cancer cells;[23] the delivery of these peptides and proteins as components within nanoparticles has shown promising improvements in vaccine efficacy.[24] Specially, protein nanoparticles have attracted incredible interest because of their highly organized structures and symmetry, ability to be specifically functionalized, and ideal size for vaccine delivery.[25] Therefore, combination of immune checkpoint inhibitors with cancer vaccines in the context of protein nanoparticles can possibly improve checkpoint inhibitor efficacy. Combination of PD-1 inhibitor with dendritic cell (DC) vaccine,[26] multipeptide vaccine,[27] and DNA vaccine[28] have been studied; in all cases higher animal survival rate was observed for combination treatment compared to immune checkpoint therapy alone. This synergistic effect could be a result of an increase in T cell response (due to the vaccine) and a decrease in the T cell inhibition (due to checkpoint inhibitor) simultaneously.

In Chapter 2, our research group demonstrated that the simultaneous delivery of CpG (adjuvant) and gp100 (melanoma MHC-I restricted antigen) within E2 nanoparticles resulted in enhanced antigen-specific IFN-γ secretion, and prolonged survival time in C57BL/6 mice.[29] Also in Chapter 3, our data confirmed that in a HLA-A2 transgenic mouse model, significantly higher IFN-γ secretion and cell lysis activity can be achieved when HLA-A2 restricted human cancer-testis antigens and CpG were coupled to the E2 nanoparticle.[30]

In this chapter, we investigated the therapeutic effect of CpG-gp-E2 immunization rather than the preventive effect evaluated in the previous study (Chapter 2).[29] We tested different schedule/regimen of nanoparticle immunization in order to find an effective one in inducing anti-tumor responses. T cell proliferation, and PD-1 and CTLA-4 expressions on T cells were also examined. We also evaluated the therapeutic effects of combination therapy of antigen-E2 delivery vaccine with anti-PD-1 antibody in a B16-F10 melanoma model in C57BL/6 mice. To our knowledge, our study is the first one to test the combination of a protein-based nanoparticle vaccine and immune checkpoint inhibitors.

4.3. Methods

4.3.1. Materials

Reagents were purchased from Fisher Scientific and antibodies were from Life Technologies unless otherwise noted. Complete RPMI used in this study for splenocytes was compromised of RPMI 1640 (Mediatech) with 10% heat-inactivated FBS (Hyclone), 1mM sodium pyruvate (Hyclone), 100 μg/ml of streptomycin (Hyclone), 0.1 mM nonessential amino acids (Lonza), 2 mM L-glutamine (Lonza), and 100 units/ml penicillin.

4.3.2. Cell Line

B16-F10, a murine melanoma cell line, was purchased from ATCC. B16-F10 was cultured in DMEM supplemented with 10% FBS, as suggested by the manufacturer. Cells were incubated at 37^{o}C, under 5% CO_2, and were passaged 2-3 times a week [cells were passaged if they were > 90% confluent]. 1.5 ml of 0.5% trypsin (37^{0}C) was added to B16-F10 cells (T-25 flask). Cells (+trypsin) were placed at 37^{o}C incubator until cells were detached [~ 5 min]. Then, cells were checked under microscope. The side of the flask was tapped to disperse any cell lumps. Seven mls of fresh warm media (DMEM + 10% FBS) was added to dilute the trypsin. Cells were spun down for 5 min at 300 × g. The supernatant was discarded and cells were resuspended in fresh media. Cells were stained in trypan blue and cells were counted using hemocytometer. B16-F10 [4 times diluted] were placed in a new T-25 flask. Only cells with passage # ≤ 15 were used for the experiments.

4.3.3. E2 Purification and Characterization

Expression, purification, and characterization of the D381C protein nanoparticle (abbreviated as E2 in this study) were performed as previously described.[31] In summary, *E. coli* strain BL21(DE3) containing E2 gene was cultured in Luria-Bertani medium containing 100 μg/ml ampicillin. Expression was induced by adding 1mM of IPTG when the culture reached the optical density of 0.6-0.9 measured at 600 nm. Cells were harvested and stored at -80^{o}C. Cells were lysed using French pressure cell (Thermo Scientific), and the insoluble fraction was removed by centrifugation. Soluble part was heated at 70^{o}C for 20 min. Denatured native *E.coli* protein aggregates were removed by centrifugation at 90,000 × g for 1 hr. The recovered supernatant was loaded to a HiPrep Q Sepharose anion exchange

column followed by a Superose 6 size exclusion column.[31] Purity of the E2 nanoparticle was confirmed with SDS-PAGE. Dynamic light scattering was used to check the size, and assembly of the particles.

As previously described, lipopolysaccharide was removed using Triton X-114 (Sigma) extraction, and endotoxin levels were evaluated using an LAL ToxinSensor kit (Genscript).[32] Briefly, Triton X-114 (Sigma) was added to the E2 nanoparticle at 1% [v/v] ratio, incubated at 4°C for 5 min, vortexed, and incubated at 37°C for 5 min. The mixture was then centrifuged at 18,000 × g and 37°C for 30 seconds. E2-containing aqueous portion was transferred to a new microcentrifuge tube. This process was repeated ≥ 8 times. Triton was removed with detergent removal spin columns (Pierce). LPS levels were below 5 EU/mg of E2 protein nanoparticle (LAL ToxinSensor gel clot assay, Genscript).

4.3.4. CpG and Antigen Epitope Conjugation

5' benzaldehyde-modified CpG 1826 [5'-tccatgacgttcctgacgtt-3'] with a phosphorothioated backbone was synthesized by Trilink. The $gp100_{25-33}$ antigen epitope, CKVPRNQDWL, a CTL-restricted epitope from human gp100,[33] was synthesized by Genemed Synthesis. CpG and antigen epitope conjugation and characterization were performed as previously described.[29,30] Briefly, CpG 1826 modified with a 5'-benzaldehyde was attached to the cysteines in the internal cavity of E2 nanoparticles using a N-β-maleimidopropionic acid hydrazide (BMPH) linker. TCEP-reduced peptides with N-terminal cysteines were conjugated to the lysines on the surface of the E2 nanoparticle by incubating the nanoparticle with a sulfo-SMCC linker.

4.3.5. Zeta Potential Measurements

To measure zeta potential, the diffusion barrier method with monomodal analysis were used because of its compatibility with physiological ionic strengths of our protein nanoparticle. Malvern capillary cells were filled with buffer (50 mM potassium phosphate at pH 7.4 with 100 mM NaCl), and 150 µl of nanoparticles (at 1.3 mg/ml) were gently injected to the bottom of the cells. Zeta potential was measured with a Malvern Zetasizer (Nano ZS).

4.3.6. Mice

Female C57BL/6 mice (~ 6 weeks) were obtained from Jackson Laboratory. All animal studies were carried out in accordance with protocols approved by the Institute for Animal Care and Use Committee (IACUC) at the University of California, Irvine.

4.3.7. Tumor Challenge for Different Immunization Schedule, Section 4.4.2.

10^5 of B16-F10 melanoma cells (in 100 µl DMEM, no FBS) were subcutaneously inoculated in the right flank of female C57BL/6 mice, and tumor size was measured daily with a caliper. Tumor volume was calculated as (0.5 × shortest diameter^2 × longest diameter). All mice were sacrificed on day 14, if they were not already sacrificed due to tumor size.

4.3.8. Tumor Challenge for Combination & Re-Challenge Study, for Section 4.4.5.

10^4 of B16-F10 melanoma cells [in 100 µl DMEM, no FBS] were subcutaneously inoculated in the right flank of female C57BL/6 mice, and tumor size was measured daily

with a caliper. Mice were sacrificed when tumor reached 1.5 cm in diameter.

4.3.9. Nanoparticle Immunization

All immunizations with CpG-gp-E2 nanoparticle was done subcutaneously at the base of the tail. Different immunization schedule/regimen were tested in this study which is discussed in more detail in the Result and Discussion section. Briefly, mice were assigned into three different immunization schedule groups [see Figure 4.2.A]. Group II received a single immunization of 50 μg CpG-gp-E2 in 120 μl of PBS. Groups III and IV received a prime immunization of 50 μg of CpG-gp-E2 in 120 μl of PBS, followed by a booster [50 μg CpG-gp-E2] on days 7 and 10, respectively. Mice in control group [group I, Figure 4.2.A] received two injections of 120 μl PBS.

4.3.10. PD-1 Inhibitor Injection

Anti-PD-1 antibody [Bio X Cell, clone RPM1-14] was administered by intraperitoneal (IP) injection. Mice received 5 injections of 100 μg anti-PD1 (in 200 μl PBS) every 3 days starting at day 9. However, 4 mice (2 mice from anti PD-1 and 2 from combined group) received only 3 injections of anti-PD-1 because they had to be sacrificed due to their tumor size.

4.3.11. IFN-γ ELISpot

For IFN-γ ELISpot, we used the Ready-Set-Go kit (eBioscience). Single-cell suspensions in RPMI were prepared from isolated spleens, and added at 10^6 cells/well to

PVDF ELISpot plates that were pre-coated with an anti-mouse IFN-γ antibody. Cell were incubated with either 10 μg/ml of the relevant peptide or an irrelevant peptide (SIINFEKL) for 24 hrs at 37°C. Unstimulated cells in RPMI were plated and served as a negative control. Positive control wells contained 2% PHA-M (Gibco). IFN-γ spots were developed following the manufacturer's protocol. Plates were scanned and quantified using an ELISpot reader (Cellular Technology) and immunospot analysis software (Immunospot Analysis Pack).

4.3.12. Flow Cytometry Staining

Single-cell suspension from tumors and spleens isolated from mice were prepared to check for various cell types and cell surface markers. RBCs were depleted with ACK lysing buffer. Cells were washed 2 times in PBS and counted with a hemocytometer. Cells were stained with primary antibodies or appropriate isotype controls in PBS + 1% BSA (FACS buffer) for 30 min on ice, followed by 2 washes with FACS buffer. Data was analyzed by NovoCyte Flow Cytometer for CD3, CD4, CD8, FoxP3, PD-1, MHC-I, CTLA-4, and PD-L1. For gp100 cells were stained with primary antibody in FACS buffer for 30 min on ice, followed by 2 washes with FACS buffer. Cells then were incubated with secondary antibody in FACS buffer for 30 min, followed by 2 washes (FACS buffer). For analysis, a typical forward-side scatter gate was set to exclude dead cells and aggregates.

4.3.13. Statistical Analysis

Data are presented as mean ± standard deviation for particle characterization of at least 3 independent experiments, using Microsoft Excel. Data for different nanoparticle immunizations regimen are presented as mean ± error of the mean (S.E.M.) of 2

independent experiments (n_{total}=7), using GraphPad Prism. Statistical significance was determined by one-way ANOVA using post-hoc Tukey's test. Statistical analysis of survival curves in the combination study was determined by Log-rank (Mantel-Cox) of 3 independent experiments (n_{total} =15), using GraphPad Prism. Statistical analysis of survival curve in re-challenge study was determined by Log-rank (Mantel-Cox) of 3 independent experiments (n_{total} =7), using GraphPad Prism. Data for tumor cell surface marker expressions (*e.g.,* MHC-I) presented as mean ± S.E.M. of 2 independent experiments (n_{total}=4), using GraphPad Prism; statistical significance was determined by one-way ANOVA using post-hoc Tukey's test. P-values less than 0.05 were considered significant.

4.4. Results and Discussion

4.4.1. Conjugation of CpG and gp100 to E2 Nanoparticles

Both CpG and $gp100_{25\text{-}33}$ were successfully conjugated to E2 nanoparticle. These results are consistent with those previously described.[29,30] As previously reported, the lower band on CpG-E2 at ~28 kDa is the unconjugated E2 monomer (~28 kDa), and the band at ~ 35 kDa suggests the conjugation of one CpG molecule (~7 kDa) to E2 monomer [Figure 4.1.A]. Simultaneous conjugation of CpG and gp100 to E2 nanoparticle resulted in two broad bands [Figure 4.1.A]. The band between 35-40 kDa confirms the simultaneous conjugation of gp100 and CpG to the E2 monomers (CpG-gp-E2). Also, dynamic light scattering revealed a hydrodynamic diameter of 27.8 ± 0.6, 27.6 ± 0.9, and 29.0 ± 0.9 nm for E2, CpG-E2, and CpG-gp-E2 respectively [Figure 4.1.B], which is within the optimal reported size for lymphatic drainage of 20-45 nm.[34–36] The zeta potential of E2, CpG-E2, and CpG-gp-E2 nanoparticles were -12.4 ± 1 mV, -11.3 ± 0.5, and -11.7 ± 1 mV, respectively, confirming that conjugation of gp100 peptide and CpG to E2 nanoparticles did not change

the overall surface charge compared to the E2 nanoparticle itself. TEM image [Figure 4.1.C] confirms that the size and structure of nanoparticles remain intact after conjugation.

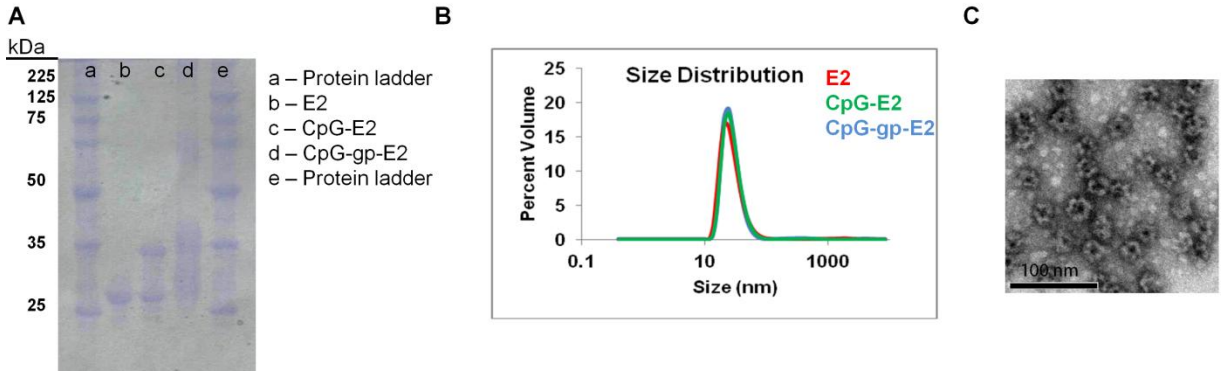

Figure 4.1. Characterization of Functionalized Nanoparticles. A) SDS-PAGE shows successful conjugation of CpG and gp100 to E2 nanoparticles. **B)** DLS reveals nanoparticle sizes of approximately 30 nm. **C)** TEM image confirms intact nanoparticles after conjugation.

4.4.2. A Booster of CpG-gp-E2 Nanoparticle Seven Days After the Prime Immunization Resulted in the Highest IFN-γ Secretion and the Slowest Tumor Growth

Antigen load is crucial for establishing a long-lived and protective T cell responses.[37] Therefore, optimal vaccination regimen is required to increase the anti-tumor responses. Therefore, we tested different schedule of CpG-gp-E2 nanoparticle immunization [Figure 4.2.A] to discover the most effective regimen in inducing anti-tumor responses against B16-F10 melanoma, in a C57BL/6 mouse model. Our data revealed that group III [Figure 4.2.A] that received a booster injection seven days after the prime immunization resulted in the highest antigen-specific IFN-γ secretion [Figure 4.2.B] and enhanced anti-tumor responses [Figure 4.2.C].

C57BL/6 mice were inoculated with 10^5 of B16-F10 cells. Different vaccine schedule/regimen of CpG-gp-E2 [Figure 4.2.A] were investigated and ELISpot results and tumor size data are presented in Figures 4.2.B and 4.2.C, respectively. All mice were

sacrificed on day 14 and spleens and tumors (if existed) were isolated to check for various cell types and cell surface markers using flow analysis (sections 4.4.3. & 4.4.4.).

Single immunization with 50 μg of CpG-gp-E2 [group II, Figure 4.2.A] resulted in negligible amount of IFN-γ secretion [Figure 4.2.B]. IFN-γ is a cytokine that is secreted predominantly by activated CD8 T cells. Therefore, measuring IFN-γ secretion could be an indirect way for checking the presence of CD8 T cell responses, a response that is needed to conquer the tumor cells. We previously reported high frequencies of gp100-specific IFN-γ secretion after a single immunization of CpG-gp-E2 nanoparticle.[29] However, in the previous work the IFN-γ secretion was evaluated seven days after immunization compared to day 14 investigated in this study. Lack of IFN-γ secretion in splenocytes 14 days after immunization could be explained by migration of antigen-specific cytotoxic T cells to the target site; T cell migration generally happens within the first week of cell-mediated immunity.[38] One possible explanation, other than T cell migration, could be the induction of $FoxP3^+$ CD4 T cells which can cause T cell suppression.[39,40] However, we did not detect an increase in $FoxP3^+$ CD4 T cell percentage [Figure 4.2.D]. Therefore, lack of IFN-γ response is not likely due to induction of FoxP3-expressing CD4 T cells.

Prime immunization of 50 μg of CpG-gp-E2 nanoparticle on day 0 followed by a booster on day seven [group III, Figure 4.2.A] showed the highest IFN-γ secretion [Figure 4.2.B] and an enhanced anti-tumor responses [Figure 4.2.C] compared to other groups, suggesting the presence of a higher cytotoxic CD8 T cell responses. Higher IFN-γ secretion and also a slower tumor growth observed in group III compared to group II with a single CpG-gp-E2 administration suggest that booster immunization is needed for inducing a stronger therapeutic response. Also, negligible levels of IFN-γ observed for the splenocytes

pulsed with an irrelevant SIINFEKL peptide [Figure 4.2.B] confirms that the response generated from immunization was antigen-specific and it was not due to a non-specific immune responses to the E2 delivery platform itself. IFN-γ secretion and anti-tumor responses that we observed for group III are comparable to a study previously reported which delivered the gp100 epitope within a heat-shock protein nanoparticle formulation delivery system.[41] Our data are also similar to previous studies of delivering different melanoma-specific TAAs, using polymeric nanoparticle platforms.[42,43]

Booster immunization 10 days after the prime immunization [group IV, Figure 4.2.A] resulted in a significantly lower amount of IFN-γ secretion compared to group III, ($p < 0.0001$) [Figure 4.2.B]. The significant difference that was observed in IFN-γ levels secreted from splenocytes of groups III and IV [Figure 4.2.B] could be due to kinetics of T cell activation. IFN-γ analysis using ELISpot in our study was performed on day 14 which is four days after the booster immunization in group IV. Lack of INF-γ secretion in group IV [Figure 4.2.B] suggests that after immunization, T cells require more than four days to be activated and secrete IFN-γ cytokine. On the other hand, high levels of IFN-γ that was detected seven days after booster immunization in group III [Figure 4.2.B] implies that T cells are activated by day seven after immunization. Therefore, this data suggests that T cell activation possibly happens somewhere between four to seven days after booster immunization. Our data is similar to a study previously reported the peak of T cell activation on day 5 following antigen administration in a PLGA nanoparticle.[44]

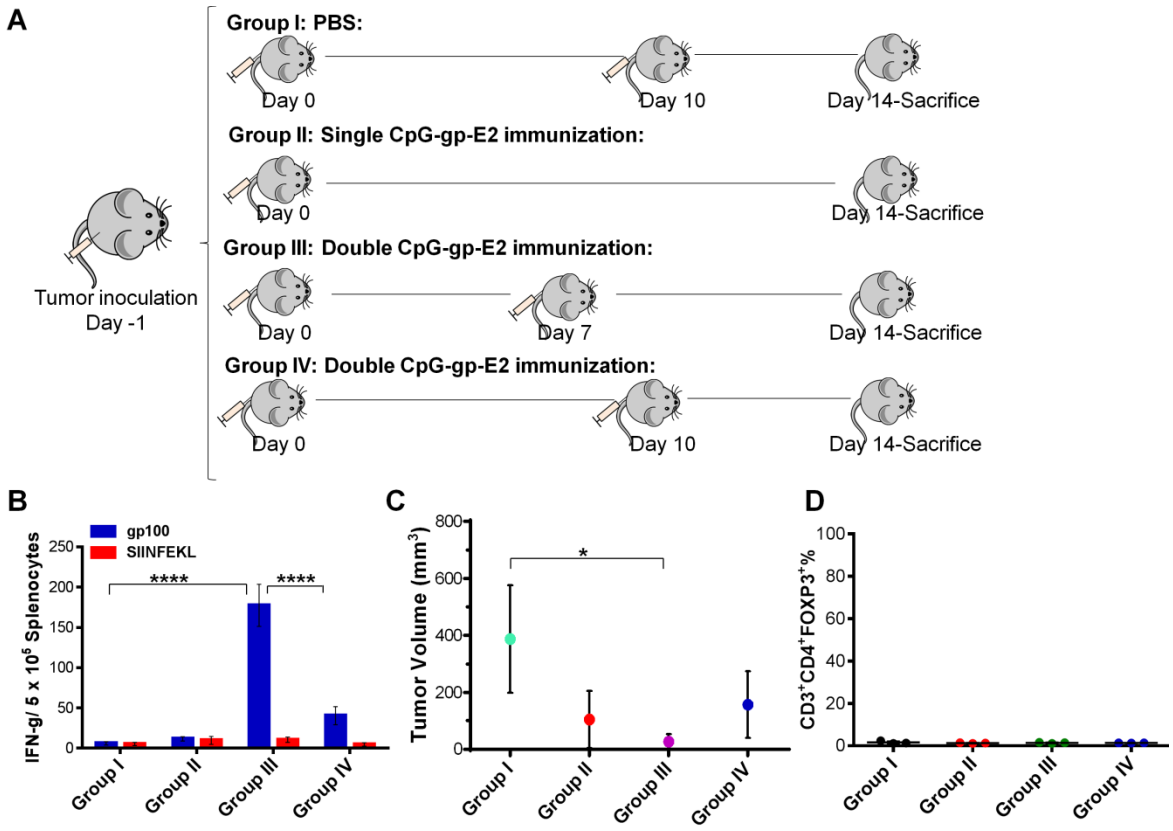

Figure 4.2. ELISpot Analysis of Splenocytes and Tumor Size Data on Day 14. A) Schematic of different nanoparticle immunization regimen/schedule [groups II-IV]. **B)** Summary of averaged ELISpot data, which evaluated antigen-specific IFN-γ secretion. C57BL/6 mice were immunized with different regimen [groups II-IV], and splenocytes were pulsed *ex vivo* in the presence of relevant peptide [gp100] or irrelevant peptide [SIINFEKL] and analyzed for specific IFN-γ secretion. Higher gp100 epitope-specific IFN-γ secretion was observed for group II [n_{total}=7]. **C)** Tumor size on day 14. Double immunization with CpG-gp-E2 (group III) significantly decreased the tumor growth compared to other groups [n_{total}=7]. **D)** $CD4^+FoxP3^+$ cell percentage in splenocytes. Immunization with CpG-gp-E2 nanoparticle did not increase the T_{reg} percentage. $CD4^+FoxP3^+$ cell percentage was only examined for 3 mice [n_{total}=3] per each group [*p < 0.05; ****p < 0.0001].

4.4.3. Double Immunization with CpG-gp-E2 Nanoparticle Increased the CD8 T Cell Count in Spleen

Tumor infiltrating lymphocytes, mainly cytotoxic CD8 T cells, are responsible for killing the cancer cells and destroying the tumor.[45,46] It has been reported in some cases that higher CD8 T cell responses can be achieved in the presence of activated CD4 T cells.[47]

Therefore, in this experiment we examined if immunization with CpG-gp-E2 nanoparticle could increase the T cell proliferation in spleens isolated from mice. It is well accepted that anti-tumor T cell activation and proliferation are initiated within secondary lymphoid tissues such as spleen. Therefore, we first examined the T cell proliferation in spleen.

Our data confirmed that T cells are proliferated in the splenocytes isolated from the mice that received double immunization of CpG-gp-E2 nanoparticle, groups III and IV. Spleens isolated from mice immunized with CpG-gp-E2 nanoparticle and specifically spleens isolated from group III were larger in size compared to PBS control group [Figure 4.3.A]. This increase in size could be an indication of lymphocytes proliferation. Nanoparticle-mediated delivery of CpG was also previously shown by others to increase spleen size.[48]

Examination of spleens isolated from group III and IV revealed proliferation in both CD8 [Figure 4.3.E] and CD4 T cells [Figure 4.3.F], although the overall percentage of these cell types have not changed significantly [Figure 4.3.C, 4.3.D]. Representative flow data are presented in Figure 4.3.B. Higher T cell proliferation observed in splenocytes isolated from groups III and IV (double immunization) compared to group II (single immunization) supports the need of a booster immunization for inducing a greater T cell proliferation [Figure 4.3.E, 4.3.F]. We observed approximately twice as many CD8 T cells in spleens isolated from group III compared to PBS control group, ($p < 0.0001$) [Figure 4.3.E]. Also, CD8 T cell count in splenocytes isolated from group IV is significantly higher than CD8 T cell count of splenocytes in PBS group, ($p < 0.001$) [Figure 4.3.E].

Furthermore, higher CD4 counts [Figure 4.3.F], with no increase in percentage of $FoxP3^+$ [Figure 4.2.D], was observed in splenocytes of group III compared to the PBS

control group. Since the gp100 epitope that we used in our system is an MHC-I restricted (CD8) epitope it was somewhat surprising to observe an increase in CD4 T cell frequencies. However, this increase could be a result of homeostatic expansion of CD4 or activation of autoreactive CD4 T cells.[49] One other possible explanation could be the presence of a CD4-restricted epitope (T-helper epitope) in the E2 nanoparticle itself. However, further investigations are needed to discover the possibility of the presence of any T-helper epitope within the E2 nanoparticle.

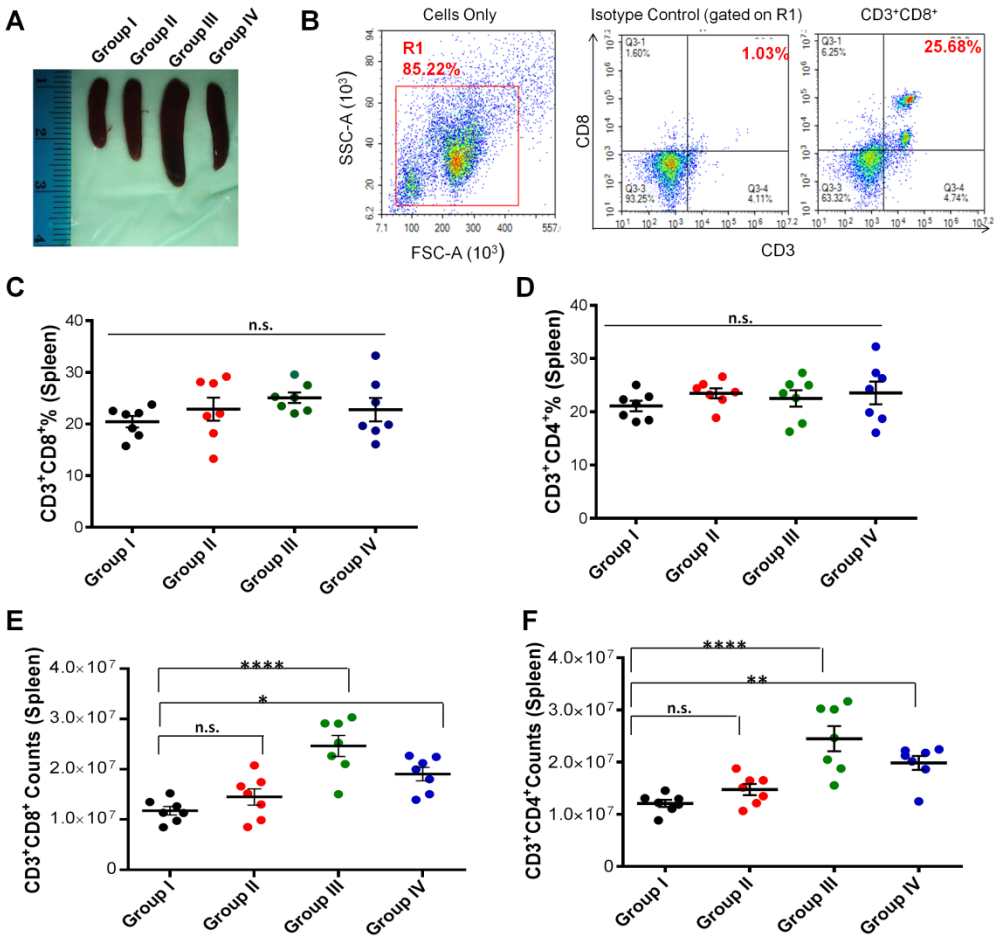

Figure 4.3. T Cell Population in Splenocytes. A) A representative of spleens isolated from different groups. Spleen isolated from group III is considerably larger in size compared to other groups. **B)** A representative data of flow cytometry. **C)** No differences have been observed in CD8 T cell percentage between groups. **D)** No differences have been observed in CD4 T cell percentage between groups. **E)** Significantly higher CD8 T cell count was observed for groups with double CpG-gp-E2 nanoparticle immunization [groups III & IV]. **F)** Significantly higher CD4 T cell count was observed for groups with double CpG-gp-E2 nanoparticle immunization [groups III & IV]. C57BL/6 mice inoculated with B16-F10 received different nanoparticle immunizations [groups II-IV]. Splenocytes were isolated and stained for T cell subsets and analyzed with flow cytometer. Higher CD8 and CD4 T cell counts were observed for groups that received double immunizations of CpG-gp-E2, groups III & IV, [$n_{total} = 7$], *$p < 0.05$; **$p < 0.01$; ***$p < 0.001$.

4.4.4. Double Immunization with CpG-gp-E2 Increased Percentage of Tumor Infiltrating T cell in the Tumor Mass/Microenvironment

Tumor microenvironments (TME) contain immune cells such as T cells. Since tumor infiltrating cytotoxic CD8 T cells are usually a major component of anti-tumor responses,[45] we evaluated the percentage of CD8 T cells in the tumor mass. Others reported that high anti-tumor responses observed in breast, glioblastoma, and cervical cancers were in association with elevated levels of cytotoxic $CD8^+$ T cells in the TME.[50]

Immunization with CpG-gp-E2 nanoparticles (groups II-IV) significantly increased CD8 T cell percentage in tumor microenvironment, with group III showing the most significant increase, ($p < 0.01$) [Figure 4.4.A]. Vaccination with CpG-gp-E2 (group III) resulted in ~ 10 fold increase in CD8 T cell percentage compared to the PBS control group [Figure 4.4.A]. Also, single and double vaccinations (groups II & IV) resulted in ~ 5 fold increase compared to the PBS control group [Figure 4.4.A]. Because tumors were only detected in 2 mice in group III, we have fewer tumor data points for this group compared to other groups [Figure 4.4.C, 4.4.E]. Data of group III demonstrating higher IFN-γ responses [Figure 4.2.B], enhanced splenocyte CD8 T cell count [Figure 4.3.E], elevated CD8 T cell percentage in TME [Figure 4.4.A], and slower tumor growth [Figure 4.2.C] suggest that the CD8 T cells elicited from immunization are possibly responsible for the observed anti-tumor responses.

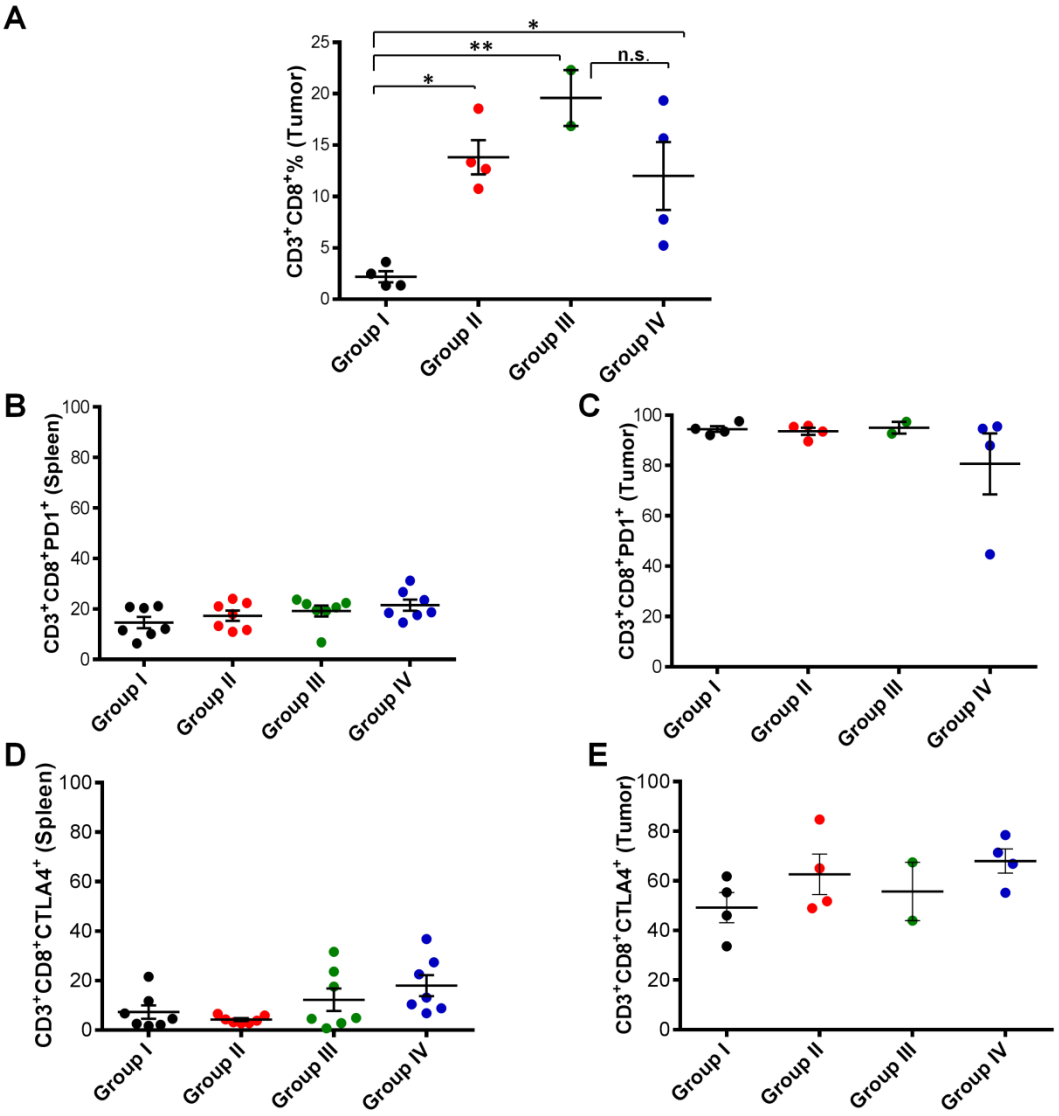

Figure 4.4. CD8 T Cell Percentage in Tumor Mass. A) Higher CD8 T cell percentage in TME was observed for the groups that were immunized with CpG-gp-E2 nanoparticle [groups II-IV]. **B)** PD-1 expression on splenocytes CD8 T cells. **C)** High PD-1 expression levels was observed on TILs, CD8 T cells. **D)** CTLA-4 expression on splenocytes CD8 T cells. **E)** High CTLA-4 expression levels was observed on TILs, CD8 T cells. C57BL/6 mice that were challenged with B16-F10 received different regimen of CpG-gp-E2 immunization. Tumor was isolated and checked for CD8 T cell responses. Higher CD8 T cell percentage was observed for groups that received double immunizations of CpG-gp-E2. Higher levels of PD-1 and CTLA-4 expressions were observed on TILs compared to CD8 T cells of splenocytes,*$p < 0.05$; **$p < 0.01$.

To evaluate the potential for immune checkpoint inhibitor treatment in combination with CpG-gp-E2 vaccine (section 3.5), we first assessed PD-1 and CTLA-4 expression on CD8 T cells. Tumor-infiltrating CD8 T cells highly expressed PD-1 and CTLA-4 in all groups [Figure 4.4.C, 4.4.E], whereas the expression of these molecules was significantly lower on CD8 T cells within the spleen [Figure 4.4.B, 4.4.D].

Naïve CD8 T cells scan the secondary lymph organs (*e.g.,* spleen) in search of their cognate antigen epitope. T cells are activated only if the TCR recognize their unique antigen epitope.[51] Therefore, after CpG-gp-E2 nanoparticle immunization, and in early stages of T cell activation within spleen, T cells are activated if their TCR binds to the gp100 epitope-MHC-I complex. However, T cells remain naive, with no PD-1 or CTLA-4 expression, if their TCRs cannot recognize the gp100 epitope. Therefore, it is not surprising that after CpG-gp-E2 nanoparticle immunization only a small percentage of T cells in spleen, with TCR specific for gp100, are activated and express PD-1 and/or CTLA-4 [Figure 4.4.B, 4.4.D]. However, high PD-1 and CTLA-4 expression levels on tumor-infiltrating lymphocytes (TILs) [Figure 4.4.C, 4.4.E] indicates the presence of activated T cells in the TME. High expression of PD-1 and CTLA-4 on TILs has been also observed previously by others.[52,53]

Our data implied that double immunization with CpG-gp-E2 nanoparticle (group III, Figure 4.2.A) would be the most effective in inducing CD8 T cell, specific IFN-γ, and antitumor responses compared to other groups studied in this work. Therefore, we hypothesized that immunization with CpG-gp-E2, using group III immunization regimen, in combination with checkpoint inhibitor treatment would increase the efficacy compared to each treatment separately. However, our initial combination study of CpG-gp-E2

nanoparticle with anti-CTLA-4 did not result in any animal survival improvements, compared to each treatment separately (see Appendix B). This poor outcome could possibly be improved by optimizing the experimental design. Our data indicates a relatively higher PD-1 expression than CTLA-4 on TILs [Figure 4.4.C, 4.4.E]. Therefore, blocking PD-1 should be more promising than blocking the CTLA-4. Furthermore, it has been reported that PD-1 blockade treatment has a lower incidence rate of immune-adverse events compared to CTLA-4.[16,54] Also, human clinical trials blockade of the PD1-PDL1 interaction is more effective than blockade of the CTLA4 pathway. Therefore, we decided to explore the effects of combination study of CpG-gp-E2 with anti-PD-1 instead of optimizing our experimental design with anti-CTLA-4.

4.4.5. Combination of CpG-gp-E2 Nanoparticle Vaccine with Anti-PD1 Antibody Significantly Increased Animal Survival

As our hypothesis predicted, administration of CpG-gp-E2 nanoparticle in combination with anti-PD-1 therapy significantly increased survival of tumor-bearing mice, compared to each treatment separately. C57BL/6 mice were inoculated with 10^4 of B16-F10 cells. Mice were randomly assigned into four different groups: anti-PD-1, CpG-gp-E2, combination of both, and PBS as a control [Figure 4.5.A]. Our data showed that immunization with CpG-gp-E2 nanoparticle alone significantly increased animal survival (median survival of 36 days), compared to PBS-injected mice (median survival of 26 days; $p < 0.001$) [Figure 4.5.B]. This data has demonstrated the CpG-gp-E2 nanoparticle ability in inducing anti-tumor responses, which is consistent with our prior data [Chapter 2].[55] Treatment with anti-PD1 antibody alone also prolonged survival time (median survival of 31 days), compared to PBS group (median survival of 26 days, $P < 0.01$), but not as effective

as combination treatment [Figure 4.5.B]. Our data is consistent with prior mouse studies demonstrating the ability of anti-PD-1 antibody (alone) in inducing partial anti-tumor responses,[26,27,56] and with clinical results showing a fraction of survival about 20%. [5,6]

Interestingly, the group that received combination treatment of CpG-gp-E2 particle and anti-PD-1 showed the most significant survival compared to CpG-gp-E2 alone ($P < 0.001$) or anti-PD1 ($p < 0.001$)[Fig. 5]. All animals in CpG-gp-E2 group were sacrificed by day 53 (0% survival). Also, all animals in anti-PD-1 group were sacrificed by day 45, except one mouse that stayed tumor free (~5% survival). However, approximately 50% of mice that received combination treatment stayed tumor-free until end of the experiment (day 60) [Figure 4.5.B].

The significant increase in animal survival of the combined group confirms the advantages of combinatory treatment compared to each treatment alone. in Current clinical therapies using anti-PD-1 antibodies do not result in long-term remission for the majority of patients.[5] Our data indicates that the low therapeutic outcome of PD-1 inhibitor treatment can possibly be improved if the treatment is administered in combination with E2 antigen-delivery nanoparticle. Our data is similar to a study previously reported a higher survival (~ 30% tumor-free mice) for animals that received dendritic cell vaccination and anti-PD-1 in combination, compared to each treatment separately. [26] Enhanced anti-tumor responses was also observed when anti-PD-1 antibody was administered in combination with multi-peptide vaccine.[27]

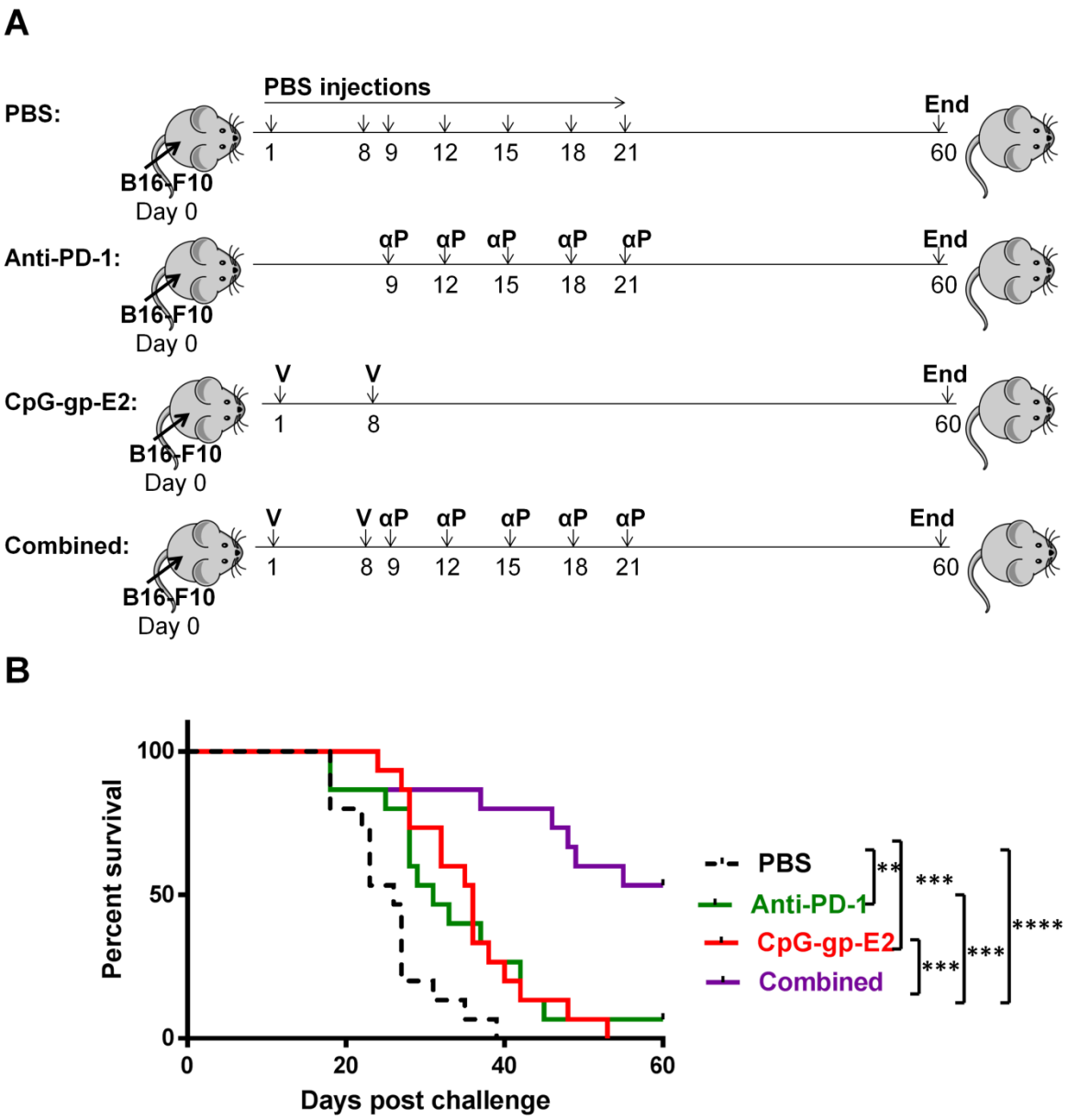

Figure 4.5. Survival Curve of Animals in Combination Study. A) Schematic of anti-PD-1 and CpG-gp-E2 administration regimen in different groups [V = vaccine; αP = anti-PD-1]. B) Combination of CpG-gp-E2 nanoparticle immunization and anti-PD-1 treatment increased survival time compared to each immunization/treatment separately. C57BL/6 mice were inoculated with B16-F10 cells followed by treatment groups of control [PBS], checkpoint inhibitor alone [anti-PD-1], nanoparticle alone [CpG-gp-E2], and combination of anti-PD-1 with CpG-gp-E2 [combined] [n_{total} = 15], **p< 0.01; ***p < 0.001; ****p < 0.0001.

One of the features expected by administration of a cancer vaccine is the induction of memory cells that can be expanded on recall and protect individuals against recurring cancer.[57] Therefore, generating memory responses after cancer treatment should be an ultimate goal of cancer vaccines. To investigate whether memory cells were generated after our combination treatment, we re-challenged the tumor-free mice from the combined group with 10^4 of B16-F10 cells. Mice did not receive any further nanoparticle immunization or anti-PD1 therapy; and naive (unimmunized) mice were used as control for this study. A significant increase was observed in survival time of re-challenged mice from the combined group compared to naive control group ($p < 0.01$) [Figure 4.6]. The significant increase in the survival time of re-challenged mice suggests that memory responses can be elicited after combination treatment of the nanoparticle with anti-PD-1 antibody. Induction of memory cells and tumor protection upon re-challenge was also previously shown by others, after administration of CpG and ovalbumin-conjugated nanoparticles.[58] Also, accumulation of memory T Cells was observed following combination therapy of multi-peptide cancer vaccine and anti-PD-1 antibody.[27]

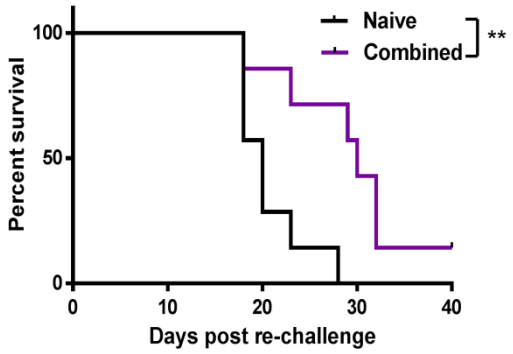

Figure 4.6. Survival Curve of Mice from the Combined Group after Tumor Re-Inoculation. Tumor free mice from combination study were re-inoculated with B16-F10 with no further immunizations. Combination of CpG-gp-E2 nanoparticle immunization and anti-PD-1 treatment increased the survival time upon tumor re-challenge (n_{total} = 7), **p < 0.01.

Furthermore, at the end of the combination experiment, tumors were examined for MHC-I, gp100, and PD-L1 expression (4 mice were chosen randomly from each group to be tested). It has been known that tumor cells can escape immune responses by MHC-I downregulation, antigen mutation or downregualtion and/or PD-L1 upregulation.[59] Our data indicates a low MHC-I expression in tumor cells isolated from PBS, CpG-gp-E2, anti-PD-1, and combined groups [Figure 4.7.A]. Low expression of MHC-I in such a low immunogenic tumor model, B16-F10, is not surprising, as other studies have also detected low expression of MHC-I on B16 melanoma cells.[60,61]

Interestingly, immunization with CpG-gp-E2 nanoparticles alone or in combination with anti-PD-1, significantly dropped the levels of MHC-I expression compared to the PBS control group [Figure 4.7.A]. MHC-I expression is a critical step in the induction of tumor rejection.[62,63] Lower MHC-I expression in CpG-gp-E2 and combined groups implies that tumor cells eventually downregulated the levels of MHC-I expression to evade the higher/stronger specific CD8 T cell responses in the TME. Furthermore, we did not detect

any gp100-antigen downregulation in any of the groups [Figure 4.7.B], suggesting that tumor escape is likely not due to changes in antigen expression levels on the tumor cells.

Combination treatment of anti-PD-1 with CpG-gp-E2 nanoparticle resulted in PD-L1 downregulation [Figure 4.7.C]. This suggests that cancer cells downregulated PD-L1 to possibly attenuate the anti-PD-1 therapy and produce resistance to the drug. Our data is similar to a study previously reported PD-L1 promoter methylation and subsequently PD-L1 down-regulation in non-small cell lung cancer (NSCLC) in the mouse model.[64] It was also reported that adaptive resistance to PD-1 treatment was associated with upregulation of alternative immune checkpoints such as T-cell immunoglobulin mucin-3 (TIM-3), and not PD-L1 upregulation.[65]

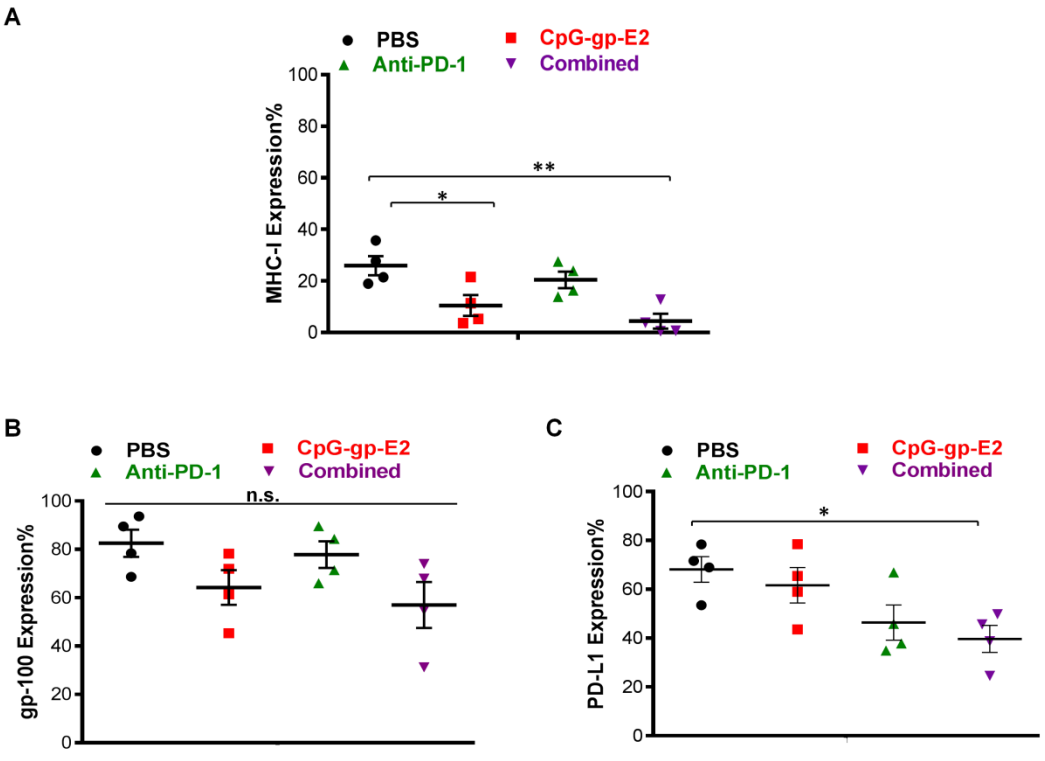

Figure 4.7. Expression of MHC-I, gp100, and PD-L1 on Tumor Cells. A) MHC-I expression level was significantly decreased on tumor cells isolated from CpG-gp-E2 and combined groups compared to the PBS group. **B)** gp-100 expression levels remained almost the same within the groups. **C)** PD-L1 expression was downregulated in the combined group compared to the PBS control group (n = 4), *p < 0.05, **p < 0.01.

4.5. Conclusions

In this study, we have investigated the effects of combination of our protein nanoparticle-antigen platform with anti-PD-1 antibody. We examined different nanoparticle administration regimens in order to find the most effective schedule in mounting cell-mediated anti-tumor immune responses. We found that a booster seven days after prime immunization with E2-antigen delivery formulations resulted in an increase in specific IFN-γ frequencies, elevated CD8 T cell counts in both spleen and tumor microenvironment, and a slower tumor growth. Further, we observed a significantly higher

animal survival time when anti-PD-1 antibody treatment was combined with CpG-gp-E2 nanoparticle (~ 50% remission), compared to each therapy/vaccine separately, with only ~5% remission for anti-PD-1 treatment separately. Additionally, we found that tumor escape could be due to MHC-I downregulation on the tumor cells. Altogether, this work shows the advantage of combination of anti-PD-1 therapy with E2-antigen delivery system as an effective way to significantly increase the efficacy of the immune checkpoint inhibitor treatment. Combination therapy of anti-PD1 with protein-based nanoparticle vaccines could be promising for enhancing cancer treatment efficacies.

4.6. Acknowledgment

Flow cytometer was carried out at the UCI Flow Cytometry Core Facility, Institute for Immunology. This work was supported by the National Institute of Health (R21EB017995) and the National Cancer Institute of the National Institutes of Health (P30CA062203).

4.7. References

1. Pardoll, D. M. The blockade of immune checkpoints in cancer immunotherapy. *Nat. Rev. Cancer* **12,** 252–264 (2012).
2. Villadolid, J. & Amin, A. Immune checkpoint inhibitors in clinical practice : update on management of immune-related toxicities. *Trans Lung Cancer Res*. **4,** 560–575 (2015).
3. Fife, B. T. & Bluestone, J. A. Control of peripheral T-cell tolerance and autoimmunity via the CTLA-4 and PD-1 pathways. *Immunol. Rev.* **224,** 166–182 (2008).
4. Francisco, L. M., Sage, P. T. & Sharpe, A. H. The PD-1 pathway in tolerance and autoimmunity. *Immunol. Rev.* **236,** 219–242 (2010).
5. Postow, M. A., Callahan, M. K. & Wolchok, J. D. Immune checkpoint blockade in cancer therapy. *J. Clin. Oncol.* **33,** 1974–1982 (2015).
6. Maio, M., Grob, J. J., Aamdal, S., Bondarenko, I., Robert, C., Thomas, L., Garbe, C., Chiarion-Sileni, V., Testori, A., Chen, T. T., Tschaika, M. & Wolchok, J. D. Five-year survival rates for treatment-naive patients with advanced melanoma who received ipilimumab plus dacarbazine in a phase III trial. *J. Clin. Oncol.* **33,** 1191–1196 (2015).
7. Topalian, S. L., Drake, C. G. & Pardoll, D. M. Immune checkpoint blockade: A common denominator approach to cancer therapy. *Cancer Cell* **27,** 451–461 (2015).
8. Sharpe, A. H. & Pauken, K. E. The diverse functions of the PD1 inhibitory pathway. *Nat. Rev. Immunol.* **18,** 153–167 (2018).
9. Chambers, C. a & Allison, J. P. Co-stimulation in T cell responses. *Curr. Opin. Immunol.* **9,** 396–404 (1997).
10. Chen, L. Co-inhibitory molecules of the B7-CD28 family in the control of T-cell immunity. *Nat. Rev. Immunol.* **4,** 336–347 (2004).
11. Huang, J. F., Yang, Y., Sepulveda, H., Shi, W., Hwang, I., Peterson, P. a, Jackson, M. R., Sprent, J. & Cai, Z. TCR-Mediated internalization of peptide-MHC complexes acquired by T cells. *Science* **286,** 952–954 (1999).
12. Sansom, D. M. CD28, CTLA-4 and their ligands: Who does what and to whom? *Immunology* **101,** 169–177 (2000).
13. Linsley, P. S., Greene, J. L., Brady, W., Bajorath, J., Ledbetter, J. A. & Peach, R. Human B7-1 (CD80) and B7-2 (CD86) bind with similar avidities but distinct kinetics to CD28 and CTLA-4 receptors. *Immunity* **1,** 793–801 (1994).
14. Blank, C., Gajewski, T. F. & Mackensen, A. Interaction of PD-L1 on tumor cells with PD-1 on tumor-specific T cells as a mechanism of immune evasion: Implications for tumor immunotherapy. *Cancer Immunol. Immunother.* **54,** 307–314 (2005).
15. Iwai, Y., Ishida, M., Tanaka, Y., Okazaki, T., Honjo, T. & Minato, N. Involvement of PD-L1 on tumor cells in the escape from host immune system and tumor immunotherapy by PD-L1 blockade. *Proc. Natl. Acad. Sci.* **99,** 12293–12297 (2002).
16. Buchbinder, E. I. & Desai, A. CTLA-4 and PD-1 pathways similarities, differences, and implications of their inhibition. *Am. J. Clin. Oncol. Cancer Clin. Trials* **39,** 98–106 (2016).
17. Lipson, E. J. & Drake, C. G. Ipilimumab: An anti-CTLA-4 antibody for metastatic melanoma. *Clin. Cancer Res.* **17,** 6958–6962 (2011).
18. Larkin, J., Chiarion-Sileni, V., Gonzalez, R., Grob, J. J., Cowey, C. L., Lao, C. D., Schadendorf, D., Dummer, R., Smylie, M., Rutkowski, P., Ferrucci, P. F., Hill, A.,

Wagstaff, J., Carlino, M. S., Haanen, J. B., Maio, M., Marquez-Rodas, I., McArthur, G. A., Ascierto, P. A., Long, G. V., Callahan, M. K., Postow, M. A., Grossmann, K., Sznol, M., Dreno, B., Bastholt, L., Yang, A., Rollin, L. M., Horak, C., Hodi, F. S. & Wolchok, J. D. Combined Nivolumab and Ipilimumab or Monotherapy in Untreated Melanoma. *N. Engl. J. Med.* **373,** 23–34 (2015).

19. Melero, I., Gaudernack, G., Gerritsen, W., Huber, C., Parmiani, G., Scholl, S., Thatcher, N., Wagstaff, J., Zielinski, C., Faulkner, I. & Mellstedt, HMelero, I., Gaudernack, G., Gerritsen, W., Huber, C., Parmiani, G., Scholl, S., Thatcher, N., Wagstaff, J, H. Therapeutic vaccines for cancer: an overview of clinical trials. *Nat Rev Clin Oncol* **11,** 509–524 (2014).
20. Van Der Burg, S. H., Arens, R., Ossendorp, F., Van Hall, T. & Melief, C. J. M. Vaccines for established cancer: Overcoming the challenges posed by immune evasion. *Nat. Rev. Cancer* **16,** 219–233 (2016).
21. Chowdhury, P. S., Chamoto, K. & Honjo, T. Combination therapy strategies for improving PD-1 blockade efficacy: a new era in cancer immunotherapy. *J. Intern. Med.* **283,** 110–120 (2018).
22. Ali, O. A., Lewin, S. A., Dranoff, G. & Mooney, D. J. Vaccines Combined with Immune Checkpoint Antibodies Promote Cytotoxic T-cell Activity and Tumor Eradication. *Cancer Immunol. Res.* **4,** 95–100 (2016).
23. Wong, K. K., Li, W. W. A., Mooney, D. J. & Dranoff, G. *Advances in Therapeutic Cancer Vaccines*. *Advances in Immunology* **130,** 191-249 (2016).
24. Zhao, L., Seth, A., Wibowo, N., Zhao, C., Mitter, N., Yu, C. & Middelberg, A. P. J. Nanoparticle vaccines. *Vaccine* **32,** 327–337 (2014).
25. Neek, M., Kim, T. I & Wang, S. W. Protein-based nanoparticles in cancer vaccine development. *Nanomedicine Nanotechnology, Biol. Med.* **15,** 164–174 (2019).
26. Antonios, J. P., Soto, H., Everson, R. G., Orpilla, J., Moughon, D., Shin, N., Sedighim, S., Yong, W. H., Li, G., Cloughesy, T. F., Liau, L. M. & Prins, R. M. PD-1 blockade enhances the vaccination-induced immune response in glioma. *JCI Insight* **1,** 1–13 (2016).
27. Karyampudi, L., Lamichhane, P., Scheid, A. D., Kalli, K. R., Shreeder, B., Krempski, J. W., Behrens, M. D. & Knutson, K. L. Accumulation of memory precursor cd8 t cells in regressing tumors following combination therapy with vaccine and anti-pd-1 antibody. *Cancer Res.* **74,** 2974–2985 (2014).
28. Chen, J., Chen, L., Zhang, H. & Quan, Y. Enhancing the antitumour-specific immunity of a lung DNA vaccine in vivo by fusion expression of MAGE-A3 and soluble PD-1. *Biotechnology & Biotechnological Equipment* **31,** 1064-1069 (2017).
29. Molino, N. M., Neek, M., Tucker, J. A., Nelson, E. L. & Wang, S. Biomaterials Viral-mimicking protein nanoparticle vaccine for eliciting anti-tumor responses. *Biomaterials* **86,** 83–91 (2016).
30. Neek, M., Tucker, J. A., Kim, T. I, Molino, N. M., Nelson, E. L. & Wang, S. W. Co-delivery of human cancer-testis antigens with adjuvant in protein nanoparticles induces higher cell-mediated immune responses. *Biomaterials* **156,** 194–203 (2018).
31. Dalmau, M., Lim, S., Chen, H. C., Ruiz, C. & Wang, S. W. Thermostability and molecular encapsulation within an engineered caged protein scaffold. *Biotechnol. Bioeng.* **101,** 654–664 (2008).
32. Molino, N. M., Anderson, A. K. L., Nelson, E. L. & Wang, S. W. Biomimetic protein nanoparticles facilitate enhanced dendritic cell activation and cross-presentation.

ACS Nano **7,** 9743–9752 (2013).
33. Kalli, F., Machiorlatti, R., Battaglia, F., Parodi, A., Conteduca, G., Ferrera, F., Proietti, M., Tardito, S., Sanguineti, M., Millo, E., Fenoglio, D., Palma, R. De, Inghirami, G. & Filaci, G. Comparative analysis of cancer vaccine settings for the selection of an effective protocol in mice. *J Transl Med*. 120, 1–11 (2013).
34. Reddy, S. T., van der Vlies, A. J., Simeoni, E., O'Neil, C. P., Swartz, M. A. & Hubbell, J. A. Exploiting lymphatic transport and complement activation in nanoparticle vaccines. *Nat. Biotechnol.* **25,** 1159-1164 (2007).
35. Bachmann, M. F. & Jennings, G. T. Vaccine delivery: a matter of size, geometry, kinetics and molecular patterns. *Nat. Rev. Immunol.* **10,** 787–96 (2010).
36. Reddy, S. T., Rehor, A., Schmoekel, H. G., Hubbell, J. A. & Swartz, M. A. In vivo targeting of dendritic cells in lymph nodes with poly (propylene sulfide) nanoparticles. *J. Control. Release* **112,** 26–34 (2006).
37. Bachmann, M. F. & Jennings, G. T. Vaccine delivery : a matter of size , geometry , kinetics and molecular patterns. *Nat. Publ. Gr.* **10,** 787–796 (2010).
38. Lawrence, C. W. & Braciale, T. J. Activation, Differentiation, and Migration of Naive Virus-Specific CD8 + T Cells during Pulmonary Influenza Virus Infection. *J Immunol.* **2,** 1209-1218 (2004).
39. Liston, A. & Gray, D. H. D. Homeostatic control of regulatory T cell diversity. *Nat. Publ. Gr.* **14,** 154–165 (2014).
40. Josefowicz, S. Z., Lu, L. & Rudensky, A. Y. Regulatory T cells Mechanisms of Differentiation and Function. *Annual Review of Immunology* 30, 531-564 (2012).
41. Wang, X., Chen, X., Manjili, M. H., Repasky, E., Henderson, R. & & Subjeck, J. R. Targeted Immunotherapy Using Reconstituted Chaperone Complexes of Heat Shock Protein 110 and Melanoma-associated Antigen gp100 1. *Cancer Res.* **63,** 2553–2560 (2003).
42. Xu, Z., Ramishetti, S., Tseng, Y. C., Guo, S., Wang, Y. & Huang, L. Multifunctional nanoparticles co-delivering Trp2 peptide and CpG adjuvant induce potent cytotoxic T-lymphocyte response against melanoma and its lung metastasis. *J. Control. Release* **172,** 259–265 (2013).
43. Zhang, Z., Tongchusak, S., Mizukami, Y., Kang, Y. J., Ioji, T., Touma, M., Reinhold, B., Keskin, D. B., Reinherz, E. L. & Sasada, T. Induction of anti-tumor cytotoxic T cell responses through PLGA-nanoparticle mediated antigen delivery. *Biomaterials* **32,** 3666–3678 (2011).
44. Iii, E. F. P., Hackett, R. H., Akai, H., Igarashi, K., Finbloom, D. S. & Larner, A. C. Modulation of Interferon Signaling in Human Fibroblasts by Phorbol Esters. **12,** 4486–4495 (1992).
45. Mahmoud, S. M. A., Paish, E. C., Powe, D. G., Macmillan, R. D. & Grainge, M. J. Tumor-Infiltrating CD8 (+) Lymphocytes Predict Clinical Outcome in Breast Tumor-Infiltrating CD8 Lymphocytes Predict Clinical Outcome in Breast Cancer. *J Clin Oncol*. 29:1949-1955 (2011).
46. Andersen, M. H., Pedersen, L. Ø., Capeller, B., Bro, E., Becker, C. & Straten, P. Advances in Brief Spontaneous Cytotoxic T-Cell Responses against Survivin-derived MHC Class I-restricted T-Cell Epitopes in Situ As Well As ex Vivo in Cancer Patients. *Cancer Res.* **1.** 5964–5968 (2001).
47. Knutson, K.L. & Disis, M.L. Tumor antigen-specific T helper cells in cancer immunity

and immunotherapy. *Cancer Immunol Immunother.* 54, 721-728 (2005).
48. Bourquin, C., Anz, D., Zwiorek, K., Lanz, A.-L., Fuchs, S., Weigel, S., Wurzenberger, C., von der Borch, P., Golic, M., Moder, S., Winter, G., Coester, C. & Endres, S. Targeting CpG Oligonucleotides to the Lymph Node by Nanoparticles Elicits Efficient Antitumoral Immunity. *J. Immunol.* **181,** 2990-2998 (2008).
49. Min, B., Yamane, H., Hu-Li, J. & Paul, W. E. Spontaneous and Homeostatic Proliferation of CD4 T Cells Are Regulated by Different Mechanisms. *J. Immunol.* **174,** 6039–6044 (2005).
50. Maimela, N. R., Liu, S. & Zhang, Y. Fates of CD8+ T cells in Tumor Microenvironment. *Comput. Struct. Biotechnol. J.* **17,** 1–13 (2018).
51. Zhang, N. & Bevan, M. J. CD8 + T Cells: Foot Soldiers of the Immune System Introduction to Cytotoxic T Cells. *Immunity* **35,** 161–168 (2011).
52. Bialkowski, L., Van der Jeught, K., Bevers, S., Tjok Joe, P., Renmans, D., Heirman, C., Aerts, J. L. & Thielemans, K. Immune checkpoint blockade combined with IL-6 and TGF-β inhibition improves the therapeutic outcome of mRNA-based immunotherapy. *Int. J. Cancer* **143,** 686–698 (2018).
53. Kondo, Y., Ohno, T., Nishii, N., Harada, K., Yagita, H. & Azuma, M. Differential contribution of three immune checkpoint (VISTA, CTLA-4, PD-1) pathways to antitumor responses against squamous cell carcinoma. *Oral Oncol.* **57,** 54–60 (2016).
54. Iwai, Y., Hamanishi, J., Chamoto, K. & Honjo, T. Cancer immunotherapies targeting the PD-1 signaling pathway. *J. Biomed. Sci.* **24,** 1–11 (2017).
55. Molino, N. M., Neek, M., Tucker, J. A., Nelson, E. L. & Wang, S. W. Biomaterials Viral-mimicking protein nanoparticle vaccine for eliciting anti-tumor responses. *Biomaterials* **86,** 83–91 (2016).
56. Fu, J., Malm, I. J., Kadayakkara, D. K., Levitsky, H., Pardoll, D. & Kim, Y. J. Preclinical evidence that PD1 blockade cooperates with cancer vaccine TEGVAX to elicit regression of established tumors. *Cancer Res.* **74,** 4042–4052 (2014).
57. Sad, S. & Krishnan, L. Maintenance and attrition of T-cell memory. *Crit. Rev. Immunol.* **23,** 129–147 (2003).
58. de Titta, A., Ballester, M., Julier, Z., Nembrini, C., Jeanbart, L., van der Vlies, A. J., Swartz, M. A. & Hubbell, J. A. Nanoparticle conjugation of CpG enhances adjuvancy for cellular immunity and memory recall at low dose. *Proc. Natl. Acad. Sci.* **110,** 19902–19907 (2013).
59. Rabinovich, G. A., Gabrilovich, D. & Sotomayor, E. M. Immunosuppressive Strategies that are Mediated by Tumor Cells. *Annu. Rev. Immunol.* **25,** 267–296 (2007).
60. Riond, J., Rodriguez, S., Nicolau, M. L., Saati, T. Al & Gairin, J. E. In vivo major histocompatibility complex class I (MHCI) expression on MHCIlowtumor cells is regulated by γδ T and NK cells during the early steps of tumor growth. *Cancer Immun.* **9,** 1–11 (2009).
61. Mansour, M., Pohajdak, B., Kast, W. M., Fuentes-Ortega, A., Korets-Smith, E., Weir, G. M., Brown, R. G. & Daftarian, P. Therapy of established B16-F10 melanoma tumors by a single vaccination of CTL/T helper peptides in VacciMax. *J. Transl. Med.* **5,** 20-28 (2007).
62. Turcotte, S., Katz, S. C., Shia, J., Jarnagin, W. R., Kingham, T. P., Allen, P. J., Fong, Y., D'Angelica, M. I. & DeMatteo, R. P. Tumor MHC Class I Expression Improves the Prognostic Value of T-cell Density in Resected Colorectal Liver Metastases. *Cancer*

Immunol. Res. **2,** 530–537 (2014).
63. Garrido, F., Aptsiauri, N., Doorduijn, E. M., Garcia Lora, A. M. & van Hall, T. The urgent need to recover MHC class I in cancers for effective immunotherapy. *Curr. Opin. Immunol.* **39,** 44–51 (2016).
64. Zhang, Y., Xiang, C., Wang, Y., Duan, Y. & Liu, C. PD-L1 promoter methylation mediates the resistance response to anti-PD-1 therapy in NSCLC patients with EGFR-TKI resistance. **8,** 101535–101544 (2017).
65. Koyama, S., Akbay, E. A., Li, Y. Y., Herter-sprie, G. S., Buczkowski, K. A., Richards, W. G., Gandhi, L., Redig, A. J., Rodig, S. J., Asahina, H., Jones, R. E., Kulkarni, M. M., Kuraguchi, M., Palakurthi, S., Fecci, P. E., Johnson, B. E., Janne, P. A., Engelman, J. A., Gangadharan, S. P., Costa, D. B., Freeman, G. J., Bueno, R., Hodi, F. S., Dranoff, G., Wong, K. & Hammerman, P. S. Adaptive resistance to therapeutic PD-1 blockade is associated with upregulation of alternative immune checkpoints. *Nat. Commun.* **7,** 1–9 (2016).

CHAPTER 5

DISPLAY OF CPG DNA on E2 NANOPARTICLES FOR DENDRITIC CELL TARGETING

Portions of this chapter have been slightly modified and published as: Molino, N. M*., Neek, M*., Tucker, J. A., Nelson, E. L. & Wang, S. W. Display of DNA on Nanoparticles for Targeting Antigen Presenting Cells. *ACS Biomater. Sci. Eng.* **3,** 496–501 (2017).

* Authors contributed equally to the work and are considered co-first authors.

5.1. Abstract

Efficient delivery of antigens to antigen presenting cells (APCs) is of paramount concern in vaccine design. Here, we investigated the feasibility of targeting dendritic cells by conjugating a CpG DNA oligonucleotide to an E2 protein nanoparticle surface (CpG-PEG-E2). Uptake of CpG-PEG-E2 significantly increased ~ 4-fold for APCs *in vitro* and approximately 2-fold for dendritic cells *in vivo*, relative to bare nanoparticle. Compared to E2-alone or E2 functionalized solely with polyethylene glycol (PEG), the CpG-PEG-E2 accumulated within draining lymph nodes and demonstrated prolonged retention up to at least 48 hr, parameters which are critical for vaccine design

5.2. Introduction

Immunotherapy has emerged as a revolutionary approach in cancer treatment.[1] Cancer immunotherapies engage one's own immune system for targeted tumor destruction, eradication of metastases, and production of immunological memory.[2] Cancer vaccines have long been a strategy to elicit anti-tumor immunity. However, finding an optimal delivery method has been facing so many challenges. [3]

The ability to supply sufficient amounts of antigen and immune-modulating compounds to lymphatics,[4] and more specifically delivery to professional antigen presenting cells (APCs), such as dendritic cells (DCs), is critical in designing a cancer vaccine.[5] DCs are responsible for orchestration of the adaptive anti-tumor responses.[6] Engineered biomaterials represent technologies that may help to overcome antigen delivery problems.[7] It has been shown that nanoparticles naturally access lymphatics following immunization and interact with DCs and other APCs.[8] Interaction of

nanoparticles with DCs may be enhanced by displaying DC-specific antibodies.[9–11] While antibodies are tremendously specific to their target, they can be difficult to produce and would likely significantly alter the physical size and properties of the nanoparticle vaccine platform.[9] Therefore, a simple-to-employ DC-specific targeting moiety would be preferred for biomaterial design. We already demonstrated the capability of E2 nanoparticle in inducing an antigen-specific immune response (chapters 2-4). In this chapter we investigated whether E2 uptake by DCs could be improved by introducing a DC-targeting moiety to the nanoparticle.

Recently, the Toll-like receptor (TLR) 9 agonist CpG (single-stranded nonmethylated oligodeoxynucleotides containing CG motifs) was revealed as a possible ligand for DEC-205, an endocytic receptor expressed mainly by DCs and other APCs.[12] The finding that DCs may possess receptors to detect CpG-containing single stranded DNA (ssDNA) presents the opportunity to utilize a naturally occurring TLR ligand that may also serve as an APC-targeting molecule for vaccine delivery.

Our group has been developing the self-assembling (60-mer) E2 caged protein nanoparticle for biomedical applications, including cancer immunotherapy.[13–15] We have shown that E2 possesses the capability to simultaneously deliver tumor antigens and CpG to DCs for enhanced activation of antigen-specific $CD8^+$ T cells, yielding enhanced anti-tumor activity and increased survival time of tumor-bearing mice.[14]

Protein nanoparticles (*e.g.*, E2, virus-like particles [VLPs]) exhibit unique advantages over other nanoparticles for immunotherapy.[16,17] Some advantages include ideal size and optimal geometry for interaction with APCs *in situ*.[16,17] Though E2 has been successfully applied in a murine model,[14] demonstrating strong potential in cancer

immunotherapy development the *in vivo* fate of this platform has not been elucidated. In this study, our goals were to examine the biodistribution of the E2 nanoparticle vaccine platform, and in particular to investigate whether CpG display on E2 could increase affinity for DCs in secondary lymphoid organs. The studies in this chapter were done in collaboration with Dr. Nicholas Molino.

5.3. Methods

5.3.1. Materials

All buffer reagents were purchased from Fisher Scientific, unless otherwise noted. The oligodeoxynucleotide Toll-like receptor 9 ligand CpG 1826 (5'-tccatgacgttcctgacgtt-3') (CpG) and non-CpG 1982 (5'-tccaggacttctctcaggtt) were synthesized with a phosphorothioated backbone and thiol linker by TriLink Biotechnologies. The methoxy-PEG-N-hydroxysuccinimide (mPEG-NHS; molecular weight 2000 Da) and maleimide-PEG-NHS (mal-PEG-NHS; molecular weight 2000 Da) were purchased from Nanocs. Alexa Fluor 488 C5-maleimide was from Life Technologies. Fluorescently-tagged monoclonal antibodies CD11c (clone N418), CD3 (clone 145-2C11), B220 (clone RA3-6B2), F4/80 (clone BM8), DEC-205 (clone 205yekta), and rat IgG2a,κ (clone eBR2a, isotype control) were purchased from eBioscience. All cell culture media, unless otherwise noted, was comprised of RPMI 1640 (Mediatech) supplemented with 10% heat-inactivated fetal bovine serum (Gibco), 1 mM sodium pyruvate (Hyclone), 2 mM L-glutamine (Lonza), 100 units/ml penicillin (Hyclone), 100 μg/ml streptomycin (Hyclone), 50 μM 2-mercaptoethanol (Fisher), and 0.1 mM non-essential amino acids (Lonza) (complete RPMI media).

5.3.2. Animals and Cell Lines

All experiments were performed under approved protocol by the IACUC at the University of California, Irvine. Animals were housed and maintained by the ULAR. For generation of bone marrow-derived dendritic cells and for *in vivo* biodistribution assays, wild-type C57B/L6 female mice aged 6-12 weeks were used (Jackson Laboratories).

The NIH 3T3 mouse fibroblast cell line was purchased from ATCC and maintained in DMEM + 10% FBS. B3Z, a $CD8^+$ T cell hybridoma, was kindly provided by Prof. Nilabh Shastri (University of California, Berkeley). CH12, a B cell lymphoma line was kindly provided by Prof. Paolo Casali (University of Texas Health Science Center at San Antonio). Murine bone marrow-derived macrophages were kindly provided by Prof. Wendy Liu (University of California, Irvine).

5.3.3. E2 Preparation

The D381C E2 protein (E2) was prepared as previously described.[13] D381C is an E2 mutant with a non-native cysteine introduced to the internal cavity of the nanoparticle for site-directed functionalization. Briefly, proteins were expressed in *E. coli*, cells were lysed, and soluble cell lysates were applied to a HiPrep Q Sepharose anion exchange column (GE Healthcare) followed by a Superose 6 (GE Healthcare) size exclusion column for purification. The purified proteins were analyzed by dynamic light scattering (Zetasizer Nano ZS, Malvern) for size measurements. Electrospray ionization mass spectrometry and SDS-PAGE were performed for molecular weight and purity confirmation. Final protein preparations were stored in 50 mM potassium phosphate at pH 7.4 with 100 mM NaCl

(phosphate buffer). Lipopolysaccharide (LPS) was removed, and endotoxin levels were checked as described previously. [15]

5.3.4. Zeta potential measurements

Zeta potential measurements were conducted with a Malvern Zetasizer (Nano ZS) using a diffusion barrier method. This method can measure the zeta potential of low volume samples in physiological ionic strengths, a condition which is needed due to aggregation of our nanoparticles at low salt conditions. Malvern capillary cells were filled with 50 mM potassium phosphate at pH 7.4 with 100 mM NaCl, and 150 µl of nanoparticles (at ~1.3 mg/ml) were gently injected to the bottom of the buffer-filled capillary cells. Since E2 samples are of relatively high conductivity/ionic strength, the monomodal analysis mode within the Malvern software was used.

5.3.5. Bone Marrow-Derived Dendritic Cells (BMDCs)

Murine bone marrow-derived dendritic cells (BMDCs) were prepared,[15](see Appendix A) and involved plating of 2 million red blood cell-depleted bone marrow cells in 10 mL of complete RPMI containing 20 ng/mL murine GM-CSF for 8 days.

5.3.6. Internal Conjugation with Alexa Fluor 488 Fluorescent Marker and External Conjugation of Poly(ethylene glycol) and CpG

The thiol-reactive Alexa Fluor 488 C5-maleimide (Thermo Fisher) was added to a solution of E2 (D381C mutant) in phosphate buffer at a 3-fold molar excess to E2 monomer. Unreacted dye was removed by the 40 kDa molecular weight cutoff Zeba Spin Desalting Columns (Thermo Fisher).

The mPEG-NHS or mal-PEG-NHS linkers were conjugated to the external lysines on E2 by incubating at a 25-fold molar excess of PEG to E2 monomer for 2 hr at room temperature, with excess linker removed by the Zeba Spin desalting column. To the mal-PEG-NHS-functionalized E2 nanoparticle, TCEP-reduced CpG-SH or (non-CpG)-SH was added at a 10-fold molar excess to E2 monomer and incubated for 2 hr at room temperature followed by an overnight incubation at 4°C, and the reaction was quenched with L-cysteine (Fisher) at a 20-fold excess to E2 monomer. Unreacted CpG-SH and L-cysteine were removed by the Zeba Spin desalting columns. All nanoparticles [E2], PEGylated E2 [mPEG-E2], and E2 with CpG and non-CpG ligands on surface [CpG-PEG-E2] and [(non-CpG)-PEG-E2], respectively were characterized by BCA (to measure concentration), SDS-PAGE, zeta potential, and DLS (to measure particle size) as previously described. In order to determine the number of conjugated CpG molecules per E2 nanoparticle, relative band intensities on SDS-PAGE were evaluated using the NIH ImageJ software as previously described;[15] Conjugation was measured by band intensity analysis with the NIH ImageJ software normalized to protein concentration measured with the BCA assay (Pierce). Endotoxin levels of final conjugated nanoparticles were checked to confirm acceptable limits as previously discussed.[15]

5.3.7. In Vitro Uptake Assays

Cells were prepared at 1 million cells/mL in complete RPMI for BMDCs, BMDMs, CH12 B cells, and B3Z T cells or DMEM + 10% FBS for NIH 3T3 cells. E2, mPEG-E2, CpG-PEG-E2, or (non-CpG)-PEG-E2 was added to the cells at either 5 μg/mL or 1 μg/mL for 1 hr at 37°C. Cells were harvested and prepared in PBS + 1% BSA (Fisher) and 0.02% sodium azide (FACS buffer) for flow cytometry analysis on the BD Accuri C6 flow cytometer. Mean

fluorescence intensity (MFI) is reported as relative to cells only (background fluorescence) and represents the mean ± standard deviation of at least 3 experiments. For discrimination of surface bound versus internalized fluorescent particles, cells were incubated with 0.5% trypsin for 30 min at 37°C to remove surface-bound proteins.

5.3.8. Biodistribution and In Vivo Cell Interaction

E2, mPEG-E2, and CpG-PEG-E2 protein nanoparticles (50 μg in PBS) were administered subcutaneously in the left hock region of 6-12 week old female C57BL/6 wild-type mice, which has a well-described unilateral drainage pattern.[18] Following 6 hr or 48 hr, secondary lymphoid tissues were isolated from euthanized animals and passed through a 70 μM cell strainer with 1 mL PBS. Cells from the draining lymph nodes were prepared for flow cytometry analysis in FACS buffer and labeled with fluorescently-tagged monoclonal antibodies.

5.3.9. Statistical Analysis

Statistical analyses were carried out using Microsoft Excel and GraphPad Prism. Data is reported as mean ± standard deviation for particle characterization and DEC-205 expression, and mean ± standard error of the mean (S.E.M.) for all else, of at least three independent experiments unless otherwise noted. For *in vitro* assays, each datum is the result of duplicate measurements (unless otherwise noted). Statistical significance was determined by one-way ANOVA using post-hoc Tukey's test (comparing all means) for *in vitro* and *in vivo* cellular uptake assays, to determine differences between the nanoparticle formulations, and t-test for *in vivo* biodistribution experiments (pairwise comparison of experimental groups to background fluorescent control).

5.4. Results and Discussion

5.4.1. CpG Conjugation and Characterization

E2 nanoparticles were conjugated with green fluorescent dye through non-native internal cavity cysteines (E2 mutant D381C, herein simply abbreviated "E2"), in order to facilitate tracking.[13] For ligand display, we conjugated 5' thiol-terminated CpG 1826 or non-CpG ssDNA oligodeoxynucleotide 1982 to solvent-exposed lysines on the E2 nanoparticle surface via a bifunctional amine- and thiol-reactive poly(ethylene glycol) (PEG; average molecular weight 2000 Da) linker. CpG 1826 is known to activate DCs, while non-CpG 1982 has served as a negative control for such prior studies.[19–22] These nanoparticles are abbreviated CpG-PEG-E2 and (non-CpG)-PEG-E2, respectively. Methoxy-terminated amine-reactive PEG conjugated to the surface-accessible lysines on E2 served as a control devoid of DNA (mPEG-E2; average PEG molecular weight of 2000 Da) (See Methods in Supporting Information). We have previously shown that surface-bound 2000 Da PEG can inhibit cellular interaction with E2 and may serve as a flexible linker to facilitate ligand/receptor interaction on cells[23,24] PEG linkers larger than 2000 Da have been shown to increase nanoparticle size and polydispersity.[10]

We characterized our functionalized E2 to ensure that external conjugation of CpG did not significantly alter E2 size or cause aggregation [Figure 5.1.A]. SDS-PAGE of functionalized E2 nanoparticles revealed protein between ~30-40 kDa for mPEG-E2, consistent with heterogeneous attachment of one or more 2000 ± 200 Da PEGs per E2 subunit [Figure 5.1.A]. For the CpG-PEG-E2 and (non-CpG)-PEG-E2 samples, bands were observed at ~28 kDa (consistent with E2, no conjugation), ~30-32 kDa (E2 + PEG, no attached CpG), and ~35 kDa (E2 + PEG + CpG), supporting a 60-mer particle with varying

degrees of conjugation. Bands at ~60 kDa and above are artifacts that are consistently observed when conjugating the bifunctional PEG linker with E2, and this control is shown in the lane of malPEG-E2 [Figure 5.1.A]. Unreacted maleimides were quenched with L-cysteine. We estimated a conjugation ratio of 16 ± 5 CpG/E2 nanoparticle within the range achieved for a synthetic nanoparticle system, when adjusting for the difference in particle diameter.[25] In order to determine the number of conjugated CpG molecules per E2 nanoparticle, relative band intensities on SDS-PAGE were evaluated using the NIH ImageJ software as previously described.[15] Depending on the conformation of the PEG (*i.e.* brush or mushroom), the polymer may not be fully extended and the maleimide may not be easily accessible to react with the thiol-terminated CpG.[26]

Dynamic light scattering (DLS) revealed no significant changes in average particle sizes [Figure 5.1.B], demonstrating that conjugation of PEG and ssDNA to E2 did not cause large increases in particle size or aggregation. Zeta potential measurements showed modest shifts in nanoparticle surface charge, relative to -12 ± 1 mV for bare E2 [Figure 5.1.C]. Furthermore, the measured increase in negative surface charge of ssDNA-containing E2, relative to the more neutral PEGylated E2, is consistent with surface conjugation of DNA.

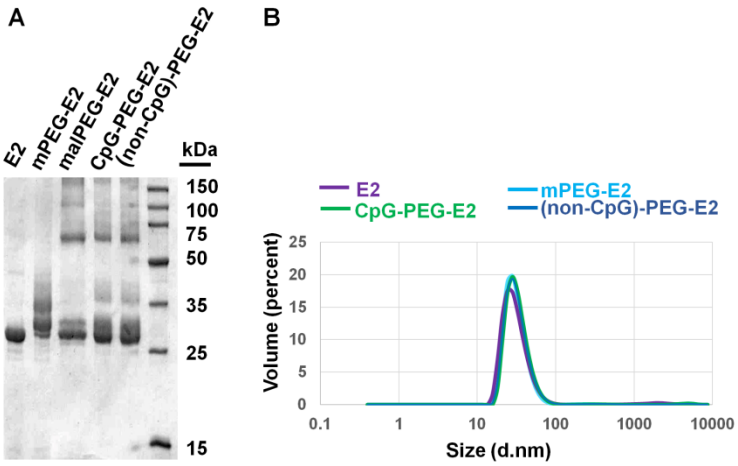

Sample	Size (d.nm)	Zeta (mV)
E2	29.1 ± 1.3	-12 ± 1
mPEG-E2	30.4 ± 0.8	-7 ± 0.5
CpG-PEG-E2	32.0 ± 0.8	-18 ± 0.7
(non)-CpG-PEG-E2	31.4 ± 0.7	-16 ± 1.4

Figure 5.1. SDS-PAGE, Hydrodynamic Diameter Size, and Surface Charge Characterization of Nanoparticles. A) SDS-PAGE. The lane for mPEG-E2 indicates heterogeneous numbers of PEG polymers attached to E2 subunits. CpG-PEG-E2 and (non-CpG)-PEG-E2 nanoparticles comprise of individual subunits with no attachment of PEG or CpG/(non-CpG), attachment of PEG, and attachment of both PEG and CpG/(non-CpG). Bands >60 kDa are indicative of the attachment of bi-functional PEG linker (see lane "malPEG-E2"). This observation for PEGylated protein is consistent with other studies and has been hypothesized to be due to the complex interaction between PEG chains and SDS micelles.[27] **B)** Representative size distribution for E2, mPEG-E2, CpG-PEG-E2, and (non-CpG)-PEG-E2 nanoparticles. **C)** Average size and measured zeta potential of nanoparticles.

5.4.2. In Vitro Uptake of E2 Nanoparticles

We examined the *in vitro* association of the fluorescently-labeled nanoparticles (E2, PEGylated E2 (mPEG-E2), CpG conjugated to E2 (CpG-PEG-E2), and non-CpG ssDNA conjugated to E2 (non-CpG)-PEG-E2) with different representative cell types, including bone marrow-derived DCs (BMDCs), bone marrow-derived macrophages (BMDMs), B cells (CH12), T cells (B3Z), and fibroblasts (NIH 3T3). As expected, PEGylation (mPEG-E2) decreased uptake of E2 by all cell types tested *in vitro*, relative to non-functionalized E2 [Figure 5.2]; this decrease is consistent with observations from our previously published reports and with PEGylation of other VLPs.[28] CpG-PEG-E2 exhibited increased association

with APCs relative to non-functionalized E2 (~4-fold increase by BMDCs and BMDMs [p < 0. 001], and to a lesser extent by B cells), but not with T cells or fibroblasts.

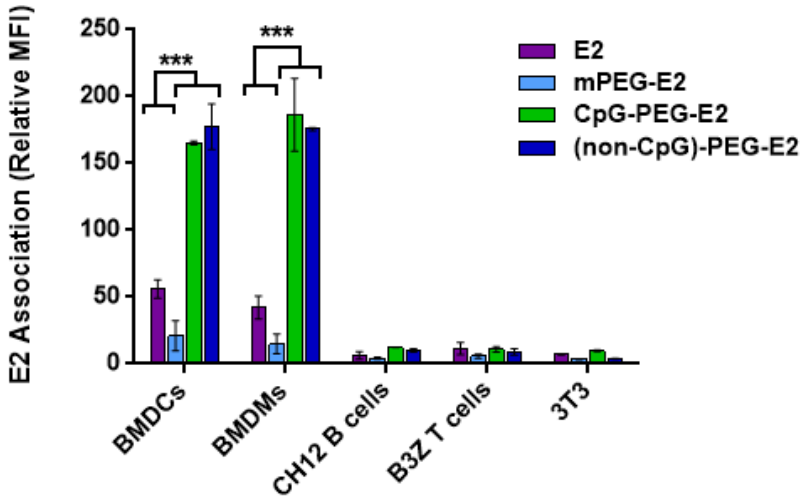

Figure 5.2. E2 Uptake by APCs. BMDCs and BMDMs show increased association with CpG-PEG-E2 and (non-CpG)-PEG-E2 nanoparticles *in vitro*, compared to their interactions with E2 and mPEG-E2. Cellular association was measured by mean fluorescence intensity (MFI) of cells incubated with 5 μg/mL E2 nanoparticle for 1 hr at 37°C. Data is reported as average ± S.E.M., relative to cellular background fluorescence (PBS), of 3 independent experiments. Statistical significance was determined with one-way ANOVA using a post-hoc Tukey's test (*** $p < 0.001$).

Trypsinization (to remove surface bound proteins) revealed that the majority of CpG-PEG-E2 nanoparticles were internalized by BMDCs and BMDMs, but not by B cells [Figure 5.3]. We also observed enhanced BMDC and BMDM uptake of E2 conjugated with non-CpG-containing ssDNA [Figure 5.2], which was an unexpected result; however, this may not be too unusual given that certain cell receptors, such as DEC-205, have also shown affinity for both CpG and DNA sequences without CpG.[12]

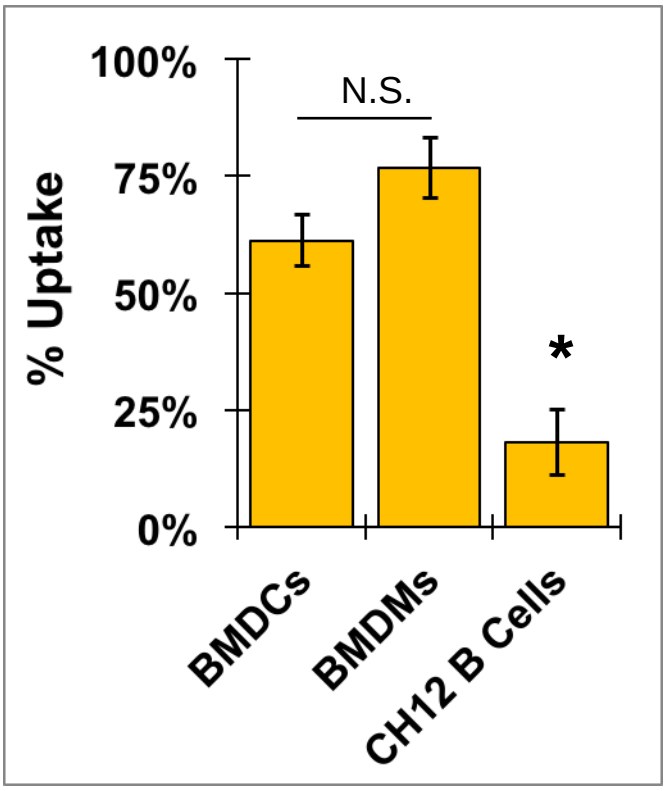

Figure 5.3. E2 Uptake by APCs after Trpsinization. The majority of E2 is internalized within BMDCs and BMDMs, but not B cells. Cells were incubated with 5 μg/mL of the CpG-PEG-E2 nanoparticle and subsequently treated with 0.5% trypsin to remove surface bound proteins. The percentage of fluorescence remaining following treatment with trypsin is shown. Data is reported as average S.E.M. of 3 independent experiments, and statistical significance was determined with a one way ANOVA followed by a post hoc Tukey's test (*$p < 0.05$). Significance for CH12 B cells was compared to both BMDCs and BMDMs.

While we expected increased CpG-PEG-E2 uptake by DEC-205$^+$ BMDC (DEC-205 expression in Figure 5.4), which we did observe [Figure 5.2] it was also notable that there was increased binding [Figure 5.2] to DEC-205$^-$ BMDMs [Figure 5.4]. It does make sense, however, that APCs likely possess multiple external sensing mechanisms for ssDNA, such as scavenger receptors,[29] although isolating and identifying each receptor involved is beyond the scope of the current study.

A

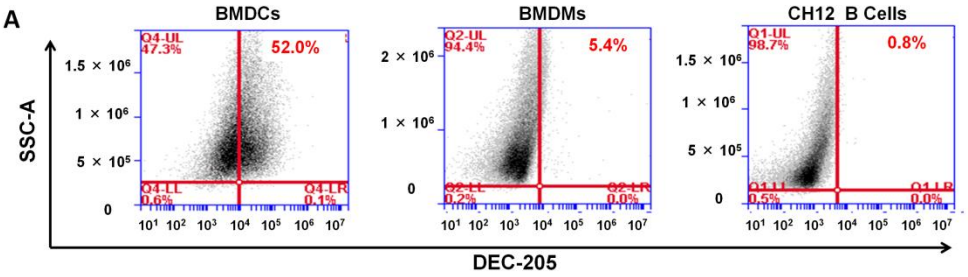

B

Cell Type	% DEC-205 Expression ± SD
BMDCs	46.4% ± 8.4
BMDMs	2.2% ± 2.7
B Cells (CH12)	0.8% ± 0.6
B3Z T cells (B3Z)	0.2% ± 0.2
Fibroblasts (NIH-3T3)	0.1% ± 0.05

Figure 5.4. DEC-205 Expression of BMDCs and BMDMs. Representative samples of BMDCs and BMDMs were labeled with fluorescently-tagged DEC-205 antibody and analyzed by flow cytometry for DEC-205 expression. A) Representative data quantifying DEC-205 expression by flow cytometry. The events to the right of the red bar are considered positive for DEC-205 expression. B. Average percent of cells residing within the gate for DEC-205 expression for the different cell types examined *in vitro*. Data are presented as average percent ± standard deviation for at least three independent experiments.

5.4.3. In Vivo Uptake of E2 Nanoparticle

We then investigated whether the observed *in vitro* targeting effect mediated by display of ssDNA was evident *in vivo* in areas of high APC-activity (*i.e.,* lymph nodes) by measuring fluorescence (MFI) of cells from individual organs. Six hours following subcutaneous administration (SC) in mice, the E2 nanoparticle was predominantly detected at the injection site, within the lymph nodes (LNs) ipsilateral to injection site. [Figure 5.5]. Further inspection revealed the E2 nanoparticle was found in 5 out of 7 LNs tested (injection site ipsilateral popliteal, inguinal, axillary, iliac, and renal, but not ipsilateral cervical or mesenteric; Figure 5.5). Due to the similarity between cellular uptake

data for CpG-PEG-E2 and (non-CpG)-PEG-E2 nanoparticles *in vitro*, only the former ssDNA-containing nanoparticle was examined *in vivo*. PEGylation (mPEG-E2) and CpG display (CpG-PEG-E2) on E2 exhibited a few notable changes in their *in vivo* fate, in that CpG-PEG-E2 was the only nanoparticle not detectable in the spleen [Figure 5.5]. Remarkably, 48 hours following administration, CpG-PEG-E2 nanoparticle was still evident in the ipsilateral dLNs [Figure 5.5], whereas E2 and mPEG-E2 were largely undetectable.

These observations indicated that a PEGylated surface alone allows the E2 nanoparticle to disperse further throughout the lymphatic and circulatory system, in agreement with the accepted properties of PEGylation in drug delivery systems,[30] including VLPs.[28,31] Display of CpG on the distal end of a PEG-linker (CpG-PEG-E2) resulted in retention of the E2 nanoparticle within proximal areas that contain DC populations, an attractive quality for vaccine design and success.[32,33] While CpG-PEG-E2 was not detected in the spleen, the draining LNs (dLNs) have been shown to play the more critical role in acute anti-viral and anti-cancer responses.[34]

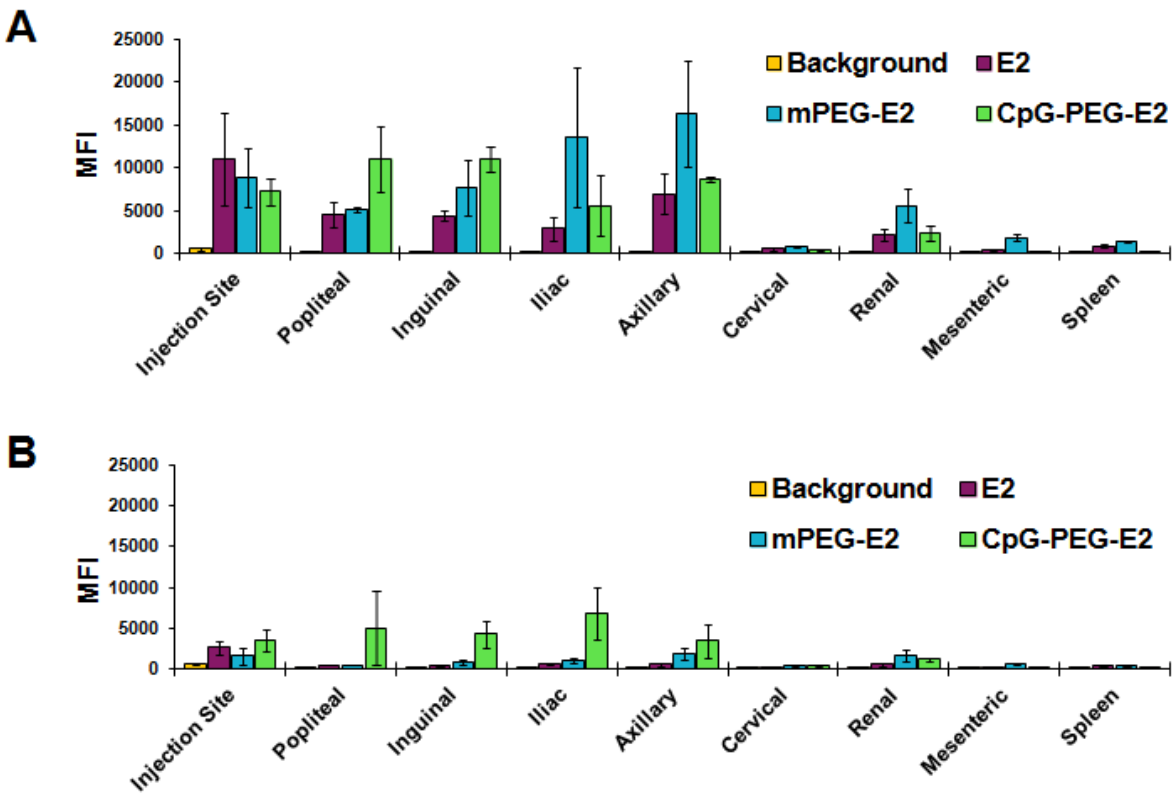

Figure 5.5. E2 In vivo Biodistribution. Distribution of nanoparticles in the lymph nodes ipsilateral to injection site, mesenteric lymph node, and spleen following injection, after (A) 6 hours and (B) 48 hours. E2, mPEG-E2, and CpG-PEG-E2 nanoparticles were administered subcutaneously. Mean fluorescence (MFI) was measured by flow cytometry of cells from relevant tissues, and background is tissue MFI from PBS-injected mice. Data is presented as average ± S.E.M. of 3 independent experiments.

To determine whether accumulation and retention of CpG-PEG-E2 nanoparticles within the dLNs was due to increased affinity for cells expressing DEC-205, we more closely examined fluorescence of DEC-205$^+$ dLN cells (*i.e.*, popliteal, inguinal, axillary, iliac, and renal LNs ipsilateral to injection site). However, consistent with our *in vitro* data, we observed no significant difference between the average fluorescence of DEC-205$^+$ cells from mice injected with CpG-PEG-E2, compared to E2 or mPEG-E2, after either 6 or 48 hours [Figure 5.6.A, 5.6.B].

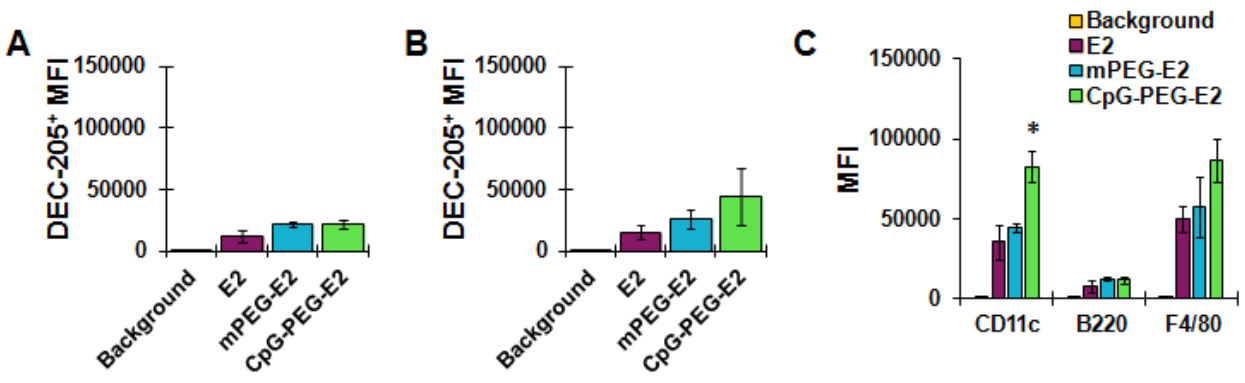

Figure 5.6. Nanoparticle Accumulation and Uptake by Cells in Draining Lymph Nodes. The MFI of DEC-205$^+$ cells in draining lymph nodes was determined **A)** 6 hr or **B)** 48 hr following subcutaneous administration of nanoparticles. E2 shows no significant preference for association with DEC-205$^+$ cells *in vivo* following surface functionalization with PEG or CpG. Data is reported as average ± S.E.M. of 3 independent experiments. **C)** Extent of nanoparticle association/uptake was measured by MFI of fluorescent-positive draining lymph node cells using flow cytometry 6 hr following subcutaneous administration. CD11c, B220, and F4/80 markers generally indicate dendritic cells, B cells, and macrophages/Langerhans DCs, respectively. Data is reported as average ± S.E.M. of 3 independent experiments. Statistical significance within a group was determined using a one-way ANOVA followed by a post hoc Tukey's test, comparing all means (* $p < 0.05$).

Interestingly, however, the overall CD11c$^+$ population (primarily DCs) from the dLNs of the CpG-PEG-E2 group showed a significant two-fold increased fluorescence compared to groups injected with E2 or mPEG-E2 nanoparticles [Figure 5.6.C]. This indicates increased broad DC association/uptake of CpG-PEG-E2, critically important for cell-mediated vaccine success,[6] and in good agreement with our *in vitro* observations [Figure 5.2]. We also observed a modest increase in CpG-PEG-E2 fluorescence of F4/80$^+$ cells, compared to groups given E2 or mPEG-E2 [Figure 5.6.C]. Altogether, our in vivo data suggests that decoration of the E2 nanoparticle with CpG oligonucelotides enhances physical association and/or uptake by DCs and macrophages within the dLNs following SC injection.

5.5. Conclusion

Here, we have demonstrated that surface display of CpG-containing ssDNA oligonucleotides significantly increased APC-specific uptake of the E2 nanoparticle. *In vitro* ssDNA decoration induced large increases in cellular uptake of E2 by DCs, macrophages, and B cells. *In vivo*, the CpG-PEG-E2 nanoparticle showed a significant increase in cellular association with DCs within the dLNs, compared to the other nanoparticles tested. These increased interactions in the presence of surface-bound ssDNA oligos, including CpG, appear to operate through multiple mechanisms. Further, CpG-PEG-E2 also demonstrated increased LN retention over 48 hr, and less presence in blood draining organs, compared to the E2 and mPEG-E2 nanoparticles. Overall, these results demonstrate that decoration of protein-based nanoparticles with CpG can increase lymph node retention and uptake by APCs, factors that are beneficial in vaccine design.

5.6. Acknowledgements

We gratefully acknowledge Prof. Aaron Esser-Kahn for use of his flow cytometer, Prof. Wendy Liu and Dr. Yoon Kim for macrophages, and Prof. Nilabh Shastri for B3Z T cells. DLS was carried out at the UCI Laser Spectroscopy Facility. This work was supported by the National Institutes of Health (R21EB017995), the National Cancer Institute of the National Institutes of Health (P30CA062203), and the University of California Cancer Research Coordinating Committee (UCCRCC-101868).

5.7. References

1. Aly, H. A., Cancer therapy and vaccination. *Journal of immunological methods **382**,* 1-23 (2012).
2. Rosenberg, S. A., Yang, J. C. & Restifo, N. P. Cancer immunotherapy : moving beyond current vaccines. *Nat. Med.* **10,** 909–915 (2004).
3. Romero, P., Banchereau, J., Bhardwaj, N., Cockett, M., Disis, M. L., Dranoff, G., Gilboa, E., Hammond, S. A., Hershberg, R., Korman, A. J., Kvistborg, P., Melief, C., Mellman, I., Palucka, A. K., Redchenko, I., Robins, H., Sallusto, F., Schenkelberg, T., Schoenberger, S., Sosman, J., Türeci, Ö., Van Den Eynde, B., Koff, W. & Couko, G. The human vaccines project: A roadmap for cancer vaccine development. *Sci. Transl. Med.* **8,** 1–8 (2016).
4. Bachmann, M. F. & Jennings, G. T. Vaccine delivery : a matter of size , geometry , kinetics and molecular patterns. *Nat. Publ. Gr.* **10,** 787–796 (2010).
5. Belz, G. T., Carbone, F. R. & Heath, W. R. Cross-presentation of antigens by dendritic cells. *Crit. Rev. Immunol.* **22,** 439–448 (2002).
6. Palucka, K. & Banchereau, J. Cancer immunotherapy via dendritic cells. *Interact. Immune Cancer Cells* **12,** 75–89 (2014).
7. Gu, L. & Mooney, D. J. Biomaterials and emerging anticancer therapeutics: Engineering the microenvironment. *Nat. Rev. Cancer* **16,** 56–66 (2016).
8. Bachmann, M. F. & Jennings, G. T. Vaccine delivery: a matter of size, geometry, kinetics and molecular patterns. *Nat. Rev. Immunol.* **10,** 787–96 (2010).
9. Aktaş, Y., Yemisci, M., Andrieux, K., Gürsoy, R. N., Alonso, M. J., Fernandez-Megia, E., Novoa-Carballal, R., Quiñoá, E., Riguera, R., Sargon, M. F., Çelik, H. H., Demir, A. S., Hincal, A. A., Dalkara, T., Çapan, Y. & Couvreur, P. Development and brain delivery of chitosan-PEG nanoparticles fnnctionalized with the monoclonal antibody OX26. *Bioconjug. Chem.* **16,** 1503–1511 (2005).
10. Cruz, L. J., Tacken, P. J., Fokkink, R. & Figdor, C. G. The influence of PEG chain length and targeting moiety on antibody-mediated delivery of nanoparticle vaccines to human dendritic cells. *Biomaterials* **32,** 6791–6803 (2011).
11. Ueno, H., Klechevsky, E., Schmitt, N., Ni, L., Flamar, A. L., Zurawski, S., Zurawski, G., Palucka, K., Banchereau, J. & Oh, S. K. Targeting human dendritic cell subsets for improved vaccines. *Semin. Immunol.* **23,** 21–27 (2011).
12. Caminschi, I., Meuter, S. & Heath, W. R. DEC-205 is a cell surface receptor for CpG oligonucleotides. *Oncoimmunology* **2,** 1–6 (2013).
13. Dalmau, M., Lim, S., Chen, H. C., Ruiz, C. & Wang, S. W. Thermostability and molecular encapsulation within an engineered caged protein scaffold. *Biotechnol. Bioeng.* **101,** 654–664 (2008).
14. Molino, N. M., Neek, M., Tucker, J., Nelson, E. L. & Wang, S. W. Biomaterials Viral-mimicking protein nanoparticle vaccine for eliciting anti-tumor responses. *Biomaterials* **86,** 83–91 (2016).
15. Molino, N. M., Anderson, A. K. L., Nelson, E. L. & Wang, S. W. Biomimetic protein nanoparticles facilitate enhanced dendritic cell activation and cross-presentation. *ACS Nano* **7,** 9743–9752 (2013).
16. Molino, N. M. & Wang, S. W. Caged protein nanoparticles for drug delivery. *Curr. Opin. Biotechnol.* **28,** 75–82 (2014).
17. Plummer, E. M. & Manchester, M. Viral nanoparticles and virus-like particles :

platforms for contemporary vaccine design. (2011). doi:10.1002/wnan.119
18. Kamala, T. Hock immunization: A humane alternative to mouse footpad injections. *J. Immunol. Methods* **328,** 204–214 (2007).
19. Utaisincharoen, P.; Kespichayawattana, W.; Anuntagool, N.; Chaisuriya, P.; Pichyangkul, S.; Krieg, A. M.; Sirisinha, S., CpG ODN enhances uptake of bacteria by mouse macrophages. *Clinical and experimental immunology **132,*** 70-75 (2003).
20. Reinis, M.; Stepanek, I.; Simova, J.; Bieblova, J.; Pribylova, H.; Indrova, M.; Bubenik, J., Induction of protective immunity against MHC class I-deficient, HPV16-associated tumours with peptide and dendritic cell-based vaccines. *International journal of oncology **36,*** 545-51 (2010).
21. Askew, D., Chu, R. S., Krieg, A. M. & Harding, C. V. CpG DNA Induces Maturation of Dendritic Cells with Distinct Effects on Nascent and Recycling MHC-II Antigen-Processing Mechanisms. *J. Immunol.* **165,** 6889–6895 (2000).
22. Switaj, T., Jalili, A., Jakubowska, A. B., Drela, N., Stoksik, M., Nowis, D., Basak, G., Golab, J., Wysocki, P. J., Mackiewicz, A., Sasor, A., Socha, K., Jakóbisiak, M. & Lasek, W. CpG immunostimulatory oligodeoxynucleotide 1826 enhances antitumor effect of interleukin 12 gene-modified tumor vaccine in a melanoma model in mice. *Clin. Cancer Res.* **10,** 4165–4175 (2004).
23. Molino, N. M., Bilotkach, K., Fraser, D. A., Ren, D. & Wang, S. W. Complement activation and cell uptake responses toward polymer-functionalized protein nanocapsules. *Biomacromolecules* **13,** 974–81 (2012).
24. Ren, D., Kratz, F. & Wang, S. W. Engineered drug-protein nanoparticle complexes for folate receptor targeting. *Biochem. Eng. J.* **89,** 33–41 (2014).
25. Milley, B., Kiwan, R., Ott, G. S., Calacsan, C., Kachura, M., Campbell, J. D., Kanzler, H. & Coffman, R. L. Optimization, Production, and Characterization of a CpG-Oligonucleotide-Ficoll Conjugate Nanoparticle Adjuvant for Enhanced Immunogenicity of Anthrax Protective Antigen. *Bioconjug. Chem.* **27,** 1293–1304 (2016).
26. Jokerst, J. V., Lobovkina, T., Zare, R. N. & Gambhir, S. S. Nanoparticle PEGylation for imaging and therapy. *Nanomedicine* **6,** 715–728 (2011).
27. Zheng, C. Y., Ma, G. & Su, Z. Native PAGE eliminates the problem of PEG-SDS interaction in SDS-PAGE and provides an alternative to HPLC in characterization of protein PEGylation. *Electrophoresis* **28,** 2801–2807 (2007).
28. O'Riordon, C. R. & Song, A. PEGylated adenovirus for targeted gene therapy. *Methods Mol. Biol.* **434,** 133–160 (2008).
29. Areschoug, T. & Gordon, S. Scavenger receptors: Role in innate immunity and microbial pathogenesis. *Cell. Microbiol.* **11,** 1160–1169 (2009).
30. Review, D. A., Jain, A. & Jain, S. K. PEGylation : An Approach for Drug. *Rev. Lit. Arts Am.* **25,** 403–447 (2008).
31. Yao, X., Yoshioka, Y., Morishige, T., Eto, Y., Watanabe, H., Okada, Y., Mizuguchi, H., Mukai, Y., Okada, N. & Nakagawa, S. Systemic administration of a PEGylated adenovirus vector with a cancer-specific promoter is effective in a mouse model of metastasis. *Gene Ther.* **16,** 1395–1404 (2009).
32. Liu, H., Moynihan, K. D., Zheng, Y., Szeto, G. L., Li, A. V., Huang, B., Van Egeren, D. S., Park, C. & Irvine, D. J. Structure-based programming of lymph-node targeting in molecular vaccines. *Nature* **507,** 519–522 (2014).

33. Cantisani, R., Pezzicoli, A., Cioncada, R., Malzone, C., De Gregorio, E., D'Oro, U. & Piccioli, D. Vaccine Adjuvant MF59 Promotes Retention of Unprocessed Antigen in Lymph Node Macrophage Compartments and Follicular Dendritic Cells. *J. Immunol.* **194,** 1717–1725 (2015).
34. Olson, M. R., McDermott, D. S. & Varga, S. M. The Initial Draining Lymph Node Primes the Bulk of the CD8 T Cell Response and Influences Memory T Cell Trafficking after a Systemic Viral Infection. *PLoS Pathog.* **8,** (2012).

CHAPTER 6

CONCLUSIONS AND FUTURE DIRECTIONS

6.1. Assembly on E2 Nanoparticle Scaffold Enhances Cell-Mediated Immune Responses Toward Cancer Antigens

6.1.1. Conclusion

In this work, we have demonstrated that prophylactic immunization with CpG-gp-E2 nanoparticles increased anti-tumor responses to gp100-expressing B16-F10 murine melanoma cells. Further, in a HLA-A2 transgenic mouse model, we found that immunization with nanoparticle formulations containing CpG and CT antigens resulted in a significantly higher specific IFN-γ release compared to formulations with unbound antigen and CpG. Also, we observed an elevated lysis activity towards human cancer cell line, A375, that expresses the target antigen. Additionally, simultaneous delivery of CpG-NYESO-E2 and CpG-MAGE-E2 nanoparticles preserved the effects of the individual antigen nanoparticles, and resulted in an additive IFN-γ secretion and lysis activity relative to each separate nanoparticle formulation. Altogether, this work shows the advantages of using the E2 nanoparticle as an effective vaccine platform to deliver cancer-testis antigens for higher cell-mediated activation.

6.1.2. Future Directions

We have shown the ability of the E2 nanoparticle in inducing effective anti-tumor responses toward TAAs. However, we have not determined the optimal nanoparticle design formulation. It would be interesting to evaluate the alternative types of adjuvants and different concentrations of both antigens and adjuvants in inducing anti-tumor responses. We have used the maximum loading capacity resulting from incubating excess CpG and peptide epitopes in the conjugation step.[1] Optimal antigen load is crucial for

establishing a long-lived and protective T cell responses.[2] Excessive antigen exposure may lead to T cell exhaustion and some of our data point to this possibility.[3,4] Therefore, different concentrations of antigen and CpG should be systematically tested.

Further, alternative TLR-activators (*i.e.* Poly-IC, ssRNA) should be explored to understand how alternative TLRs influence the immune system activation. Potential of combining multiple adjuvant for synergistic effects should be also examined; it was shown that dual TLRs can yield higher immune activation.[5] TLR9 (receptor for CpG) expression is limited in human cells, compared to the mice.[6] Therefore, it will be important to evaluate alternative adjuvant (i.e. dsRNA, Poly-IC) than CpG. Other potential intracellular receptors targets include TLR-3, TLR-7, and TLR-8.[7,8] The ligands for TLR-7 and TLR-8 are small RNA and DNA sequences.[8] Double-stranded RNA such as poly-IC is also known for TLR-3.[8]

Once we have discovered the optimal design/formulation of the nanoparticle it would be interesting to examine whether alternate routes of nanoparticle administration (IV, IM, IP) are more effective than SC; our *in vivo* immunizations have been administered by the SC route. Different routes of immunization could change the vaccine efficacy.

While the ability to mount an anti-tumor response against B16-F10 melanoma in C57BL/6 mice is remarkable, the vaccine efficacy should be evaluated in an alternative tumor models to prove that the significant effects can be recapitulated. T cell depletion studies should also be performed to study the contribution of CD8 and CD4 T cells in the observed anti-tumor responses and confirm the role of CD8 T cells.[9] It will also be interesting to examine whether the immune response generated from antigen-E2 delivery system can be effective against metastases, where cancer therapies face their major challenges.

In this work we showed that higher cell lysis against human cancer cell line was achieved after antigen-E2 delivery, in a HLA-A2 mice. However, because of the absence of a murine homologue for human HLA-A2-restricted CT antigens, we could not test these human antigens in a preclinical tumor model *in vivo*. Therefore, it would be important to examine whether the antigen-E2 nanoparticle vaccines are capable of activating human immune cells in vitro. The ability of the antigen-E2 delivery system (CpG-NYESO-E2 or CpG-MAGE-E2) in human DCs activation, and in human T cells activation and proliferation should be tested.

Finally, it would also be important to identify the physical stability of the E2 vaccine platform. Vaccines should ideally display long term stability, where they can be stored and delivered to areas that may not hold resources for long term storage conditions.

6.2. E2 Vaccine in Combination with Immune Checkpoint Inhibitors

6.2.1. Conclusion

In this work, we confirmed that double immunization with CpG-gp-E2 resulted in an increase in specific IFN-γ frequencies, elevated CD8 T cell counts, and a slower tumor growth. In this work, we tested the E2 vaccine in a therapeutic system rather than protective responses examined in Chapter 2. Further, we observed a significantly higher animal survival when anti-PD-1 antibody treatment was combined with CpG-gp-E2 nanoparticle (~ 50% remission), compared to each therapy/vaccine separately (*e.g.,* only ~5% survival of tumor-free mice in anti-PD-1 group). Additionally, we found evidence that tumor escape could be due to MHC-I downregulation on the tumor cells. Altogether,

This work shows that the E2 nanoparticle can successfully be used in combination with anti-PD-1 to improve checkpoint inhibitor treatment efficacy.

6.2.2. Future Directions

While the combination treatment was shown to be effective, the mechanism in unclear. Therefore, it is important to evaluate the contribution of different cell types that were involved in the observed anti-tumor responses. Tumor masses should be collected and checked by histology and/or flow cytometery for various cell types such as CD8, CD4, and NK cells. Also, T cell depletion investigations should be performed to study the involvement of CD8 and CD4 T cells in the observed anti-tumor responses.[9] It will also be interesting to observe whether the immune response can be effective against metastases, where conventional cancer treatments face their largest challenges.

Because anti-PD-1 acts by releasing the suppression of T cell activation without priming the specific responses towards tumors, non-specific immune-related adverse events after this treatment are not surprising.[10] Immune-related events are correlated with changes in routine blood counts; fluctuations in routine blood count could be a sign of immune-related adverse events.[11] Therefore, a complete blood count including total white blood cell count, relative neutrophil, monocyte, and lymphocyte should be performed.

We hypothesized that memory T cells were responsible for prolonging the animal survival after tumor-challenge and preliminary evidence also supports this (Chapter 4). Therefore, it would be interesting to check for existence of T memory cells after combination therapy. Five-six weeks after the last immunization, single cells isolated from

lymph nodes, spleen, and blood sample should be pulsed with the cognate antigen. CD8 and CD4 T cells should be checked for memory cell markers such as CD44 and CD45RO.[12]

Ideally, a cancer treatment approach should be applicable to a wide variety of disease types. It would be important to evaluate the effects of combination therapy in a different tumor model (such as CT26 colon cancer), to assess if the data can be recapitulated. Dosing schedules of anti-PD-1 antibody administration should be optimized for a more effective therapy. It would be important to discover the kinetics of PD-1 expression and T cell infiltration into TME; this understanding could be helpful in designing the most optimized schedule for vaccine and immune checkpoint inhibitor administration.

Also, alternative immune checkpoint inhibitors other than anti-PD-1 (*e.g.,* LAG-3, TIM-3)[13,14] could be tested to discover the most effective one in our system. It was shown by others that therapy with dual immune checkpoint inhibitors yield higher anti-tumor responses.[15] Therefore, it will be interesting to evaluate the effects of simultaneous therapy of 2 immune checkpoint inhibitor in combination with antigen-E2 delivery system, however, due to the likelihood of side effects, immune-adverse events should be monitored.

6.3. E2 Nanoparticle Uptake and DC Targeting

6.3.1. Conclusion

Our E2 nanoparticle *in vitro* demonstrated the ability for efficient uptake by DCs. We showed that conjugation of CpG and (non)-CpG motifs on the E2 surface greatly enhanced DC uptake *in vitro*. The E2 nanoparticle is within the optimal size for lymphatic drainage,[16] our studies showed that E2 drains primarily to the lymph nodes (LN) after subcutaneous

injection. Also, surface display of the CpG DNA resulted in nanoparticle accumulation in the LN ; with an enhanced LN retention time, compared to the E2 nanoparticles alone.

6.3.2. Future Directions

It would be interesting to explore other potential aptamers, such as DC-targeting peptides.[17] Also, different linkers could be used for aptamer conjugation. Linkers may affect the density of aptamers conjugated to the E2 nanoparticle and also alter the cell uptake kinetics.[18,19] While PEG-2000 (molecular weight of 2000 Da) was used for this study, different PEG linker with varying molecular weights should be tested to measure differences in kinetics.

It would be also interesting to determine after how long the nanoparticles are cleared from the body. Therefore, *in vivo* distribution could be investigated via live-imaging, and further examination for various cell types and uptake could be performed through flow cytometry. Since, CpG DNA is also a ligand for TLR-9, we would expect that DC are activated after taking up CpG-PEG-E2 nanoparticles. Therefore, DC activation should also be checked in future experiments.

6.4. Reference

1. Molino, N. M., Anderson, A. K. L., Nelson, E. L. & Wang, S. W. Biomimetic protein nanoparticles facilitate enhanced dendritic cell activation and cross-presentation. *ACS Nano* **7,** 9743–9752 (2013).
2. Bachmann, M. F. & Jennings, G. T. Vaccine delivery: a matter of size, geometry, kinetics and molecular patterns. *Nat. Rev. Immunol.* **10,** 787–96 (2010).
3. Critchfield, J., Racke, M., Zuniga-Pflucker, J., Cannella, B., Raine, C., Goverman, J. & Lenardo, M. T cell deletion in high antigen dose therapy of autoimmune encephalomyelitis. *Science.* **263,** 1139–1143 (1994).
4. Yi, J. S., Cox, M. A. & Zajac, A. J. T-cell exhaustion : characteristics , causes and conversion. *Immunology.* **2,** 474–481 (2010).
5. Fox, C. B., Sivananthan, S. J., Duthie, M. S., Vergara, J., Guderian, J. A., Moon, E., Coblentz, D., Reed, S. G. & Carter, D. A nanoliposome delivery system to synergistically trigger TLR4 AND TLR7. *J. of Nanobiotechnology.* 7–12 (2014).
6. Krieg, A. M. Toll-like receptor 9 (TLR9) agonists in the treatment of cancer. *Oncogene* **9,** 161–167 (2008).
7. Kay, E., Scotland, R.S., Whiteford, J. R. Toll-like receptors : Role in inflammation and therapeutic potential. *Biofactor* **44,** 284–294 (2014).
8. Bauer, S. *Toll-Like Receptors (TLRs) and Innate Immunity. Nature Reviews Immunology* **1**, 135–145 (2001)
9. Laky, K. & Kruisbeek, A. M. In vivo depletion of T lymphocytes. *Curr. Protoc. Immunol.* **2016,** 4.1.1-4.1.9 (2016).
10. Michot, J. M., Bigenwald, C., Champiat, S. & Collins, M. ScienceDirect Immune-related adverse events with immune checkpoint blockade : a comprehensive review. *Eur. J. Cancer* **54,** 139–148 (2016).
11. Fujisawa, Y., Yoshino, K., Otsuka, A. & Funakoshi, T. Fluctuations in routine blood count might signal severe immune-related adverse events in melanoma patients treated with nivolumab. *J. Dermatol. Sci.* **88,** 225–231 (2017).
12. Dutton, R. W., Bradley, L. M. & Swain, S. L. T CELL MEMORY. *Annual Review of Immunology* **16,** 201-203 (1998).
13. Tsai, H. F. & Hsu, P. N. Cancer immunotherapy by targeting immune checkpoints: Mechanism of T cell dysfunction in cancer immunity and new therapeutic targets John T Kung. *J. Biomed. Sci.* **24,** 1–8 (2017).
14. Bialkowski, L., Van der Jeught, K., Bevers, S., Tjok Joe, P., Renmans, D., Heirman, C., Aerts, J. L. & Thielemans, K. Immune checkpoint blockade combined with IL-6 and TGF-β inhibition improves the therapeutic outcome of mRNA-based immunotherapy. *Int. J. Cancer* **143,** 686–698 (2018).
15. Perez-Gracia, J. L., Labiano, S., Rodriguez-Ruiz, M. E., Sanmamed, M. F. & Melero, I. Orchestrating immune check-point blockade for cancer immunotherapy in combinations. *Curr. Opin. Immunol.* **27,** 89–97 (2014).
16. Bachmann, M. F. & Jennings, G. T. Vaccine delivery : a matter of size, geometry, kinetics and molecular patterns. *Nat. Publ. Gr.* **10,** 787–796 (2010).
17. Curiel TJ, Morris C, Brumlik M, Landry SJ, Finstad K, Nelson A, Joshi V, Hawkins C, Alarez X, Lackner A, et al.: Peptides identified through phage display direct

immunogenic antigen to dendritic cells. *J Immunol* **172**, 7425-7431(2004).
18. Steinmetz, N. F. & Manchester, M. PEGylated viral nanoparticles for biomedicine: The impact of PEG chain length on VNP cell interactions in vitro and Ex vivo. *Biomacromolecules* **10,** 784–792 (2009).
19. Stefanick JF, Ashley JD, Kiziltepe T, Bilgicer B: A systematic analysis of peptide linker length and liposomal polyethylene glycol coating on cellular uptake of peptide-targeted liposomes. *ACS Nano*, **7,** 2935-2947 (2013).

APPENDIX A

Appendix A.1 DNA and Protein Sequences

E2 amino acid and DNA sequence

Full native pyruvate dehydrogenase E2 sequence from *Geobacillus stearothermophilus* (This is where the numbering is based on, for our different mutants)

```
1       MAFEFKLPDI GEGIHEGEIV KWFVKPGDEV NEDDVLCEVQ NDKAVVEIPS PVKGKVLEIL VPEGTVATVG QTLITLDAPG
81      YENMTFKGQE QEEAKKEEKT ETVSKEEKVD AVAPNAPAAE AEAGPNRRVI AMPSVRKYAR EKGVDIRLVQ GTGKNGRVLK
161     EDIDAFLAGG AKPAPAAAEE KAAPAAAKPA TTEGEFPETR EKMSGIRRAI AKAMVHSKHT APHVTLMDEA DVTKLVAHRK
241     KFKAIAAEKG IKLTFLPYVV KALVSALREY PVLNTSIDDE TEEIIQKHYY NIGIAADTDR GLLVPVIKHA DRKPIFALAQ
321     EINELAEKAR DGKLTPGEMK GASCTITNIG SAGGQWFTPV INHPEVAILG IGRIAEKPIV RDGEIVAAPM LALSLSFDHR
401     MIDGATAQKA LNHIKRLLSD PELLLMEA
```

Our E2-WT DNA sequence in pET-11a plasmid

```
1       ATGCTGTCTG TTCCTGGTCC CGCTGCTGCA GAGGAAAAGG CTGCTCCAGC GGCTGCGAAA CCGGCTACTA CTGAAGGTGA
81      ATTCCCTGAA ACCCGTGAAA AAATGTCTGG TATCCGTCGT GCAATCGCGA AAGCCATGGT TCACTCTAAA CACACCGCGC
161     CACACGTTAC CCTGATGGAT GAAGCAGACG TTACCAAACT GGTTGCGCAC CGTAAAAAAT TCAAGGCGAT TGCGGCGGAA
241     AAAGGTATCA AACTGACCTT CCTGCCGTAC GTTGTTAAAG CTCTGGTTTC GGCTCTGCGT GAATACCCGG TTCTGAACAC
321     CTCTATTGAC GACGAGACCG AAGAAATCAT CCAGAAACAC TACTACAACA TCGGTATCGC TGCGGACACT GATCGTGGTC
401     TGCTGGTTCC TGTGATTAAA CACGCGGACC GTAAACCGAT CTTCGCGCTC GCTCAGGAAA TCAACGAACT GGCTGAGAAA
481     GCTCGTGACG GTAAACTGAC TCCTGGTGAA ATGAAAGGCG CGTCTTGCAC TATTACCAAC ATCGGCTCTG CAGGTGGTCA
561     GTGGTTCACC CCAGTTATCA ACCACCCGGA AGTTGCGATC CTGGGTATTG GTCGTATAGC CGAAAAGCCG ATCGTTCGTG
641     ACGGTGAAAT CGTTGCTGCT CCGATGCTGG CCCTGTCTCT GTCTTTCGAT CATCGTATGA TTGATGGCGC GACCGCACAG
721     AAAGCCCTGA ACCACATCAA ACGTCTGCTG TCCGACCCGG AACTGCTGCT GATGGAAGCT taa
```

Our E2-WT protein sequence (numbering for our mutants for example D381C is based on the full native pyruvate dehydrogenase E2 sequence; see above).

```
1       MLSVPGPAAA EEKAAPAAAK PATTEGEFPE TREKMSGIRR AIAKAMVHSK HTAPHVTLMD EADVTKLVAH RKKFKAIAAE
81      KGIKLTFLPY VVKALVSALR EYPVLNTSID DETEEIIQKH YYNIGIAADT DRGLLVPVIK HADRKPIFAL AQEINELAEK
161     ARDGKLTPGE MKGASCTITN IGSAGGQWFT PVINHPEVAI LGIGRIAEKP IVRDGEIVAA PMLALSLSFD HRMIDGATAQ
241     KALNHIKRLL SDPELLLMEA
```

A.2. Detailed Protocols and Additional Methods

A.2.1. Bone Marrow-Derived Dendritic Cell Preparation

1. Beginning with euthanized mouse

2. Spray animal with generous amount of 70% ethanol

3. Make sure surgical tools are all sterile

4. Cut away the tissue from the hind legs of the animal

5. For a good video on this, go to:

http://www.jove.com/video/769/culture-of-myeloiddendritic-cells-from-bone-marrow precursors

6. Make sure you remove enough skin and tissue to expose the hip joint

7. It's common for bleeding to occur here, if you sever the femoral artery

8. Remove the hind legs from the animal by cutting at the hip joint

9. Be very careful not to break the femur

10. Continue to remove tissue until the bones are exposed

- **a.** Remove the feet
- **b.** Separate the femur and tibia at the knee joint

11. You can use all four leg bones, just the femur, or just the tibias, depending on how many cells you need

- **a.** All four bones →30-40 million cells
- **b.** 2X Femurs →20-30 million cells
- **c.** 2X Tibias →5-10 million cells

12. Rinse bones in 70% ethanol for about a minute

13. Rinse the bones in a small amount of ice cold PBS

14. Set the bones in ice cold PBS on ice.

15. Using straight scissors, cut both epiphyses from the bone and place back in ice cold PBS until next step

16. Prepare ~ 7 ml of ice cold PBS in a petri dish and fill a 3 ml syringe with ice cold PBS

17. 27 gauge needle on end of syringe

18. Insert the needle into one end of the bone and flush out the marrow with PBS into the 7 mls of PBS in the petri dish

- **a.** The bone will go from brownish to bright white as the marrow is flushed to the

dish

b. Flush with more PBS as necessary to get all of the marrow out

19. Using a 10 ml serological pipette, pipette the marrow/PBS solution up and down for several minutes, until the marrow is broken up into a more homogeneous solution (single cell suspension)

20. Insert a 70 µm mesh tissue strainer to a 50 ml conical tube and apply the 10 mls of marrow to the mesh

a. If there are red clumps on the mesh, you can break that up with the tip of the pipettes.

21. Rinse the petri dish with 10 ml of fresh ice cold PBS, and apply that to the strainer

22. Centrifuge the marrow cells at 300 x g for 5 minutes

23. Decant the supernatant, break up the pellet, and add 3 mls of ACK lysing buffer for 2 minutes at room temperature

a. After 2 minutes, quench with 10-20 mls of ice cold PBS

24. Centrifuge at 300 x g for 5 minutes

25. Decant, break up pellet, and add 10-20 mls of PBS

a. You should notice that the pellet is now white, instead of red

b. Take 100 µl for cell counting

26. Centrifuge at 300 x g for 5 minutes

27. Resuspend the cells at 2 million cells/ml in pre-warmed BMDC media

28. Add 1 ml of cell suspension to a sterile bacteriological non-treated petri dish (2 million cells total)

29. Bring the volume in the dish up to 10 ml with pre-warmed media

30. Supplement the media with 20 ng/ml of mouse recombinant GM-CSF (day 0)

31. On Day 3, add 10 ml of fresh pre-warmed DC media (now 20 ml total)

a. Supplement with 10 ng/ml GM-CSF (i.e. 20 µl of 10 µg/ml stock)

32. On Day 6, remove 10 ml from each culture (50% of the media), centrifuge at 300 x g for 5 min, and resuspend the non-adherent cells in 10 ml of prewarmed DC media

a. Supplement with 10 ng/ml fresh GM-CSF (i.e. 20 µl of 10 µg/ml stock)

33. Add the non-adherent cells in fresh media back to the culture dishes

34. On Day 8, you should notice that the cells have proliferated

a. Harvest the cells by gently pipetting the media against the plate with a 10 ml serological pipette

35. Centrifuge at 300 x g for 5 min

36. Plate the immature BMDCs in whatever plate or at whatever concentration is appropriate for your experiment

A.2.2. *Splenocyte Cell Preparation*

1. Pre-warm Full RPMI (10% FBS, 1% antibiotic/antimycotic) at 37oC.

Make 1000X βME by adding 3.7 ul of BME to 1 ml of RPMI.

2. Add 50 ul of 1000X BME into 50 mL of Full RPMI to make Complete RPMI.

3. Sacrifice mouse and extract spleen and/or lymph nodes, place in 1 mL Complete RPMI.

4. (empty) through strainer.

5. Spin for 5 min on setting, then aspirate media.

6. Gently resuspend in 1 mL ACK, then add 4 mL slowly. Incubate for 4 minutes MAX.

Quench reaction with 25 mL RPMI. (skip step to step 7 if working with lymph nodes)

7. Spin for 5 min on setting 4. Aspirate media.

8. Resuspend in 10 mL RPMI.

9. Count cells. 90 µL Trypan blue + 10 µL cells. Stain for 2 minutes. Count cells, calculate the average of 2 quadrants and divide by dilution factor to obtain number of million cells/mL.

10. Dilute cells to desired concentration with Complete RPMI

A.2.3. *PEGylation of E2 Surface Amines*

1. Determine concentration of the E2 protein with BCA,

    a. Molecular weight of D381C monomer: 28105 Da

2. React the NHS-PEG2000-maleimide with the E2 protein at 30 molar excess of NHS to the E2 monomer:

    a. For example for 1 mg/ml E2 → ~ 1 mg/ml → 1 / 28105 = ~ 36 µM (with respect

to E2 monomer) → 36 μM * 30 = 1 mM

b. PEG stock at 10 mM (maleimide-PEG2000-NSH) or 100 mM (mPEG2000-NHS) in DMSO

3. Add PEG to E2, mix, and keep at room temperature for 1-2 hour
4. Apply the reaction to a 40 kDa cutoff Zeba spin desalting column
    a. From Pierce – follow the manufacturer's instructions
5. Options for reacting with free maleimide group:
    a. Add L-cysteine at ~ 20-fold molar excess to E2 monomer
    b. Add cysteine containing peptide at 5-10 molar excess to E2 monomer
6. React thiol containing compound with maleimide for 2 hr at room temperature
7. Remove excess unreacted cysteine or peptide with desalting column
8. Measure protein concentration with BCA

A.2.4. *CH12 and B3Z Cell Maintenance*

CH12 B cells should be maintained at the density between 50,000 – 200,000 cells/ml (absolutely not over 300,000 cells/ml at any time or 700,000 cells/mL for B3Z) in 5 ml of RPMI plus FBS, antibiotics and β-mercaptoethanol in a T-50 culture flask. It is important to split almost every day due to the 8 hour-doubling time of this cell line.

For maintenance:

1. Transfer cells into a 15 mL conical Falcon tube.
2. Spin for 4 minutes on setting 3 in a clinical centrifuge. Meanwhile, wash the T-50 culture. flask with 6 mL of PBS or use a new flask, and set up the hemocytometer.
3. Wash cell pellet with 2 mL of PBS, aspirate. Resuspend cells in 2 mL of fresh full medium.
4. Count cells and split cells to 50,000 cells/mL in 5 ml.

APPENDIX B

Appendix B. Additional Results

B.1. *Tumor Challenge after Single Immunization of CpG-gp-E2. (Relevant to section 2.4.3)*

Single immunization with the CpG-gp-E2 nanoparticle did not delay the B16-F10 tumor growth or animal survival time. **A)** Mice (n = 5 per group) were immunized subcutaneously with CpG-gp-E2 (50 µg per injection; equivalent to 5 µg each of gp100 peptide and CpG ODN) at day −14, followed by tumor challenge at Day 0. **B)** Single immunization with CpG-gp-E2 did not delay the tumor growth, compared to PBS-treated control. Each line represents the tumor growth of a single animal. **C)** Immunization with CpG-gp-E2 did not prolong the animal survival, compared to PBS-treated controls. Single immunization is not sufficient enough to yield an effective anti-tumor responses.

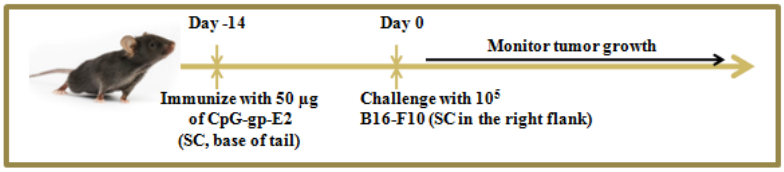

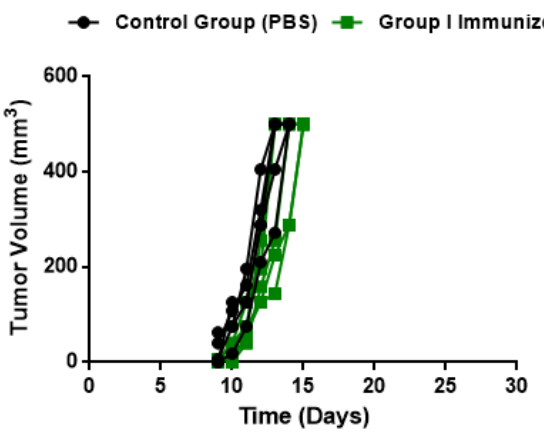

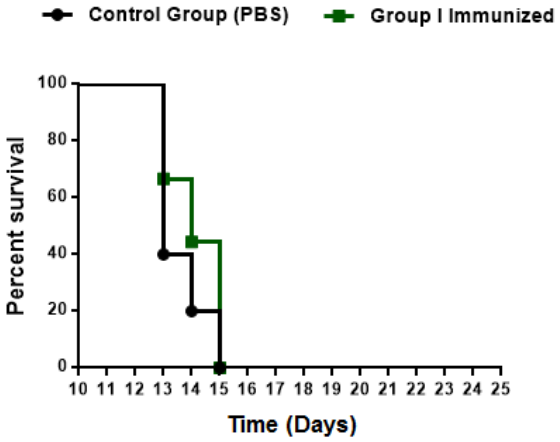

B.2. *Double Immunization with CpG-NYESO-E2, 100 μg Each Injection. (Relevant to section 3.4.2)*

HLA-A2 mice were immunized with 100 μg CpG-NYESO-E2 per dose (instead of 50 μg per dose discussed in section 3.4.2). Splenocytes of immunized mice were pulsed *ex vivo* in the presence of relevant peptide (NYESO) or irrelevant peptide (SIINFEKL) and analyzed for specific IFN-γ secretion, checked with ELISpot. No significant increase in specific IFN-γ was observed for mice receiving 100 μg CpG-NYESO-E2 immunization (per injection) compared to PBS control group ($p > 0.05$, $n=4$). Immunization with 100 μg of CpG-NYESO-E2 did not increase the IFN-γ secretion compared to 50 μg, and in fact showed a significant decreased across the cohort of mice. This could be due to increased levels of suppressive T cells, T cell exhaustion, or high antigen doses leading to increase tolerance.

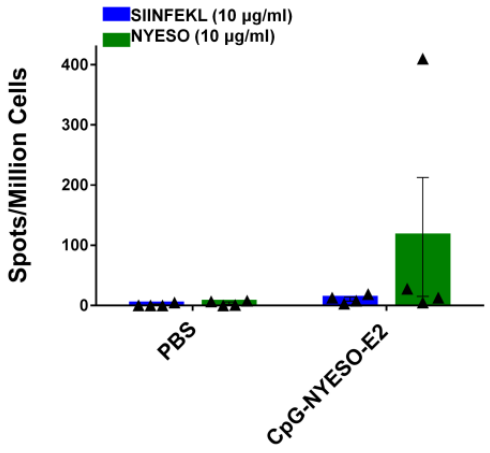

B.3. *SDS-PAGE and ELISpot Data from CpG-NYESO(p2)-E2 and CpG-MAGE(p2)-E2 Nanoparticles. (Relevant to sections 3.4.2 & 3.4.4).*

A) SDS-PAGE. Peptides were successfully conjugated to the E2 nanoparticle. **B)** Summary of averaged ELISpot data from mice immunized with 50 µg CpG-NYESO(p2)-E2 or CpG-NYESO-E2. **C)** Summary of averaged ELISpot data from mice immunized with 50 µg CpG-MAGE(p2)-E2 or CpG-MAGE-E2. HLA-A2 mice were immunized, and splenocytes of immunized mice were pulsed *ex vivo* in the presence of relevant peptide or irrelevant peptide (SIINFEKL) and analyzed for specific IFN-γ secretion. No significant increase in specific IFN-γ secretion was observed for mice receiving CpG-NYESO(p2)-E2 or CpG-MAGE(p2)-E2 compared to PBS control group ($p > 0.05$, $n \geq 3$). Our data showed that immunization with nanoparticle formulations of the NYESO(p2) epitope (C-ILTIRLTAA) [CpG-NYESO(p2)-E2] and MAGE(p2) epitope (C-KVAELVHF) [CpG-MAGE(p2)-E2] did not result in any significant increase in the IFN-γ secretion. This could be due to their low *in vivo* immunogenicity.

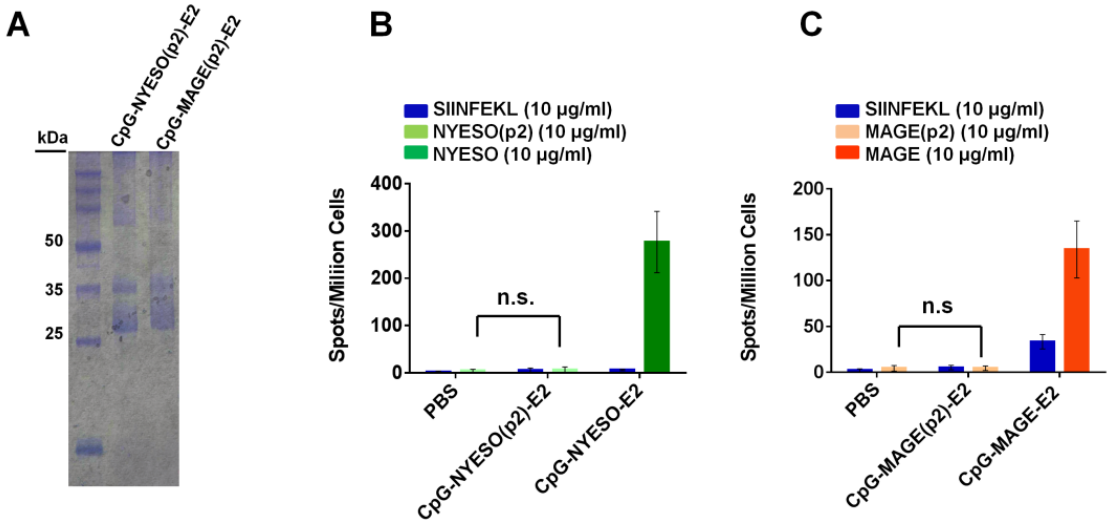

B.4. *ELISpot Data Using Splenocytes from Co-Immunization with CpG-NYESO-E2 and CpG-MAGE-E2 Nanoparticles (50 µg each, 100 µg total per dose). (Relevant to section 3.4.6.)*

HLA-A2 mice were immunized with different formulations (a-d). Splenocytes of immunized mice were pulsed *ex vivo* in the presence of relevant peptide (NYESO or MAGE) or irrelevant peptide (SIINFEKL) and analyzed for specific IFN-γ secretion. Lower IFN-γ secretion was observed for NYESO epitope when mice were immunized simultaneously with CpG-NYESO-E2 and CpG-MAGE-E2 (50 µg each, 100 µg total per dose) compared to CpG-NYESO-E2 alone (50 µg per dose)**.** Co-immunization with higher doses (compared to section 3.4.6) of CpG-NYESO-E2 and CpG-MAGE-E2 nanoparticles (50 µg each, 100 µg total per dose) did not amplify the specific-IFN-γ secretion, relative to each formulation separately; in fact, both IFN-γ and lysis effects were lower than the effects of each individual antigen-nanoparticle alone. This observation could be due to T cell exhaustion or peptide competition on the MHC of the antigen presenting cells (e.g., DCs) or on the T cell receptors.

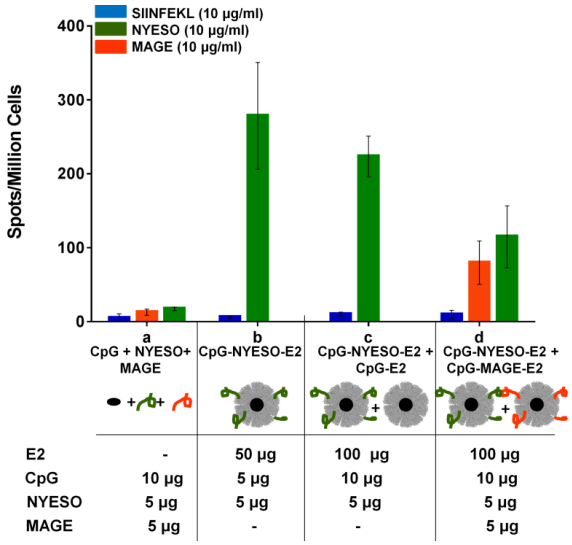

B.5. *Cell Lysis Assay Using Splenocytes from Co-Immunization with 50 μg CpG-NYESO-E2 and 50 μg CpG-MAGE-E2 Nanoparticles (100 μg total per dose, 2 immunization). (Relevant to section 3.4.6.)*

A) Vaccine components of different formulation groups (a-c). **B)** Summary of averaged lysis data. Mice received immunizations with different formulations (a-c); splenocytes isolated from mice co-immunized with CpG-NYESO-E2 and CpG-MAGE-E2 nanoparticles (50 μg each, 100 μg total per dose) did not increase the lysis activity toward A375, relative to each CpG-NYESO-E2 or CpG-MAGE-E2 formulation alone at 50 μg per dose (100:1 effector: target ratio). **C)** Dose-response lysis ability towards A375 and MCF-7 cell lines at different effector: target ratio. Co-immunization with higher doses (compared to section 3.4.6) of CpG-NYESO-E2 and CpG-MAGE-E2 nanoparticles (50 μg each, 100 μg total per dose) did not amplify the lysis activity, relative to each formulation separately; in fact, both IFN-γ and lysis effects were lower than the effects of each individual antigen-nanoparticle alone. This observation could be due to T cell exhaustion or peptide competition on the MHC of the antigen presenting cells (e.g., DCs) or on the T cell receptors.

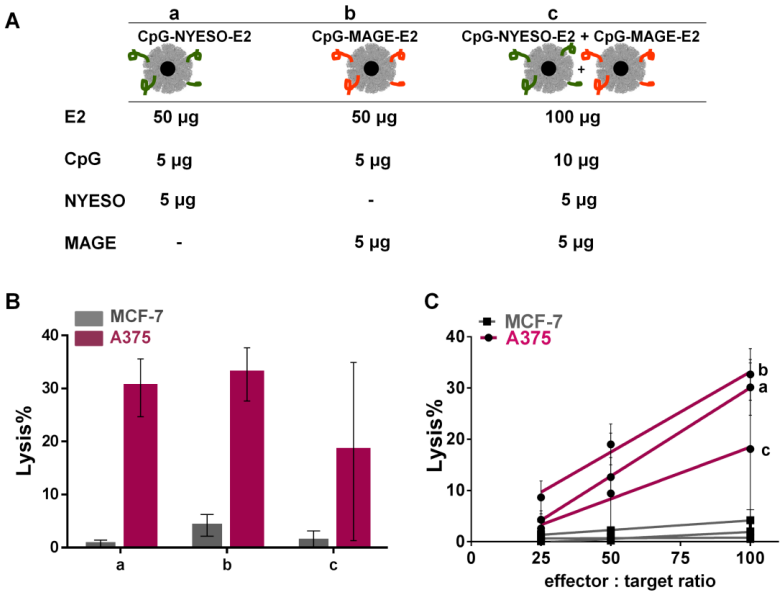

B.6. *HPLC Analysis of Peptide and CpG Conjugation to the E2 Nanoparticle*

Numbers of peptides attached to the E2 nanoparticle was analyzed by HPLC (Shimadzu system) with a Zorbax C18 column over a water: acetonitrile gradient at 0.6 ml/min of total flow. Concentration of pump A (water) dropped from 95% to 5% over 35 minutes. Peptides and E2 were conjugated using sulfo-SMCC linker. As a negative control, peptides and E2 were combined in the presence of water instead of linker. Without removing unbound peptides, peptide-conjugated E2 and negative control samples (H2O was used instead of the linker) were examined by HPLC. The area difference in peptide peak between peptide-conjugated E2 and unbound samples were measured, and was used to determine the amount of remaining unconjugated peptide in the solution which was quantified with a standard curve of free peptide.

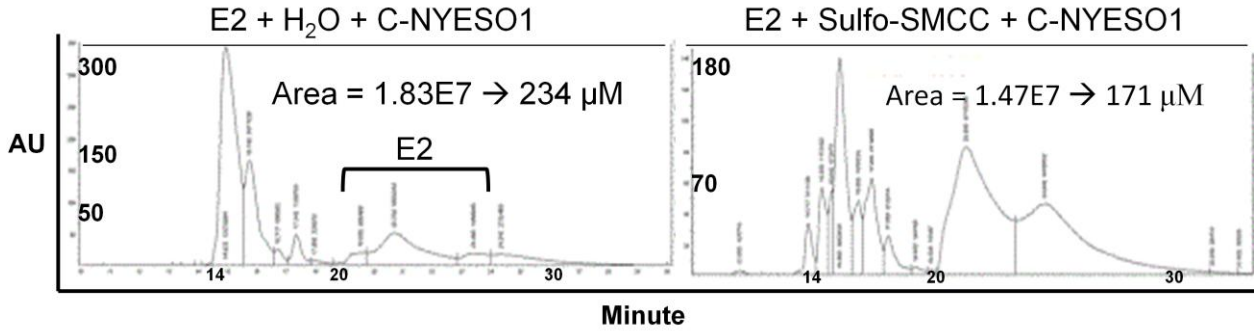

B.7. *Combination of CpG-gp-E2 with Anti-CTLA4 Did Not Increase the Efficacy Compared to Each Treatment Alone*

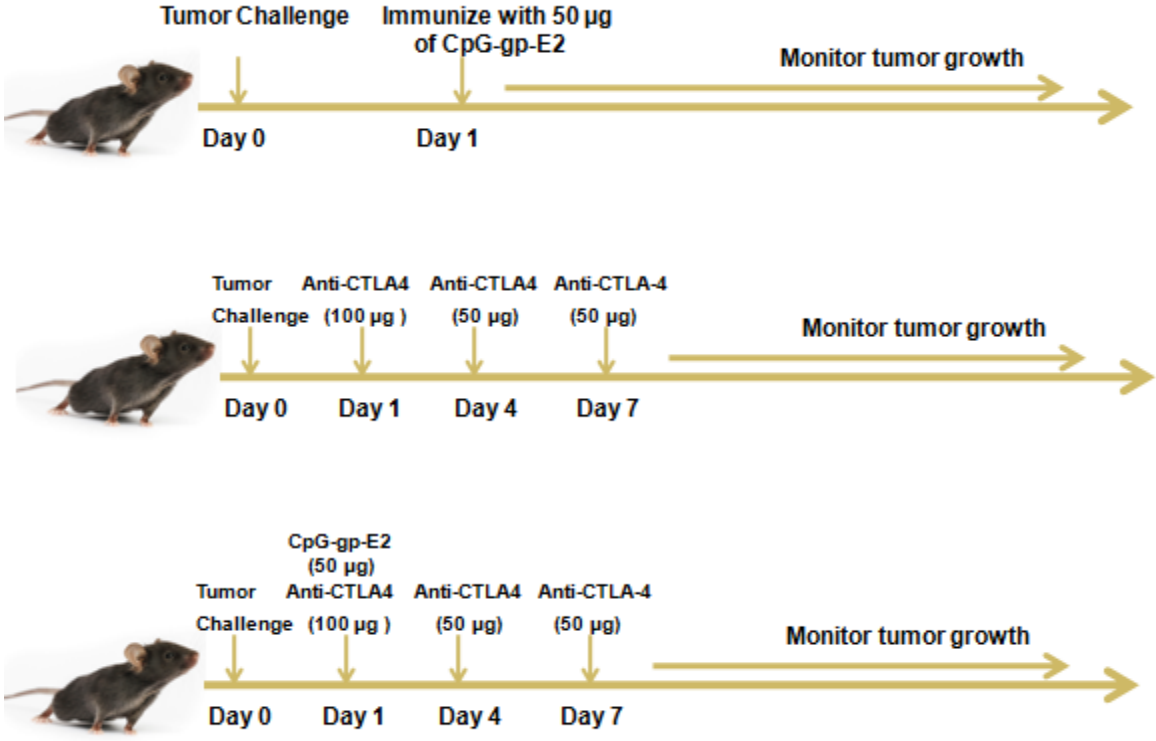

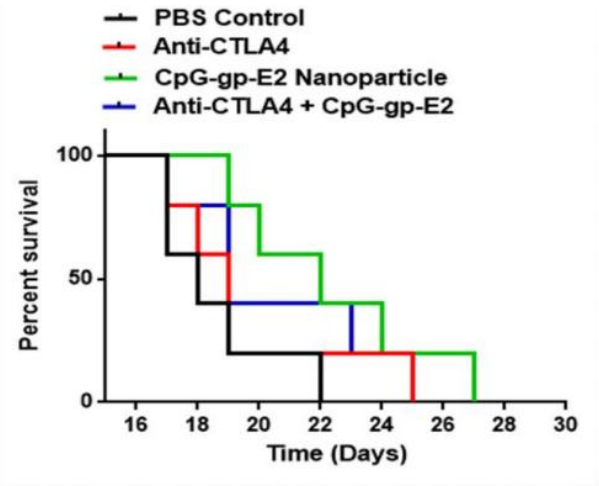

P value (Log-rank) comparison of:
PBS with nanoparticle group: 0.049*
PBS with anti-CTLA4 group: 0.45
PBS with combined study group: 0.15
Nanoparticle with combined group: 0.43

B.8. *NK Cells Count per Spleen after Immunization with CpG-gp-E2 Nanoparticle. (Relevant to section 4.4.3)*

Mice were immunized (groups II-IV). All mice were sacrificed on day 14 and spleens were stained for NK cells. Immunization with CpG-gp-E2 nanoparticle did not change the NK cell population in spleen, compared to the PBS control group.

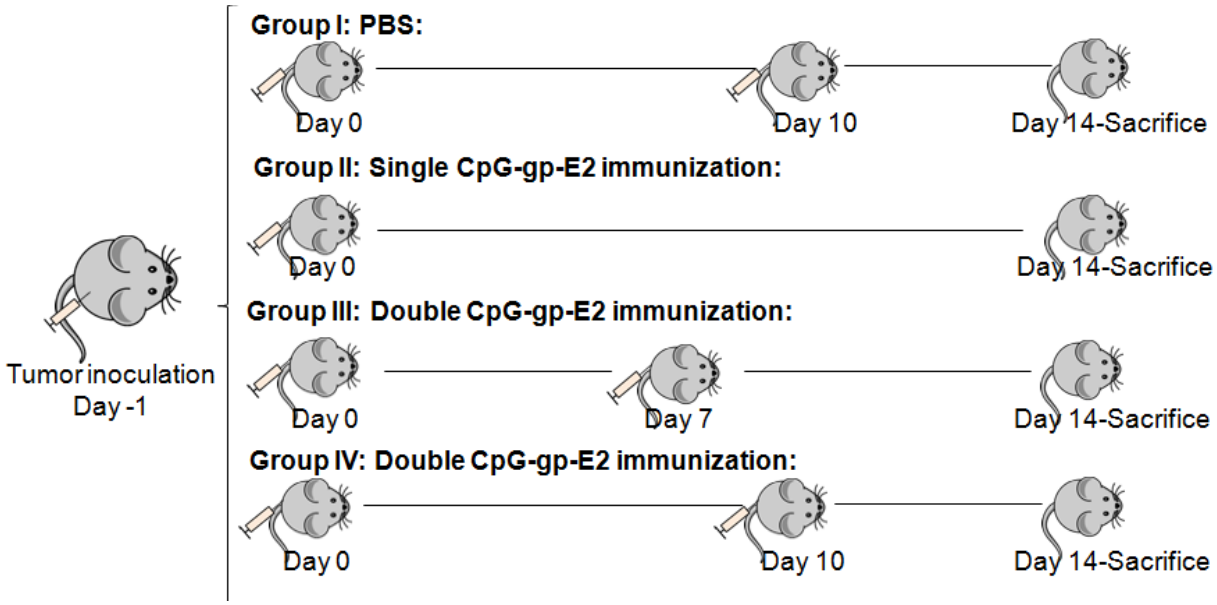

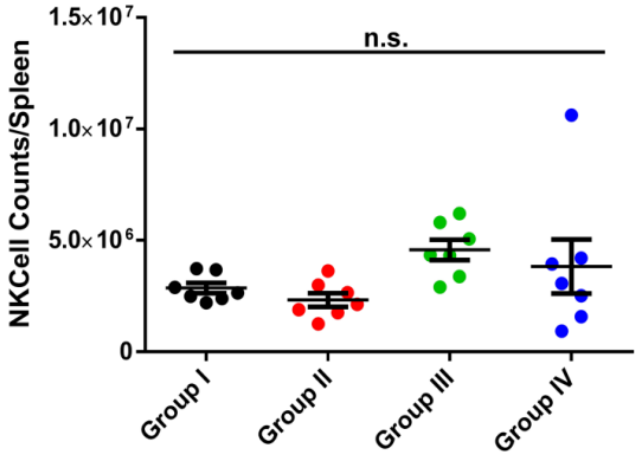

B.9. *Imidazoquinoline Conjugation to the Interior of the E2 Nanoparticle*

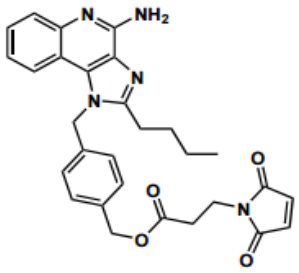

Imidazoquinoline with ester linker

Imidazoquinoline is a ligand of TLR7 and TLR8 which can be used as an adjuvant in cancer vaccines. Imidazoquinoline with ester linker was synthesized by Dr. Carl Vogel at UCI. We attempted to conjugate the imidazoquinoline molecule from the maleimide end to the cysteine of D381C. However imidazoquinoline is a very hydrophobic molecule and it had to be dissolved in organic solvent. In contrast, E2 protein nanoparticles denature in presence of > 25% of organic solvent. Solubility of imidazoquinoline was less than 0.06 mg/ml in 25% of DMSO, urea, ethanol, guanidine, and NMP which is not high enough to perform the conjugation. Therefore, we couldn't find a solvent that keeps both the E2 nanoparticle and the imidazoquinile happy to perform the conjugation.

We also tested Methyl tert-butyl ether (MTBE) solvent. Imidazoquinoline was partially dissolve in 25% of MTBE. E2 denatured in 25% of MTBE; we refolded the E2 by adding phosphate buffer to overtime until the percentage of MTBE dropped down to less than 1%. However, in the refolding process, we lost tremendous amount of the E2 nanoparticle to the point that we were not able to detect it anymore. We could not find a method to conjugate the imidazoquinoline to the E2 nanoparticle.